UNIVERSIDAD DE LA FRONTERA

Facultad de Ingeniería, Ciencias y Administración

Doctorado en Ciencias de Recursos Naturales

Synthesis of metal nanoparticles (Ag, Au and Cu) with antimicrobial activity by micelyum-free extract of Chilean native fungus

DOCTORAL THESIS IN FULFILLMENT OF THE REQUERIMENTS FOR THE DEGREE DOCTOR OF SCIENCES IN NATURAL RESOURCES

RAPHAEL ALEJANDRO CUEVAS ASTUDILLO

TEMUCO-CHILE

2017

“Synthesis of metal nanoparticles (Ag, Au and Cu) from micelyum-free extract of Chilean native fungus with antimicrobial activity”

Esta tesis fue realizada bajo la supervisión de la Dra. Olga Rubilar, perteneciente al Departamento de Ingeniería Química de la Universidad de La Frontera y es presentada para su revisión por los miembros de la comisión examinadora.

Raphael Alejandro Cuevas Astudillo

Dr. Francisco Matus B.

Director Programa de Doctorado en Ciencias de Recursos Naturales

Dra. Olga Rubilar A.

Dra. Maria Cristina Diez

Dra. María de la Luz Mora

Dr. Juan Carlos Parra

Director Académico de Postgrado Universidad de La Frontera

Dra. Paula Zapata

Dr. Miguel Martínez

Dedico estas simples palabras cada una de las personas que me acompañó y apoyó durante el tiempo desarrolló de mis estudios doctorales; MUCHAS GRACIAS!!!...

En especial dedico este logro a mis padres y mi familia.

…Bajo los volcanes, junto a los ventisqueros, entre los grandes lagos, el fragante, el silencioso, el enmarañado bosque chileno...

…Quién no conoce el bosque chileno, no conocé este planeta…

El bosque Chileno, Pablo Neruda

Dedico este trabajo a mi amado hijo Renato y a Karina por todo el tiempo que me acompañaron…

Acknowledgments

This study was possible thanks to support by FONDECYT project N° 1130854, from Comisión Nacional de Investigación Científica y Tecnológica, Chile.

I want thanks the financial support of CONICYT through Doctoral Fellowship Program 21110491 and CONICYT Internship in Brazil 21110491 and Operational expenses CONICYT Scholarship 21110491.

I want also thanks to Environmental Nanobiotechnology group (UFRO-Chile) and Environmental Biotechnology Center (UFRO-Chile). Similarly thank the research group Ecological Chemistry, IQ-UNICAMP (Brazil).

Contents

Index Table

Index Figure

Summary

The biogenic synthesis of metal nanoparticles by fungi is more advantageous in comparison with other microorganisms, produce nanoparticles in form intra and extracellular way due to the high secretion of proteins and enzymes that are involved in the reduction of metal ions and limiting nanoparticles. In this context, the white rot fungi are potential biofactories for metal nanoparticle production due to rich extracellular enzyme system as ligninases, peroxidases and reductases as laccase. Therefore, this work aims evaluate the synthesis of metal (Cu, Ag and Au) nanoparticles (Me-NPs) by oxide-reductase enzyme of mycelium-free extract of native white rot fungus to be used as antimicrobial agent. A screening of different white rot fungi of native forest to Sourther Chile obtained from the culture collection of the Environmental Biotecnology Laboratory of Universidad de La Frontera, was evaluated for its potential for synthesis of Ag nanoparticles under acid and alkaline conditions. Later, the fungus that showed higher ability for synthesized silver nanoparticles was used also for synthesized Cu and Au nanoparticles under differente conditions of synthesis (different metal salts and pH conditions). The metal nanoparticles (Cu, Ag and Au-NP) formation were evaluated spectrophotometrically by UV-Vis (200-800 nm) for identifying the formation of plasmonic bands and characterized by electron microscopy TEM or/and SEM, determination of average size by DLS, Fourier Transforms Infrared spectroscopic (FTIR) and X-ray difrattion. Subsequently with the results obtained a possible mechanism of the formation of metal nanoparticles using white rot fungus was proposed. Finally, antimicrobial activity studies of metal nanoparticles (Cu, Ag and Au - NP) were development with *Escherichia coli* and *Staphylococcus aureus* bacterial strains. Disc diffusion assays were performed with 100 µg of nanoparticles to evaluate the inhibitory effect of metal nanoparticles on bacterial strains of *E. coli* and *S. aureus*. Continued, studies were analyzed tests the effects on bacterial growth by increasing the optical density in the liquid medium with increasing concentration in solution 100, 250 and 500 µg/mL were analyzed.
The results showed that the fungal extracts produced from *Stereum hirsutum*, *Anthracophyllum discolor* and *Trametes versicolor* demonstrated to have potential for the synthesis of metal nanoparticles, but the better result was obtained in the synthesis using mycelium-free extract produced from *S. hirsutum* with alkaline pH conditions in solution. The Ag nanoparticles synthetized by mycelium-free extract produced from *S. hirsutum* had an average size of 100 nm and it was effective in the formation of silver nanoparticles zero valent. The Cu nanoparticles synthetized by *S. hirsutum* combined with $CuCl_2$ under basic conditions was effective obtaining monodisperse and spherical nanoparticles between 4 and 5 nm in size. And the maximum absorbance peak was observed to 620 nm, associated with the form of copper oxide. The Au nanoparticles were predominant spherical shape and a dispersal of size 100 nm aproximatelly. The XRD scan spectroscopy demonstrated the presence of Ag, Cu and Au nanocristal in the nanoparticles. The FTIR spectra for all the metal nnaoparticles revealed bands in the regions of 3280 and 2924 cm^{-1} which are reported as type movements of stretching vibrations in primary and secondary amines. The bands near 1029 cm^{-1} are reported to be C-N stretching vibrations of aromatic and aliphatic amines, and another band of interest found in this study was observed at 1243 and 1244 cm^{-1} are designated as bending vibration movements I and III amides. In addition, the analysis results of SDS-PAGE protein profile present in the extract produced from fungal *S. hirsutum*, the presence of bands 12.9, 15.9, 36.9, 47.4 and 61.0 kDa were observed molecular weight. These evidences suggest that the release of extracellular protein by white rot fungi may have resulted in the formation and stabilization of biogenic metal nanoparticles synthesized. A possible mechanism explaining the formation of metal nanoparticles using white rot fungus is by laccase enzyme, which was proposed in our reserach. The formation of

nanoparticle that could explain the formation of the nanoparticles by the interaction of the metal ion with the disulfide bridges in the structure presenting the laccase enzyme: 1) It is by reducing the ion metal action of the redox potential present in T1 copper having a cysteine residue in conformation and 2) it is possible to break the sulfur bridges sulfur stabilizing the molecule in domain 1 of the structure.

In relation to the results obtained of antimicrobial activity, it showed that there copper nanoparticles were no inhibitory effect on bacterial growth of *E. coli* and *S. aureus* in liquid medium and the same result was observed in the diffusion assay plate. A possible cause of the lack antimicrobial activity of copper nanoparticles synthesized from the extract of white rot fungus *S. hirsutum* can be attributed to these enveloping biopolymer nanoparticles. But, antibacterial activity of silver and gold nanoparticles demonstrated that the MIC of silver nanoparticle for bacteria strain *E. coli* and *S. aureus* were 30 and 80 µg/mL respectively. Complementarily, gold nanoparticles were 40 and 60 µg/mL solution for *E. coli* and *S. aureus* respectively. The results of the development work investigate may indicate that the biogenic silver nanoparticles synthesized from extract of *S. hirsutum* have better antimicrobial activity that biogenic Au-PN. The results obtained in studies of staining for the production of reactive oxygen species (ROS), confirming qualitatively generation of ROS by means of the Confocal Microscope images. Addition, flow cytometer studies were performed to quantify the production of ROS species, the results showed an extra generation in average 15% of species ROS. In relation to mechanism of antimicrobial activity of silver nanoparticles are not fully characterized, but in this direction hypothetical mechanism: (a) silver nanoparticle direct damage to cell membranes and (b) the silver nanoparticle and silver ion generation of reactive oxygen species (ROS). In conclusions the use of mycelium-free extract from white rot fungus for the production of different metal nanoparticles proved to be effective in the process of synthesizing the metal nanoparticles (Ag, Au and Cu), this results show a high potential for research and development in the area of nanobiotechnology from the use of white rot fungi. Besides, the process of reduction being extracellular using mycelium-free extract from white rot fungus is fast that may lead to the development of an easy bioprocess and ecofriendly for synthesis of metal nanoparticles. In general, the reaction of synthesis of the nanoparticles using fungal extract the reaction proceeded at room temperature without the need to deliver energy to the system. The antimicrobial activity of silver and gold nanoparticles has the potential to inhibit bacteria growth and/or kill the bacterial cell of *S. aureus* and *E. coli*, the antibacterial activities of NPs depend on main factors type metal NPs used and type of bacteria (gram-negative and gram-positive). Finally, the use of white rot fungi in the synthesis of biogenic nanoparticles to develop industrial or biomedical applications will be favored by the nonpathogenic nature of these organisms.

.

CHAPTER I: GENERAL INTRODUCTION

General Introduction

Nanotechnology represents a field of study that has been of great interest in recent years due to unusual properties that exhibit materials with dimensions between 1 and 100 nm. Metal nanoparticles (Me-NPs) have been synthesized by various physical and chemical processes; however, these methods are costly, inefficient and generate hazardous wastes that are risks to the environment (Azim et al., 2009). There is therefore an urgent need to develop environmentally friendly biological processes for nanoparticles synthesis. In this context, the synthesis biogenic of stable Ag nanoparticles (Fayaz et al, 2010; Vigneshwaran et al., 2006), CuS nanoparticles (Hosseini et al., 2012) and Au nanoparticles (Kitching et al., 2015) by fungi have been reported.

The synthesis biogenic of nanoparticles can be categorized as intracellular and extracellular according to where the nanoparticles are synthesized (Ahmad et al., 2002; 2003). However, extracellular synthesis is the technique most frequently used due to that the nanoparticles are obtained via a simple and easy process. Several studies (Durán et al., 2005; Gericke and Pinches, 2006a; Sanghi et al., 2009; Jain et al., 2011) have demonstrated that the formation mechanism is due to the action of a large number of enzymes secreted by the fungi. Durán et al. (2005) reported that nitrate reductase is the main enzyme involved in the biogenic synthesis of Ag nanoparticles by *F. oxysporum.*

Currently in the processes of synthesis of biogenic Me-NPs is taking more interest the use of white rot fungi strains. Likewise, Sanghi et al. (2011) demonstrated that the laccase enzyme secreted by the white rot fungus *Phanerochaete chrysosporium* is responsible for the formation of gold nanoparticles (Au-NPs). In this context, white rot fungi isolated from template forests in southern Chile might have a high potential for synthesizing Me-NPs due to their high production of extracellular enzymes such as laccase and peroxidases (Tortella et al., 2008; Rubilar et al., 2007), the white rot fungi have shown an ability to synthesize biogenic Me-NPs (Sanghi et al., 2011; Sanghi and Verma, 2010; Sanghi et al., 2009). Therefore, the main of this study was to evaluate the synthesis of Me-NPs (Cu, Ag and Au -NP) by oxide-reductase enzyme of mycelium-free extract of native white rot fungus and to be used as potential antimicrobial agent. The main activities of this study were (a) selection of a fungal mycelium-free extract of a fungus strain with best capacity for the synthesis of Me-NPs; (b) evaluation of the synthesis of Me-NPs by oxide-reductase enzyme of a mycelium-free extract of native white rot fungus and to proposed a synthesis mechanism for their production. And (c) evaluation of biocide activity of Me-NPs previously synthesized.

1.1.- Synthesis of metal nanoparticles from fungal extract

Many microorganisms including bacteria, fungi, actinomycetes and yeast have been shown to be capable of synthesizing Me-NPs (Durán et al., 2010; Narayanan and Sakthivel, 2010; Zhang et al., 2011). However, synthesis by fungi is more advantageous compared to other microorganisms. In this context, diverse strains of fungi have been used for synthesis of Me-NPs (Table 1.1).
Adinallity, many fungi have been studied for their nanoparticles formation, including *Cladosporium cladosporioides* (Balaji et al., 2009), *Fusarium semitectum (*Basavaraja et al., 2008), *Trichoderma Reesei* (Vahabi et al., 2008), *Trichoderma viride* (Fayaz et al., 2009), *Penicillium brevicompactum* (Shaligram et al., 2009), *Aspergillus niger* (Jaidev et al., 2010), *Candida albicans* (Ahmad et al., 2013), *Penicillium* sp (Honary et al., 2012), among others. In the context, it is possible to indicate

that *Fusarium oxysporum* is the most widely used and reported strain (Husseiny et al., 2015; Ghaseminezhad et al., 2012; Syed et al., 2012; Durán et al., 2007; 2005; Bansal et al., 2005).

Moreover, fungi are easy to handle during their cultivation; most fungi have a high tolerance towards metals and also secrete a large number of proteins that enable a greater production of nanoparticles formation (Mohanpuria et al., 2008). The synthesis of nanoparticles by fungi occurs mainly due to a reaction of reduction/oxidation, being the enzymes the main responsible for reducing metal compounds into their respective nanoparticles. The synthesis of nanoparticles by fungi can be developed intracellular or extracellularly.

Table 1.1 Metal nanoparticles synthetized by proteins using of different fungi strains

Fungal strains	Metal	Reference
Fusarium oxysporum	Ag	Ghaseminezhad et al. (2012)
Candida albicans	Ag	Ahmad et al. (2013)
Fusarium solani	Ag	El-Rafie et al. (2012)
Fusarium oxysporum	Ag	Husseiny et al. (2015)
Trichoderma asperellum	Au	Mukherjee et al. (2012)
Candida albicans	Au	Ahmad et al. (2013)
Fusarium oxysporum	Ba-Ti	Bansal et al. (2006)
Fusarium oxysporum	Ti	Bansal et al. (2005)
Fusarium oxysporum	CuS	Hosseini et al. (2012)
Penicillium sp.	Cu	Honary et al. (2012)
Fusarium oxysporum	ZnS	Mirzadeh et al. (2013)
Fusarium oxysporum	Pt	Syed et al. (2012)
Fusarium semitectum	Au/Ag	Sawle et al. (2008)
Neurospora crassa	Au/Ag	Castro-Longoria et al. (2012)
Aspergillus flavus	TiO_2	Rajakumar et al. (2012)
Aspergillus aeneus NJP12	ZnO	Jain et al. (2013)
Verticillium sp	Fe_3O_4	Bharde et al. (2006)

In intracellular synthesis, nanoparticles are produced mainly on the inner surface of the cell membrane and cell cytoplasm (Senapati et al., 2004; Mukherjee et al., 2001a), whereas extracellular synthesis is produced by protein, polysaccharides and/or organic acid secreted by fungi (Rodriguez et al., 2013; Jain et al., 2011; Balaji et al., 2009). Both cultivation methods have been widely studied (Mukherjee et al., 2008; Durán et al., 2005; Mukherjee et al., 2002), however, extracellular synthesis is the technique most frequently used because a large number of nanoparticles free of cells are produced, allowing a relatively simpler processing.

The extracellular synthesis of nanoparticles by fungi basically consists in the separation of biomass from the culture medium to remove growth media components that could interfere in the reaction with metal ion. The biomass is cultivated in distilled water where the fungi secrete a wide variety of components (protein, polysaccharides and organic acid) involved in the reduction and capping of nanoparticles. Then, the biomass is filtered and the solution is used to synthesize nanoparticles, where metals like Cu, Ag or Au, among others, are added as salts (Durán et al., 2005; Bhainsa et al., 2006; Balaji et al., 2009) (Figure 1.1).

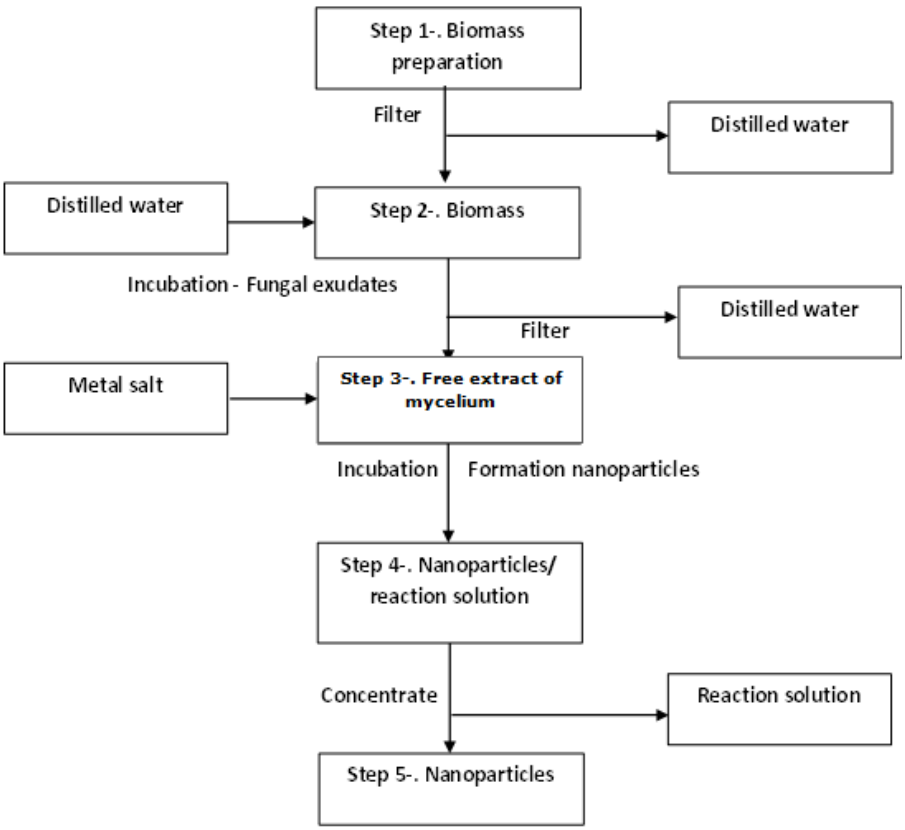

Figure 1.1 Process diagram of extracellular synthesis of metal nanoparticles using a fungal free-extract mycelium.

The bio-transformed products are measured by UV-Vis spectroscopy at different time intervals to determine the change in the light absorption profile of the solution and increase in their intensity. Extracellular synthesis of gold, copper, silver, zirconia, titanium, magnetite, silica and barium by fungi has been reported (Narayanan and Sakthivel, 2010). Studies conducted by Bhainsa and D'Souza (2006) showed that when silver nitrate is added to a filtered solution of *Asperguillus fumigates*, monodisperse silver nanoparticles (Ag-NPS) 5-25 nm in size were produced in 10 min. Hosseini et al. (2012) demonstrated that *F. oxysporum* was capable of producing copper sulfite nanoparticles with a mean size of 3 nm from a copper sulfate solution. In the same way, Ahmad et al. (2003) demonstrated extracellular synthesis of Ag-NPs in the range of 5-15 nm using *F. oxysporum*.

1.2.- Synthesis of metal nanoparticle by white rot fungi

The white rot fungi have been used intensively in the degradation of environmentally hazardous compounds (Tortella et al., 2005; Rubilar et al., 2008; 2011; 2012). The ability of white rot fungi to degrade pollutant compounds is due to their highly efficient non-specific extracellular enzymatic system, composed by the ligninolytic enzyme laccase, manganese peroxidase and lignine peroxidase (Kersten et al., 1990). The non-specificity of the ligninolytic enzymes with respect to its substrate allows that wide range of compounds are oxidated and/or reduced (Kersten et al., 1990), which have also allowed use in the synthesis of Me-NPs. In this context, in Table 1.2 is possible to observe some studies on synthesis of Me-NPs by white rot fungi, mainly have been reported nanoparticles synthesized from three metals Au, Ag and Cd.

Currently interest in the use of decay fungi gaining ground in the world of research, studied reported by Sanghi et al. (2011) showed that the extracellular enzyme system of *Phanerochaete chrysosporium* was actively involved in the synthesis of Ag-NPs. Other more recent examples are those reported by Krishna et al. (2015) using *Schizophyllum radiatum* for synthesis of Ag nanoparticles and El-Batal et al. (2015) reported synthesis of Au-NPs by *Pleurotus ostreatus.* More references are presented in Table 1.2 demonstrating the growing interest in the development of this biotechnology.

Table 1. 2 Metal nanoparticles using white rot fungi strains in the synthesis process

Fungal strains	Metal	Reference
Pleurotus sajor caju	Ag	Nithya and Ragunathan (2009)
Coriolus versicolor	Ag	Sanghi and Verma (2009a)
Shizophyllum commune	Ag	Mashitua and Chan (2011)
Pycnoporus sanguineus	Ag	Chan et al. (2012a)
Schizophyllum commune	Ag	Chan et al. (2012b)
Pycnoporus sanguineus	Ag	Chan and Don (2014)
Schizophyllum radiatum	Ag	Metuku et al. (2014)
Schizophyllum radiatum	Ag	Krishna et al. (2015a)
Trametes versicolor	Ag	Durán et al. (2014)
Trametes sp	Ag	Krishna et al. (2015b)
Phanerochaete chrysosporium	Au	Sanghi et al. (2011)
Paraconiothyrium variabile	Au	Faramarzi and Forootanfar (2011)
Pleurotus ostreatus	Au	El-Batal. (2015)
Coriolus versicolor	CdS	Sanghi and Verma (2009b)
Phanerochaete chrysosporium	CdS	Chen et al. (2014)

In this respect, studies developed by Faramarzi and Forootanfar (2011) demonstrated that the laccase enzyme produced by the white rot fungus *P. variabile* is responsible for the formation of Au-NPs, but this synthesis needs external energy delivered as the temperature increases to be effective. In the same way, studies developed by Durán et al. (2014) demonstrated that the synthesis of Ag-NPs could be attributed to enzyme laccase, which was semi-purified from the white rot fungus *Trametes versicolor.* The synthesis of Me-NPs could be used with semi-purified or purified enzymes; however it is a more complex and expensive process. In this context, the use of fungal mycelium for obtaining a free extract of mycelia with the enzymatic system is an alternative that allows a relatively simple processing and a large number of nanoparticles free of cells.

1.3.- Formation mechanisms of metal nanoparticles by fungi

Several studies have attempted to describe the synthesis mechanism of Me-NPs (Jain et al., 2011; Durán et al., 2011; Durán et al., 2005). However, it is not yet well understood. Mukherjee et al. (2008) proposed that the formation mechanism of Ag-NPs starts with the bioreduction of $AgNO_3$ to produce Ag-NPs, followed by the stabilization and/or encapsulation of the nanoparticle by a suitable capping agent. Durán et al. (2005) suggested two possible mechanisms for biogenic synthesis of Ag-NPs by *F. oxysporum:* one involves the enzyme nitrate reductase and the other a shuttle quinone extracellular process. In Figure 1.2 is represented of possible mechanisms; nitrate reductase is responsible for the reduction Ag^+ to Ag^0 causing the formation of Ag-NPs, electron transfer for the

reduction of ion is through a quinone intermediate passes. The reaction is coupled to a redox reaction; divide the reduction of NAD^+ to NADH and the oxidation of nitrite to nitrate reductase.

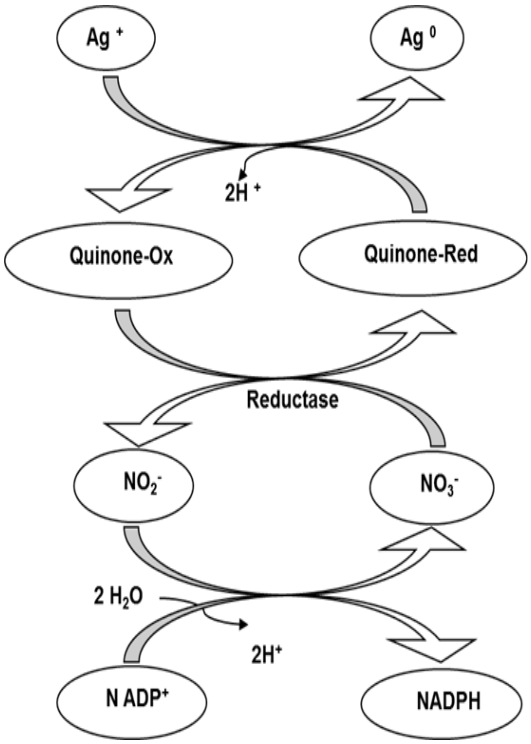

Figure 1. 2 Hypothetical silver nanoparticles synthesis based on the reductive action of nitrate, reductase (Journal Nanobiotechnology, proposed by Durán et al., 2005).

Similar results were reported regarding the synthesis of Ag-NPs by *F. acuminatum* (Ingle et al., 2008) and *Bacillus licheniformis* (Kalimuthu et al., 2008), where the formation mechanism was attributed to nitrate reductase. Likewise, Jain et al. (2011) suggested that a possible mechanism for the synthesis of the Ag-NPS by *Asperguillus flavus* might occur in two steps: the first involves a 32 kDa protein which may be the reductase enzyme secreted by the fungus, the second involves 35 kDa proteins which are bonded with nanoparticles and confer stability on the nanoparticles. With respect to other metals, studies conducted by Sanghi and Verma (2009a) demonstrated that the white rot fungus *C. versicolor* produced cadmium sulfide nanoparticles (CdS-NPs), where the thiol group of the fungal protein was the main one responsible for the synthesis of CdS-NPs. Prasad et al. (2010) suggested that a low pH environment might activate oxidase enzymes in the microorganisms due to a high oxidation potential, which would allow the Cu-NPs formation. By contrast, Sanghi et al. (2011) demonstrated that during the synthesis of Au-NPs by *P. chrysosporium* the enzyme laccase was dominant in the fungal medium, attributing this to nanoparticles formation.

Therefore, these studies demonstrate that the synthesis of metal nanoparticles is an emerging area of research that requires further study to elucidate the mechanisms.

1.4.- Characterization of metal nanoparticles synthesized by fungi

Several techniques are used to evaluate the characteristics of Me-NPs, such as ultraviolet-visible (Uv-Vis) spectroscopy, electron microscopy techniques; Fourier transformed infrared (FTIR) spectroscopy analysis, X-ray diffraction, zeta potential and particle size distribution.
The method Uv-Vis spectroscopy allows determining the formation and stability of Me-NPs by color changes of the reaction solutions. These changes are attributed to the excitation of surface

plasmon resonance in the Me-NPs (Durán et al., 2010). Studies developed by Nayak et al. (2011) demonstrated that the peak maximum of absorbance in the synthesis of silver nanoparticles by *Penicillium purpurogenum* was 420 nm, indicating that Ag^+ was reduced to Ag^0. Hosseini et al. (2012) demonstrated that copper sulfide nanoparticles showed the peak maximum after 400 nm.

In relation to the microscopy techniques, the most frequently used are transmission electron microscope (TEM), scanning electron microscopy (SEM) and energy-dispersive spectroscopy (EDS). The morphology of Me-NPs can be analyzed by TEM and SEM. The TEM technique allows visualizing the size and shape of nanoparticles. Furthermore, TEM analysis can characterize the stabilization of nanoparticles by capping around the particles to prove whether fungal proteins are responsible for covering the particle (Durán et al., 2004, Sanghi and Verma, 2009). SEM analysis enables the determination of the monodispersity of nanoparticles and elemental characterization by SEM combined with EDS.

The FTIR spectroscopy allows characterizing the protein binding with Me-NPs by identifying a secondary structure in the Me-NPs/protein interaction (Durán et al., 2010). Studies developed by Vigneshwaran et al. (2007) showed that the FTIR spectrum of the synthesis of Ag-NPs by *A. niger* revealed bands at 3280 and 2924 cm^{-1}, corresponding to the stretching vibrations of primary and secondary amines, respectively. Additionally, two bands were observed at 1379 and 1033 cm^{-1} corresponding at the C-N stretching vibrations of aromatic and aliphatic amines, respectively. Similar results were obtained by Hosseini et al. (2012) in the synthesis of copper sulfide nanoparticles by *F. oxysporum.* These results confirm the presence of protein in the Me-NPs synthesized by fungi. The X-ray diffraction allows evaluating the formation of Me-NPs demonstrating the crystalline nature, as well as the particle size.

Finally, the zeta potential and particle size distribution of Me-NPs are measured using a Zetasizer Nano. The zeta potential is a technique that determines the stability of nanoparticles electrostatic repulsion. Studies developed by Sadowski et al. (2008) demonstrated that Ag-NPs synthesized using *Penicillium* had a negative zeta potential with an isoelectric point below pH=2 at pH>8, it being thus determined that the nanoparticles are fairly stable due to electrostatic repulsion.

1.5.- Effect of reaction parameter in the synthesis of metal nanoparticles by fungi

In the area of nanotechnology the development of a protocol to synthesize metal nanoparticles with controlled of formation, particle size and morphology is the major challenge of synthesis. Studies conducted by Morones et al. (2005) demonstrated that the antimicrobial effect of Ag-NPs can be attributed mainly to their concentration, small size, monodispersity and highly specific surface areas. Under these conditions, the nanoparticles can interact directly with the microbial membranes of bacterial and fungal pathogens, thereby generating cell death (Durán et al., 2010).
Therefore, ascertaining the optimum value of reaction parameters in the synthesis of metal nanoparticles is important in antimicrobial activity. However, the studies of parameters that control the formation, size and morphology of the synthesis process have been conducted mainly with Ag and Au-NPs (Gericke and Pinches, 2006a, Gericke and Pinches, 2006b; Nayak et al., 2011), being the optimization of reaction parameter of synthesis of other metals rarely reported. Therefore, the review of reaction parameters is limited mainly at Ag and gold synthesis:

pH: The pH plays an important role during the optimization of a process that controls nanoparticle morphology. Gericke and Pinches (2006a) demonstrated that the initial pH is an important parameter in the synthesis of gold nanoparticles by *Verticillium luteoalbum.* The results showed that at pH 3 and 5 the gold nanoparticles were predominantly spherical and uniform in size with 10 nm in

diameter, whereas at pH 7 and 9 the size particle increased to 30 nm with various shapes such as triangles, hexagons, spheres and rods. A contrary effect was found by Nayak et al. (2011) in the synthesis of Ag nanoparticles by culture-filtrated of *P. purpurogenum.* At pH 4 and 5, polydisperse nanoparticles were found with an average size between 40 and 55 nm, whereas smaller particles were formed at pH 8 and 9 with an average particle size between 8 and 13 nm and a uniform shape. Similar results were obtained by Kathiresan et al. (2009) in silver nanoparticle production by *P. fellutanum.* Another study developed by Sanghi and Verma (2009) demonstrated that the synthesis of Ag nanoparticles by *C. versicolor* at pH 10 was more rapid than the culture at normal pH (5.6). Also, the nanoparticles synthesized at pH 10 were stable after three months.

Substrate concentration: The substrate concentration (concentration of metal ions) has been studied regarding the effect on the size and monodispersity of nanoparticles. Studies by Nayak et al. (2011) demonstrated that an increase in $AgNO_3$ concentration increases the formation of Ag-NPs by culture-filtrated of *P. purpurogenum.* At 5 mM $AgNO_3$ highly populated polydisperse nanoparticles were observed. However, highly monodisperse spherical nanoparticles of 8-10 nm size were obtained at a concentration of 1 mM $AgNO_3$. Gericke and Pinches (2006b) reached a similar conclusion in the synthesis of gold nanoparticles by *V. Luteoalbum*. The results showed that at Au concentrations of 250 and 500 mg L^{-1}, the nanoparticles were spherical and similar in size and morphology, whereas at 2500 mg L^{-1} nanoparticles of irregular morphology and particle aggregation were observed.

Temperature: The temperature can affect the size, morphology and reaction rate of nanoparticle formation. Fayaz et al. (2009) demonstrated that the average size of Ag-NPs synthesized by culture-filtrated of *T. viridae* decreases as the reaction temperature increases, whereas a decrease in reaction temperature results in increased particle size. These results were attributed to an increased reaction rate at a higher temperature. A contrary effect is produced in the synthesis of Au-NPs. Studies developed by Gericke and Pinches (2006b) showed that the particle size of Au nanoparticles synthesized by *V. luteoalbum* increased with the increase in temperature. However, this effect depended on the reaction time, with the particle size increases as the reaction time increased.

Reaction time: The reaction time influences the size and morphology of nanoparticles. Gericke and Pinches (2006b) determined that smaller nanoparticles with good monodispersivity were found at a reaction time of 1 h than at a longer reaction time (24 h). Sanghi and Verma (2009) demonstrated that the synthesis of Ag-NPs by *C. versicolor* under alkaline conditions reduced the reaction time for the formation of nanoparticles from 72 to 1 h.

Therefore, all the reaction parameters reviewed are possible key factors in the biogenic synthesis of metal nanoparticles with high antimicrobial activity.

1.6.- Antimicrobial properties of biogenic metal nanoparticles

In light of the increase in microorganisms resistant to multiple antibiotics and fungicides, a great deal of research has been aimed at developing new and effective cost-effective antimicrobial agents without resistance. In this context, the Ag-NPs and Cu-NPs have been studied with promising results. Ramyadevi et al. (2012) demonstrated that Cu-NPs had an inhibitory effect on human gram negative pathogenic bacteria such as *E. coli, Micrococus luteus, S. aureus, Klebsiella pneumonia* and *Pseudomonas aeruginosa.* It also exhibited an antifungal effect against *A. flavus, A. niger* and *Candida albicans.* The antimicrobial activity of Ag-NPs has been studied against diverse bacteria

such as *Staphylococcus* sp. (Fayaz et al., 2010, Jaidev et al., 2010), *Salmonella typhi* (Fayaz et al., 2010), *Bacillus* sp. (Jaidev et al., 2010), *E. coli* (Fayaz et al., 2010, Jaidev et al., 2010, Nithya et al., 2009), *Micrococcus luteus* (Fayaz et al., 2010), *Pseudomonas aeruginosa* (Nithya et al., 2009), among others. Likewise, the antimicrobial activity of Ag nanoparticles was tested against fungi such as *A. niger* (Jaidev et al., 2010) and *F. oxysporum* (Musarrat et al., 2010). The mechanism of action has been proposed by several authors. Lok et al. (2006) determined that a short exposure of Ag nanoparticles to *E. coli* resulted in an increase of cell membrane permeability and a massive loss of intracellular potassium, thereby generating the loss of cell viability. In the same way, Sondi and Salopek-Sondi (2004) treated *E. coli* with Ag-NPs and studied the effect on cell morphology using SEM microscopy. The bacterial cell showed aggregates composed of Ag-NPs and cell death, suggesting that Ag^+ binds to functional groups, resulting in protein denaturation. Ruparelia et al. (2008) determined that a similar mechanism of action is attributable to Cu-NPs. Silver and copper ions are released by the nanoparticles and these may attach to the negatively charged bacterial cell wall and generate their rupture, thereby leading to protein denaturation and cell death (Lin et al., 1998). The antimicrobial effect of nanoparticles depend of size particle and specific surface area of these, being higher the antimicrobial activity in particles with small size and high specific surface area due to that it can penetrate more facile the cell membranes and generate the cell death (Sondi and Salopek-Sondi 2004; Baker et al., 2005). In addition, the antimicrobial potency of nanoparticles is directly proportional to the concentration of nanoparticles in the solution. Sondi and Salopek-Sondi (2004) studied the antimicrobial effect of different concentrations of Ag nanoparticles (10, 50 and 100 µg cm^3) on 10^7 *E. coli.* The results showed that a higher nanoparticle concentration decreased the growth of pathogen bacteria. However, these concentrations are considerably less than the antimicrobial effect of Me-NPs and metal salts because nanomolar concentrations are used in the case of nanoparticles and micromolar ranges are used in the case of metal salts (Durán et al., 2010).

1.7 Antimicrobial application of metal nanoparticles

Nanoparticles have a wide range of antimicrobial applications in the field of medicine and agriculture. The application in medicine is based on the effectiveness of Me-NPs against many human pathogens including varied resistant bacteria. Ingle et al. (2008) reported that during the synthesis of Ag nanoparticles using *F. acuminatum* it was possible to obtain nanoparticles with a broad spectrum of antibacterial activity against different human pathogens, including multidrug resistant strains such as *S. aureus, S. typhi, S. epidermis* and *E. coli.* In this sense, the antimicrobial application of metal nanoparticles has been used in the production of sterile materials. Durán et al. (2007) studied the effect of incorporating Ag-NPs synthesized by *F. oxysporum* in cotton fabrics on the pathogenic bacterium *S. aureus*, a main cause of intrahospital infections. The results demonstrated the Ag-NPs exhibited a significant antibacterial activity against *S. aureus* (99.9% bacterial reduction).

Another application for Me-NPs is agriculture. Rickman et al. (1999) reported that nanotechnology could increase crop yields, minimizing the use of fertilizer and pesticides. Several studies have shown that Me-NPs have antifungal activity against plant pathogens such as *B. cinerea* (Oh et al., 2006; He et al., 2011), *P. expansum* (He et al., 2011) and *Raffaelea* sp. (Kim et al., 2009), demonstrating their high potential as a fungicide. In this context, the use of Me-NPs in replacing traditional fungicides is of great interest in crop protection. One field of application could be blueberry production, given that Chile is the world's largest producer of blueberries, harvesting a total of 120,121 tons/year of blueberries in 2011 (ODEPA, 2012). During blueberry production the stems, flowers and fruit are affected by *B. cinerea* and stems also are affected *F. oxysporum.* Both fungi could cause severe crop damage, generating large losses in blueberry production. Fungi are

currently controlled by the application of copper oxychloride, copper oxide and copper sulfate. However, the concentration used of theses fungicides can kill all of the plant tissue, risking injury to crop foliage and fruits. Therefore, the use of Cu-NPs and Ag-Nps could reduce this risk due to the nanomolar concentrations that are used in the case of nanoparticles.

1.8.- Hypothesis

Considering that:

- Fungi secrete proteins and enzymes that synthesized metal nanoparticles.
- Fungi isolated from forests in southern Chile have high production of protein and enzymes.
- Metal nanoparticles synthesized by fungi have been reported as antimicrobial agents against agent pathogens.

According to these statements, the following hypotheses are proposed:

I. The proteins/enzymes with reducing potential present in the mycelium-free extract of native white rot fungi will produce synthesis of metal nanoparticles (Ag, Au and Cu) with antimicrobial activity.

1.9.- General objective

I. To evaluate the synthesis of metal nanoparticles (Cu, Ag and Au) with antimicrobial activity by micelyum-free extract of Chilean native fungus.

1.9.1.-. Specific objectives

I. To select a fungal mycelium-free extract of native white rot fungus with better capacity for the synthesis of metal nanoparticles (Cu, Ag and Au).

II. To evaluate the synthesis of metal nanoparticles (Cu, Ag and Au) by oxidoreductase enzyme of a mycelium-free extract of native white rot fungus and to proposed a synthesis mechanism for their production.

III. To evaluate antibacterial activity of metal nanoparticles (Cu, Ag and Au) previously synthesized.

CHAPTER II: BIOGENIC SYNTHESIS OF METAL NANOPARTICLES (Cu, Ag AND Au) USING A MYCELIUM- FREE EXTRACT PREPARED FROM BIOMASS OF WHITE ROT FUNGUS

Extracellular biosynthesis of copper and copper oxide nanoparticles by *Stereum hirsutum* a native white rot fungus from Chilean forests. Journal of Nanomaterials Article ID 789089, 7 pages

Abstract

The fungi are known to be efficient secretors of extracellular proteins and enzymes capable of reacting with metals ions to synthesize metal nanoparticle with antimicrobial activity. In this context, the white rot fungi might have a high potential for synthesizing metal nanoparticles due to their high production of extracellular enzymes. Thus, the aim of this study was to select a fungal mycelium-free extract from white rot fungus with best capacity for the synthesis of metal nanoparticles (Cu, Ag and Au). In the first stage, the mycelium-free extract produced from biomass fungi of *Anthracophyllum discolor, Stereum hirsutum* and *Trametes versicolor* were evaluated for synthesized silver nanoparticles under acidic and alkaline condition from 1 mM of silver nitrate solution. After the selection of the better mycelium-free extract, it was used for synthesis and characterization of gold nanoparticles using a mycelium-free extract of white rot fungus in combination with 1 mM of $AuCl_4^-$ under acidic pH conditions. Finally, the synthesis of copper nanoparticle with mycelium-free extract of *S. hirsutum* and different salts metal ($CuCl_2$, $Cu(NO_3)_2$ and $CuSO_4$ at different pHs (5.0 and 9.0) were evaluated. The metal nanoparticles (Cu, Ag and Au-NP) formation were evaluated spectrophotometrically by UV-Vis (200-800 nm) for identifying the formation of plasmonic bands and characterized by electron microscopy TEM or/and SEM, determination of average size by DLS and Fourier transforms infrared spectroscopic (FTIR). Results demonstrated that the uses of mycelium-free extract of *S. hirsutum* were effective in the process of synthesis and formation of the different metal nanoparticles as silver, gold and copper/oxide copper nanoparticles, possibly being different the oxidation state of copper in the nanoparticles. As a general observation nanoparticles presented a quasi-spherical shape from the three metals used in the synthesis, observed from different techniques such as DLS and TEM results showed sizes smaller than 100 nm in the synthesis. The presence of amine groups attached to the silver and copper nanoparticles was confirmed by FTIR, suggesting that the release of extracellular protein by white rot fungi possibly performed the function of formation and stabilization of nanoparticles synthesized in aqueous medium. Additionally, SDS-PAGE profile of the proteins was developed in the fungal extract for determining the molecular weight of proteins that presumably involved in the synthesis and stabilization of metal nanoparticles. In the results of SDS-PAGE profiles of the proteins showed the presence of bands between 12 to 61 kDa, which could be engaging in the process of synthesis and stability of metal nanoparticles. These positive results increase the consciousness towards green chemistry and to the development of environmentally friendly technologies. In this specific case the use of white rot fungi for the synthesis of nanoparticles is a technology with great potential for development new products. However, the use of a fungal extract for the synthesis of metallic nanoparticles has the disadvantage of be a complex medium to determine a mechanism possible to explain the formation of the nanoparticles, since it is not possible to determine the molecules were as proteins, enzymes, sugars, organic acids and others who participated in the reduction and stabilization of the nanoparticles to be a complex mixture of different molecules previously mentioned.

2.1.- Introduction

Fungi are organisms which produce nanoparticles in extracellular way, due to the high secretion of proteins and enzymes that are involved in the reduction of metal ions for the nanoparticles formation (Narayanan et al., 2010). In the last decade, the technology of biogenic synthesizing metal nanoparticles using strains of white rot fungi has gained interest, but mainly the white rot fungus have been studied in bioremediation processes (Rubilar et al., 2007, 2008; Tortella et al., 2008; Acevedo et al., 2010; Palma et al., 2011; Behnood et al., 2013).

Currently, the use of white rot fungi for the production of metal nanoparticles (Me-NPs) are silver and gold nanoparticles (Ag-NPs and Au-NPs) mainly, and the most used fungi are *P. chrysosporium* (Vigneshwaran et al., 2006; Sanghi et al., 2011; Chen et al., 2013, 2014), *Shizophyllum commune* (Mashitua, and Chan, 2011; Chan et al., 2012b), *Schizophyllum radiatum* (Metuku et al., 2014; Krishna et al., 2015), *Pycnoporus sanguineus* (Chan et al., 2012a; Chan and Dom, 2013) and *Pleurotus sajor caju* (Nithya and Ragunathan, 2009; El-Batal et al., 2015). Recently was reported *Pleurotus sajor caju* in the synthesis of Au-NPs and applied in the decoration of industrial dyes, demonstrating the strong potential of this technology in the industry (El-Batal et al., 2015).

In relation to copper nanoparticles (Cu-NPS) not reports of the use of white rot fungi in the synthesis are presented, but information is limited to fungi such as *Penicillium* sp. and *F. oxysporum,* have been reported to synthesize copper oxide and Cu_2S nanoparticles from fungal extracts (Honary et al., 2012; Hosseini et al., 2012).

In this respect, studies developed by Sanghi et al. (2011) demonstrated that the laccase enzyme secreted by the white rot fungus *P. chrysosporium* is responsible for the extracellular formation of Au-NPs. In the same way, studies conducted by Sanghi and Verma (2009) demonstrated that the white rot fungus *C. versicolor* produced cadmium sulfide nanoparticles (CdS-NPs), where the thiol group of the fungal protein was the main one responsible for the synthesis of CdS-NPs. Prasad et al. (2010) suggested that a low pH environment might activate oxidase enzymes in the microorganisms due to a high oxidation potential, which would allow the Me-NPs formation. Moreover, Nithya and Ragunathan (2009) indicate that the protein released by the white rot fungus *Pleurotus sajor caju,* could be involved in the stabilization of nanoparticles.

Due to the non-pathogenic nature of white rot fungus, the application of this technology for production of Me-NPs with these fungi could be interesting alternative due to high biomass production and easy handling (Vigneshwaran et al., 2006, 2007, Metuku et al., 2015). In this context, the white rot fungi isolated from template forests in southern Chile might have a high potential for synthesizing Me-NPs due to their high production of extracellular enzymes such as laccase and peroxidases (Tortella et al., 2008; Rubilar et al., 2007). In addition, an extensive characterization of the nanoparticles is necessary to develop future biotechnological applications.

To achieve the objective of this study firstly, to select a fungal mycelium-free extract of a fungus strain with better capacity for the synthesis of Me-NPs (Cu, Ag and Au). The initial determination for the formation of Me-NPs are performed by UV-Visible spectrophotometer at a range of wavelength of 200-800 nm, determining the formation of surface plasmon bands. The morphology and crystallinity of Cu-NPs, Ag-NPs and Au-NPs have been studied by X-ray

diffraction. The size of the distributed Me-NPs were measured by using the principle of dynamic light scattering (DLS) and complemented by electron microscopes TEM and SEM. The participation of proteins in the synthesis process of Me-NPs was confirmed by Fourier transform infrared (FT-IR) spectroscopy .

2.2.- Methodology

2.2.1.- Chemicals:

$CuSO_4$, $Cu(NO_3)_2$ and $CuCl_2$ were used for the synthesis of copper/copper oxide nanoparticles, and $AgNO_3$ for the synthesis of silver nanoparticles and $HAuCl_4$ for the synthesis of gold nanoparticles.

2.2.2.- Microorganisms for synthesis of nanoparticles:

Native fungi from Southern Chile used were *A. discolor, S. hirsutum* and *T. versicolor* were obtained from the culture collection of the Environmental Biotechnology Laboratory of Universidad de La Frontera. The fungi were transferred from slant culture tubes (maintained at 4 °C and subcultured every 6 months) to malt extract agar (MEA) plates and incubated at 30 °C for 5-7 days before being used for inoculum preparation

2.2.3.- Preparation of fungal mycelium-free extract

Fungal inoculums was obtained by taking 5 plugs agar circular pieces (6 mm diameter) and transferred into 500 mL Erlenmeyer flasks with 100 mL of growth medium containing 15 g L^{-1} glucose, 5 gL^{-1} peptone and 2.5 gL^{-1} yeast extract at pH 5.5 and incubated for 15 days at 25ºC. Fungal biomass produced was filtered by filter paper grade 4 and washed thoroughly with sterilized deionized water. Then, approximately 8 g (wet weight) of fungal biomass was transferred into100 mL Erlenmeyer flasks containing 50 mL of sterilized deionized water and incubated in an orbital shaker (100 rpm) for 24 h at 25ºC.

2.2.4.- Synthesis of silver nanoparticles by fungal mycelium-free extract

The mycelium-free extract of *S. hisutum, T. versicolor* and *A. discolor* were adjusted to pH 5 and pH 9 with HCl and NaOH 0.1 M. Then, 50 mL mycelium-free extract were added into flasks of 100 mL and 0.5 mL $AgNO_3$ from a concentrated solution of 100 mM, were added to obtain a final concentration of 1 mM. The flasks were incubated in an orbital shaker for 72 h at 100 rpm and 25 °C in darkness. Controls only with mycelium-free extract or $AgNO_3$ were established for comparative effects. All the assays were run in triplicate.

In each flask, aliquots at 0, 12, 24, 48 and 72 h of reaction were taken periodically to evaluate the reduction of silver ions by measuring UV-Vis spectrum using a SpectronicGenesys GS. The mycelium-free extract with higher peak area and height of UV-Vis spectrum obtained for the reaction was selected for further studies.

2.2.5.- Synthesis of gold nanoparticles by fungal mycelium-free extract

The mycelium-free extract of S. hirsutum was used for synthesis of copper nanoparticles. 10 mL of each fungal extract was transferred into 50 mL amicon tubes and pH was adjusted at 5.0 and 9.0. Then, 0.25 mL of a concentrated solution (40 mM) of HAuCl4 was added separately to obtain a final concentration of 1mM. The flasks were incubated for 72 h at 200 rpm and 25 °C in the darkness.
In each amicon tubes, aliquots at 0, 12, 24, 48 and 72 h of reaction were removed periodically to evaluate the reduction of gold ions by measuring UV-Vis spectrophotometer (UV-1650 PC Shimadzu) at a range of wavelength of 200-800 nm.

2.2.6.- Synthesis of copper nanoparticles by fungal mycelium-free extract

The mycelium-free extract of *S. hirsutum* was used for synthesis of copper nanoparticles. 50 mL of each fungal extract was transferred into 100 mL Erlenmeyer flask and pH was adjusted 7.0 and 9.0. Then, 0.5 mL of a concentrated solution (100mM) of $CuCl_2$ was added separately to obtain a final concentration of 5 mM. The flasks were incubated for 72 h at 200 rpm and 25 °C in the darkness.

In each flask, aliquots at 0, 12, 24, 48 and 72 h of reaction were removed periodically to evaluate the reduction of silver ions by measuring UV-Vis spectrum using a SpectronicGenesys GS. The fungal mycelium-free extract with higher peak area and height of UV-Vis spectrum obtained for the reaction was selected for further studies.

2.2.7.- Characterization of Metal nanoparticles

2.2.7.1.- UV-Vis Spectroscopy

Preliminary silver nanoparticles were detected by UV-Vis spectrophotometer (UV-1650 PC Shimadzu) and SpectronicGenesys GS at a range of wavelength of 200-800 nm.

2.2.7.2- Fourier Transform Infrared Spectroscopy (FTIR)

Characterization of silver nanoparticles was carried out by FTIR using CARY 630 FTIR Agilent Technologies in the range 600 – 4000 cm^{-1}. FTIR reveals the biomolecules responsible for the reduction of silver ions and stabilization of Ag-NPs in the solution.

2.2.7.3.- X-Ray Diffraction (XRD) studies

XRD spectra was recorded on a Shimadzu XRD 7000 instrument, and depicted number of Bragg reflections indexed on the basis of the face centered cubic (FCC) structure of metallic silver.

2.2.7.4.- Particle size by Dynamic light scattering (DLS) and Potential Zeta analysis

The hydrodynamic diameter and zeta potential values of the produced silver nanoparticles were assessed with a Malvern Zetasizer Nanosystem (Worcestershire, UK). The aqueous suspension of the synthesized silver nanoparticles was filtered through a 0.22 μm syringe driven filter unit and the size of the distributed silver nanoparticles were measured by using the principle of dynamic light scattering (DLS) technique made in a Malvern ZetasizerNano series compact scattering spectrometer.

2.2.7.5.- Transmision Electron Microsocopy (TEM)

TEM images of the samples were obtained using a transmission electron microscope (model JEOL JEM 1200EX II), at a Filament; Tungsten Voltage, kV; 40-120kv. The elemental analysis was carried out in spectrum of energy dispersive X-ray technique.

2.2.7.6.- Scanning Electron Microscopy (SEM)

SEM micrograph was taken using a JEOL 6360LV instrument, 40kV. The samples were fixed with 2.5% glutaraldehyde overnight at room temperature followed by dehydration with gradient alcohol (10% to 95%) for 20 min and then in absolute alcohol for 2-5 min. The final specimen was prepared by coating the dehydrated sample with monolayer platinum for making the surface conducting

2.2.8.- Characterization of the proteins present in the fungal free-mycelium extract by SDS-PAGE analysis

The mycelium-free extract of *S. hirsutum*, silver nanoparticles and copper/copper oxides nanoparticles was analyzed further by one dimensional SDS-PAGE analysis (sodium dodecyl sulfate–polyacrylamide gel electrophoresis). Electrophoresis was performed using Bio-Rad Mini Protean gel system at a constant voltage of 100 kV for 120 min. After electrophoresis, the gel was stained with Coomassie Brilliant Blue dye and was observed in a gel imaging system. For estimating the molecular weight of proteins, stained molecular weight marker was run along with samples.

2.3.- Results and discussion

2.3.1.- Synthesis of silver nanoparticles using mycelium-free extract of white rot fungi

A preliminary study was performed for determining the ability of mycelium-free extract of white rot fungi for synthesized Me-NPs. The synthesis of Ag-NPs was carried out under acidic (pH 5.0) and alkaline (pH 9.0) conditions of mycelium-free extract of the fungi *A. discolor*, *S. hirsutum* and *T. versicolor*. In the first stage, the synthesis of Ag-NPs was evaluated preliminary by measuring the UV-Vis spectrum (Figure 2.1). In this sense, the formation of silver nanoparticles can be distinguished after the bioreduction of $AgNO_3$ with mycelium-free extract through visible observation of color change from yellow into brown. This bioreduction can be identified by UV-vis spectrum, due to that the surface plasmom absorption band for synthesis of Ag-NPs occurred between 400 and 420 nm. In this context, the spectrum of mycelium-free extract of *S. hirsutum* showed surface plasmom absorption band only under alkaline condition, which occurred at 400 nm, being the peak higher when the incubation time increases (Figure 2.1a and Figure 2.1d). Additionally, one band for both conditions was observed around 270 to 290 nm (Figure 2.1a). Similar results were obtained for *A. discolor* (Figure 2.1b and Figure 2.1e), but the intensity of band was lower than the intensity shown by *S. hirsutum.* A different response was observed for *T. versicolor*, where band between 270 and 290 nm were observed for both conditions but no band was detected around 400 nm (Figure 2.1c and Figure 2.1f), indicating that this strain produced no synthesis of Ag-NPs. Control without silver ions showed no change in color of the mycelium-free extract when it was incubated under the same conditions and the best peak intensity of absorbance was obtained in the alkaline pH condition, because synthesis of Ag-NPs is not possible under acidic conditions (Sanghi and Verma, 2009a; Durán et al., 2011).

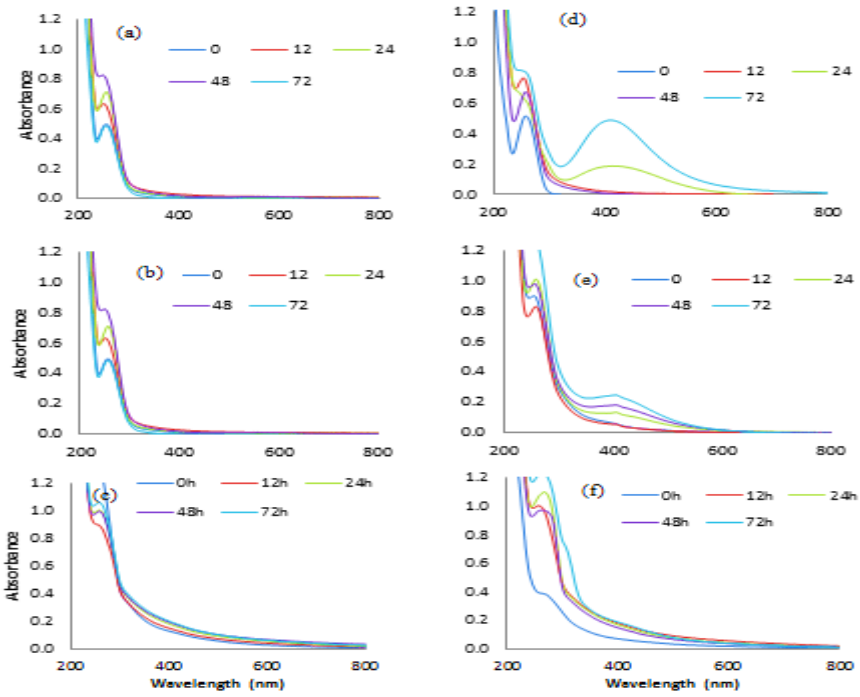

Figure 2.1 UV-Vis spectrum of silver nanoparticles synthesized from mycelium-free extract of *S. hirsutum* (a,d), *A. discolor* (b,e) *and T. versicolor* (c,f) in medium with 1 mM $AgNO_3$ for 72 hours of reaction at pH 5.0 (a, b and c) and pH 9.0 (d, e and f).

The formation of Ag-NPs can be primarily distinguished after the bioreduction of $AgNO_3$ with mycelium-free extract through visible observation of color change from yellow into brown, observer Figure 2.2.

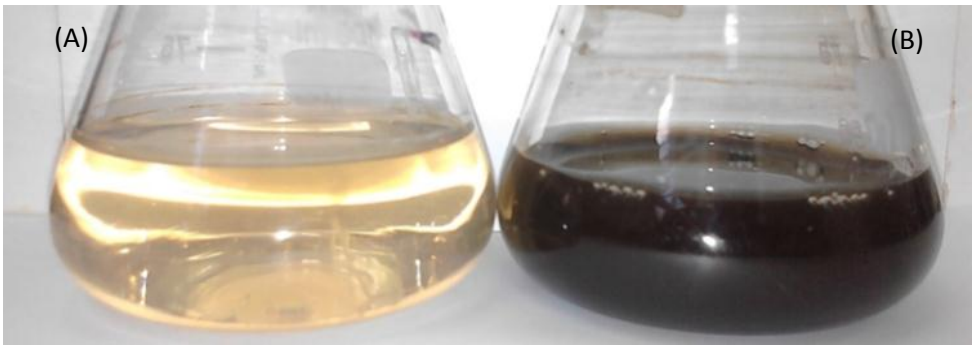

Figure 2.2 Visual identification of silver nanoparticles synthesized from fungal mycelium-free extract. (A) 0 h and (B) 72 h after reaction.

This bioreduction can be identified using UV-Vis spectrum, where the surface plasmon absorption band for synthesis of silver nanoparticles occurred between 400 and 420 nm, these results can be observed in Figure 2.3(a). A qualitative way of seeing the synthesis of Ag-NPs is to observe a change in color in mycelium-free extract solution combined with the silver salt from yellow into brown, this indicates the positive formation of Ag-NPs (Vigneshwaran et al., 2007; Du et al., 2015) and it is due to the excitation of surface plasmon vibrations in the nanoparticles (Mukherjee et al., 2002; Ahmad et al., 2003).

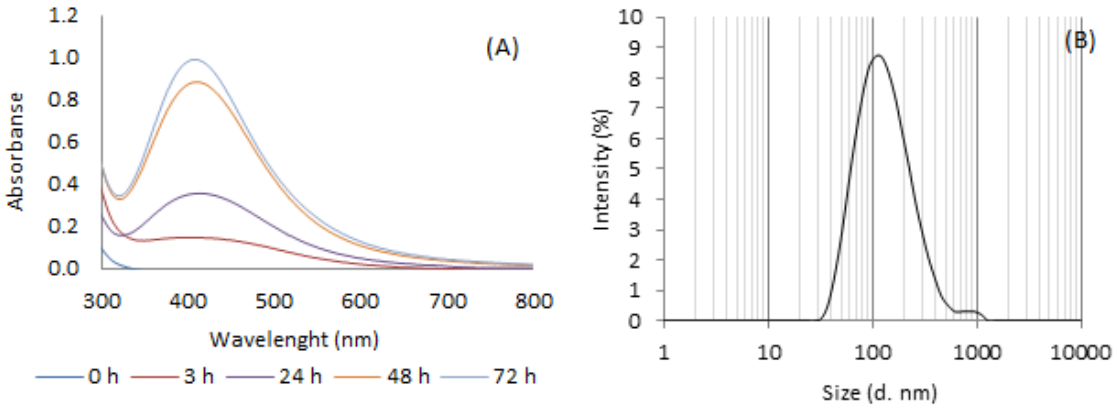

Figure 2.3 UV-Vis spectrum and (b) sizes distribution graph (Intensity) by Dynamic Light Scattering (DLS) of silver nanoparticles synthesized from mycelium-free extract of *S. hirsutum* with 1 mM of $AgNO_3$ for 72 h of reaction.

Furthermore, color change and the increase of absorbance of plasmon surface at 420 nm was indicative of the extracellular reduction of silver ions present in the solution (Ahmad et al., 2003; Durán et al., 2005), as it is shown in Figure 2.3A. It has been reported that for achieving an effective synthesis of Ag-NPs it is necessary to carry out the reduction reaction of metal ions under alkaline conditions (Kathiresan et al., 2009; Sanghi and Verma, 2009a). Complementary in Figure 2.3B was displayed the results of the size distribution by DLS of nanoparticles is obtained an average 94.3 nm in synthesis used mycelium-free extract at a concentration of 1

mM silver nitrate and Chan et al. (2013) also reported that the Ag-NPs were mainly spherical particles with average of 50 to 100 nm using *Pycnoporus sanguineus* in synthesis process. Additionally, the size of the nanoparticles is influenced by the concentration of the metal salt in solution, increasing the concentration of metal salt in solution involves increased nucleation processes.

Moreover, the results of the zeta potential in the aqueous solution had a higher variability in the results, the values range from -19 to -26 mV present with an average of -22.2 mV for the Ag-NPs produced in the mycelium-free extract and the resulting particles have good stability. Du et al. (2015) reported that the zeta potential of the nanoparticles is influenced by the pH of the solution and that this improvement in alkaline conditions increases the absolute value of the measurement thereby increasing the stability of the nanoparticle in solution. This report was reported to pH 9 a zeta potential of -13 mV and a pH 12 a zeta potential of -25.9 mV was obtained. The negative charge is indicative that the synthesized Ag-NPs obtained in alkaline pH conditions had negative surface charges and it was also observed a relationship between increasing pH and decreasing size of the resulting nanoparticles to pH 12 averaging about 60 nm in diameter was obtained (Du et al., 2015). Figure 2.4 shows the images obtained through TEM (a, b) and SEM (c,d) microscopies of nanoparticles using fungal extract of *S. hirsutum* synthesized. Clearly it is showed that well dispersed and spherical shape distribution of Ag-NPs prepared with mycelium-free extract was obtained. Besides, this spectroscopy shows stability in the nanoparticles therefore, there was no evidence of flocculation of the nanoparticles.

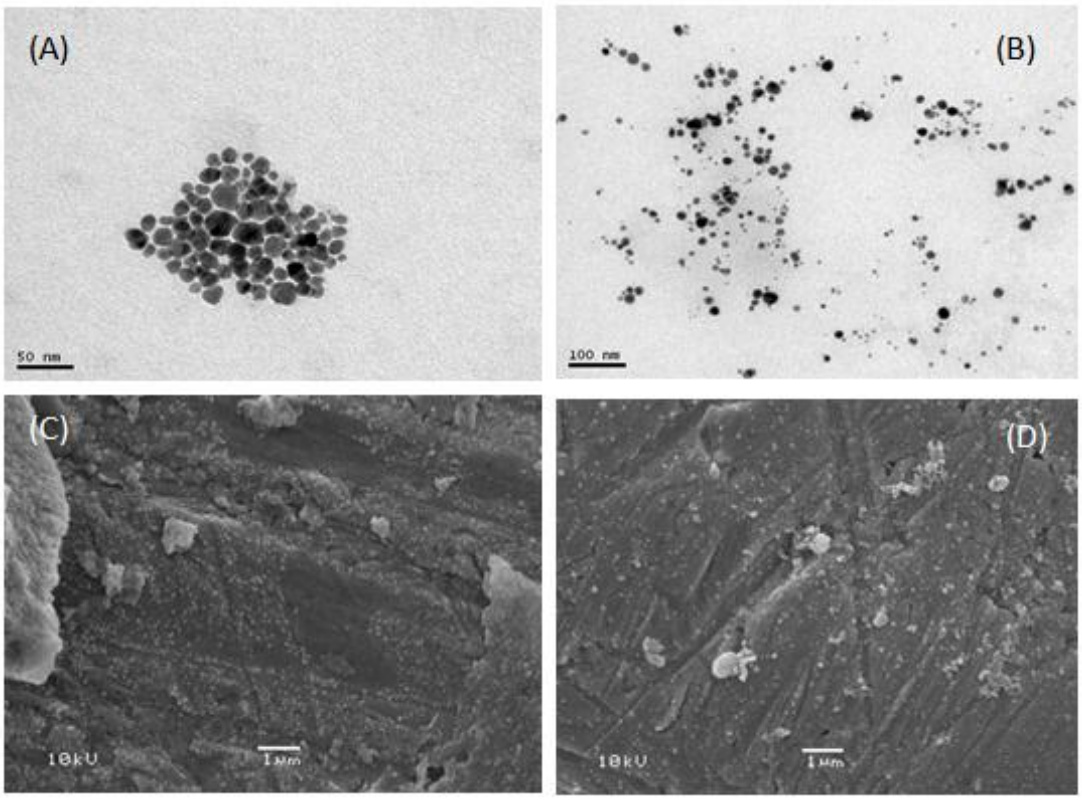

Figure 2.4 (A, B) Transmission Electron Microscopy (TEM) and (C, D) Scanning electron microscopy (SEM) images of silver nanoparticles synthesized in fungal mycelium-free extract produced using *S. hirsutum*.

The morphology of the Ag-NPs mainly been reported as spherical in the biological synthesis, but and rarely triangular, hexagonal and other shapes, this was mainly observed through the use TEM microscopy (Ahmad et al., 2003; Sanghi and Verma, 2009; Du et al., 2015). Figure 2.5 are presented results of scanning pattern of the resulting X-ray diffraction (XRD) (Figure 2.5A) and results of spectrum for Fourier transform infrared spectroscopic (Figure 2.5B). Samples were lyophilized and then were analyzed by FTIR to identify possible interactions between silver and biomolecules present in the mycelium-free extract. The results of FTIR spectrum obtained for Ag-NPs synthesized using fungal mycelium-free extract produced by *S. hirsutum* was presented in Figure 2.5B.

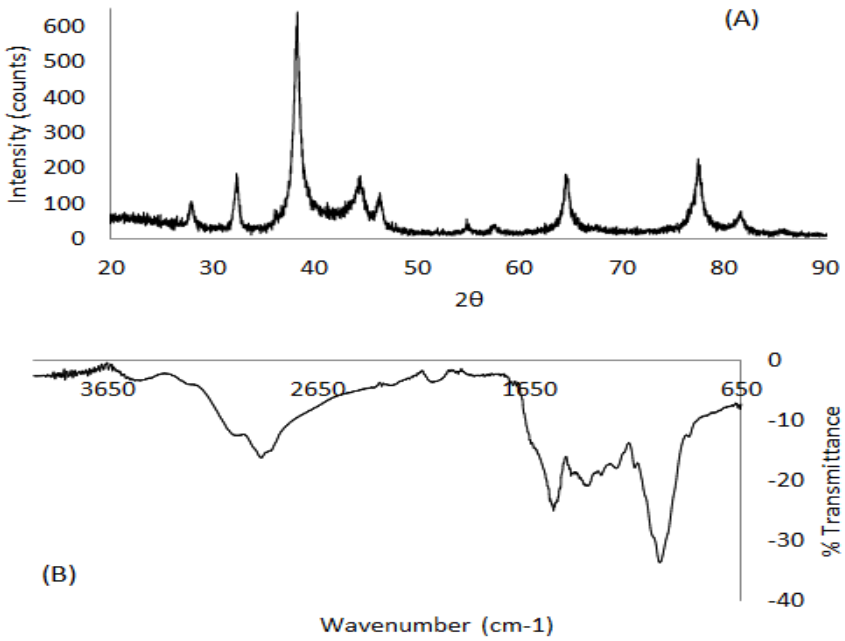

Figure 2.5 (A) Scanning pattern of the resulting X-ray diffraction and (B) spectrum for Fourier transform infrared spectroscopic (FTIR) for the silver nanoparticles synthesized from mycelium-free extract of *S. hirsutum*.

The results of the samples the following peaks in the spectrum for the bands 773, 829, 1041, 1244, 1307, 1388, 1540, 1640, 2114, 2322, 2928, 3047 and 3503 cm^{-1}. On the other hand, samples were lyophilized and then are analyzed by XDR (Figure 2.5A), the results of the diffraction pattern of X-rays obtained for the extracellularAg-NPs showed four intense peaks in the spectrum of 2θ values ranging from 20 to 90 degrees. The results of the XRD scan spectroscopy showed the following diffractions at 28.88°, 32.28°, 38.24°, 44.40°, 46.30°, 54.80°, 57.62°, 77.44° and 81.64° degrees of 2θ. The pattern of XRD exhibited intense peaks for fungal mycelium-free extract this pattern shows the presence of Ag^0 obtained in the reduction of Ag^+. Diffractions points at 38.24°, 44.40°, 64.74° and 77.44° degrees of 2θ can be indexed to the (111), (200), (220) and (311) planes of the face center cubic (FCC) structure of silver nanoparticles (Mukherjee et al., 2008; Feng et al., 2010). Morever, in the FTIR spectra obtained with the synthesized nanoparticle bands 1640 cm^{-1} and 1540 cm^{-1} type movements corresponding to bending vibrations (Vigneshwaran et al., 2007; Basavaraja et al., 2008; Shaligram et al., 2009), Chan et al., (2013) reported the same band synthesis of Ag-NPs used in the synthesis of white rot fungi. In the FTIR spectra obtained with the synthesized nanoparticle

bands found in the region of 3280 and 2924 cm^{-1}, these are reported as type movements of stretching vibrations in primary and secondary amines (Vigneshwaran et al., 2007, Chan et al., 2013), others report bands 1640 and 1540 cm^{-1} type movements corresponding to bending vibrations (Vigneshwaran et al., 2007; Basavaraja et al., 2008; Shaligram et al., 2009). The bands near 1029 cm^{-1} are reported as C-N stretching vibrations of aromatic and aliphatic amines (Shaligram et al., 2009), another band of interest is 1243 and 1244 cm^{-1} which is designated for bending vibration movements in amines I and III (Hosseini et al., 2012).

Finally, synthesis of Ag-NPs by fungi is more advantageous in comparison with other microorganisms, because the use of fungal strains provides a high generation of extracellular proteins and easy separation of biomass/supernatant by simple filtration. Moreover, various organic compounds in the supernatant are produced by fungal exudates necessary for synthesis (Sastry et al., 2003). Information about synthesis of different types of nanoparticles by white rot fungi is very limited, and at present, synthesis of Ag (Nithya et al., 2009; Sanghi and Verma, 2009ab; Chan et al., 2012, Chan et al., 2013). The specific mechanisms, by which nanoparticles are formed during their synthesis mediated by fungal strains, are not clear so far. It has been reported that reduction could be due to the NADH-dependent reductase by Durán et al., (2005) using *F. oxysporum* and Jain et al., (2011) using a inespecific enzyme and protein in the mechanism, but the overall observation and results obtained observations and results obtained confirms the presence of protein in the samples of Ag-NPs. This evidence suggests that the release of extracellular protein by white rot fungi possibly performed the function of formation and stabilization of nanoparticles synthesized in aqueous medium, but it has the limitation of only delivering general information about the involvement of proteins in the process of formation of the nanoparticles

2.3.2.- Synthesis of gold nanoparticles using fungal extract-free mycelium

The fungal filtrate with the addition of gold ions a rapid changed to purple color on completion of the reaction with gold ions for 72 h occurred uunder acidic pH conditions (Mukherjee et al., 2002; Sanghi et al., 2011; El-Batal et al., 2015). In the results of basic pH condition it was not possible to obtain the synthesis of Au-NPs. In the Figure 2.6 was observing visual identification of Au-NPs by color change in reaction solution. The appearance of a purple color in solution suggested the formation of Au-NPs (Soni and Prakash, 2012).

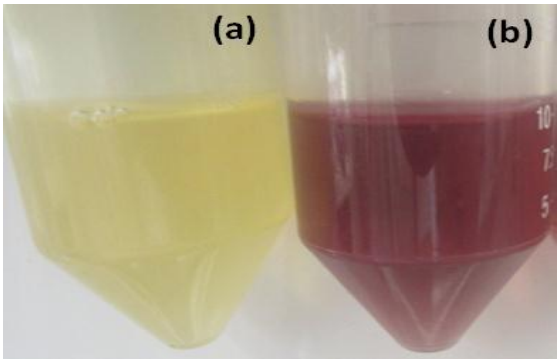

Figure 2.6 Gold nanoparticles synthesized from mycelium-free extract in reaction with $AuCl_4^-$ ions 1 mM. The (a) mycelium-free extract without $AuCl_4^-$ and (b) mycelium-free extract with $AuCl_4^-$.

In Figure 2.7 results are presented of UV-Vis spectrum of fungi *S. hirsutum* exhibited maximum absorption spectra between 540 to 560 nm. The strong surface plasmon resonance centered at 540-560 nm clearly increases in intensity with time. The solution was extremely stable, with no evidence of flocculation of the particles for three months after reaction. UV-Vis spectra in low wavelength region recorded from the reaction medium exhibited an absorption band at 265 nm and it was attributed to aromatic amino acids of proteins. It is well known that the absorption band at 265 nm arises due to electronic excitations in tryptophan and tyrosine residues in the proteins. This observation indicates the release of proteins into solution by *S. hirsutum* suggests a possible mechanism for the reduction of the metal ions present in the solution. It was previously suggested by Sanghi et al., (2011) in the biogenic Au-NPs from *P. chrysosporium* laccase levels are substantially important in the fungal media. Then, the experimental conditions were very favorable for the extracellular formation of nanoparticles in this fungal filtrate.

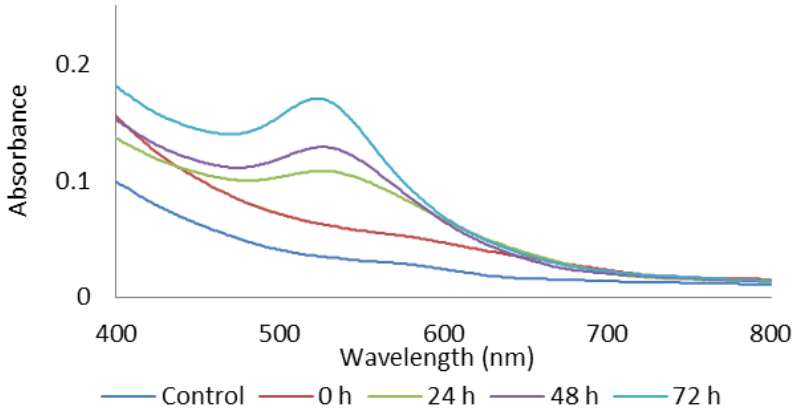

Figure 2. 7 UV-Vis absorption spectra of synthesis of gold nanoparticles using fungal mycelium-free extract (a) from *S. hirsutum*.

In Figure 2.8 is show the results obtained size distribution graph (Figure 2.8a) and X-ray diffraction pattern (Figure 2.8b). The XDR pattern spectrum of Au-NPs shows intense peaks in the spectrum of 2θ values ranging from 10 to 90. The results of the XRD scan spectroscopy showed the following values 21.11°, 27.40°, 31.74°, 38.20°, 45.54°, 56.48°, 64.50°, 66.72°, 75.30° and 84.22° degrees of 2θ, the presence of intense peaks at 38°, 45°, 65° and 75° degrees of 2θ corresponding to gold nanocrystals, which correspond to the (111), (200), (220) and (311) (Ahmad et al., 2003; Shankar et al, 2004). The lack of any peaks resembling metal or metal oxide other than for pure gold in the diffraction data confirmed the purity of the synthesized Au-NPs. An identical XRD pattern with the strain *F. oxysporum* (Ahmad et al., 2003) was observed. The data of DLS analyses supported that the average size of the synthesized nanoparticles around 100 nm and 0.3 PDI value (by intensity) and the obtained single peak indicated that the quality of the synthesized Au-NPs is good for both strains. The value of zeta potential of the nanoparticles from *S. hirsutum* such as -34.3 mV with a single peak signified that the presence of repulsion among the synthesized nanoparticles is present. *Aspergillus niger* strain exhibited zeta potential of -19.01 mV in Au-NPs of extracellular synthesis (Bhambure et al., 2009).

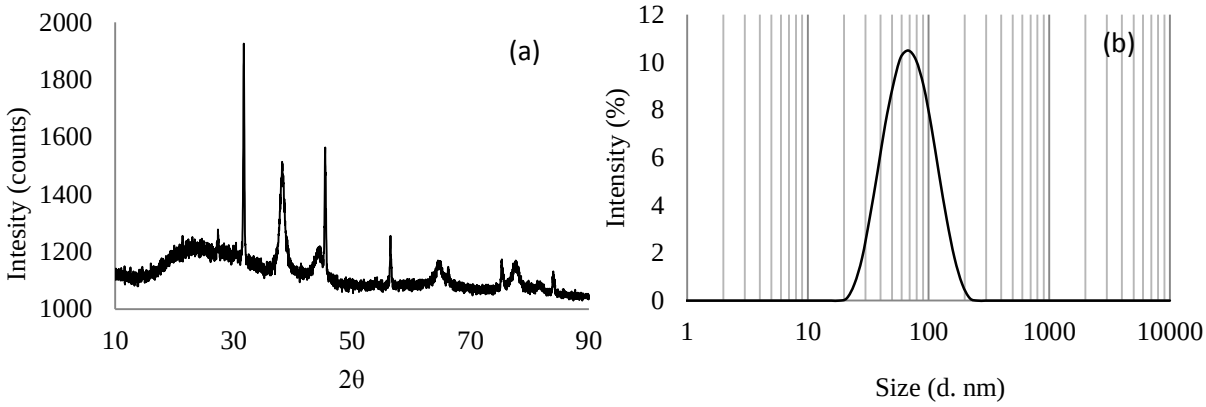

Figure 2. 8 Dynamic Light Scattering (DLS) sizes distribution graph (Intensity) and X-ray diffraction pattern of gold nanoparticles using fungal mycelium-free extract from white rot fungus**.**

Figure 2.9 shows the TEM micrograph recorded from the Au-NPs obtained using mycelium-free extract. In cases the nanoparticles were not in direct contact even with in the aggregates, indicating stabilization of the nanoparticles by a capping agent. The shape of the gold nanoparticle is spherical in both cases. At present, there are various reports and studies which state that Me-NPs produced by fungi are stabilized by fungal protein through the use FTIR (Jaidev et al., 2010; Basavaraja et al., 2008; Mukherjee et al., 2002), but few studies have established molecular weights for the proteins involved in the synthesis reaction of biogenic nanoparticles (Mukherjee et al., 2002; Jain et al., 2011; Rodrigues et al., 2013).

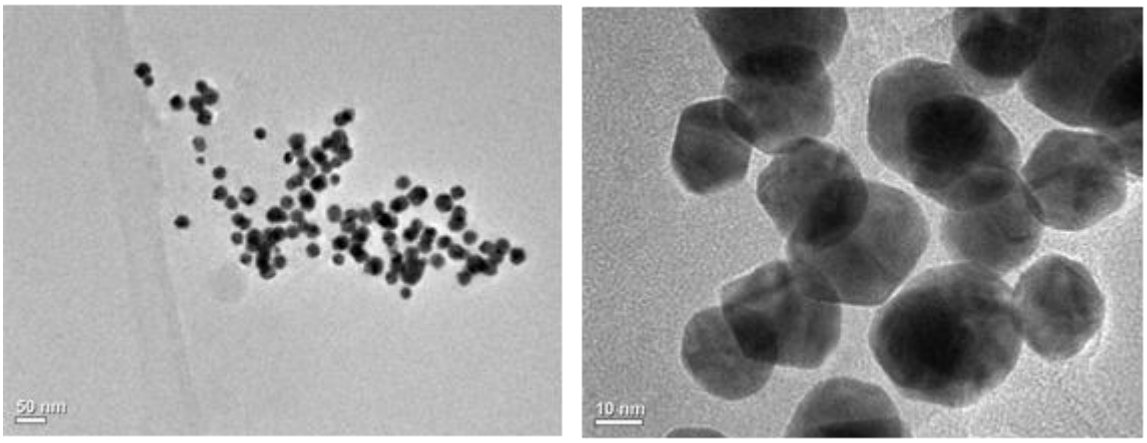

Figure 2. 9 TEM micrograph of gold nanoparticles produced using fungal mycelium-free extract Transmission Electron Micrograph (TEM) for gold nanoparticles (1 mM $HAuCL_4$) produced by white rot fungi mycelium-free extract

2.3.3.- Synthesis of copper nanoparticles using fungal mycelium-free extract

The synthesis of copper nanoparticles by mycelium-free extract of *S. hirsutum* was carried out with $CuCl_2$, $Cu(NO_3)_2$ and $CuSO_4$ as substrate at a concentration of 5 mM and different pHs (5.0, 7.0 and 9.0). The UV-Vis spectral analysis of synthesis of Cu-NPs synthesized with $CuCl_2$ at different pH is shown in Figure 2.10. At pH 5.0 no band of spectrum was observed during all incubation time (Figure 2.10). However, in the extract with pH 7.0 and 9.0 a peak of absorbance

between 590 and 630 nm was observed (Figure 2.10b y 2.10c), being the peak of absorbance higher in the extract with pH 9.0. Additionally, with pH 7.0, an increase of peak at higher incubation time was observed, being higher on 7 days (Figure 2.10b). In the spectrum at pH 9.0 the highest peak intensity was on the 5th day, whereas the intensity on the 7th day of incubation, changed to a peak from 600 to 680 nm was observed (Figure 2.1c).

The UV-Vis spectral analysis of synthesis of c Cu-NPs synthesized with $Cu(NO_3)_2$ at different pH. At pH 5.0 no bands were observed in the spectrum. However, the extract with pH 7.0 and 9.0 shows a band with weak intensity between 670 and 700 nm and under both conditions the highest peak was detected on the 5th day of incubation. Finally, the UV-Vis spectrum of Cu-NPs synthesized using in solution $CuSO_4$ at different pHs. At pH 5 similar results to the obtained with the others two copper salts evaluated were observed. However a positive response was observed at pH 7.0 and 9.0 for $CuSO_4$ copper salt. The bands in the extract with pH 7.0 were detected between 680 and 720 nm, whereas those bands in the extract with pH 9.0 were identified between 680 and 710 nm until the 5th day of incubation and 600 nm on the 7th day of incubation.

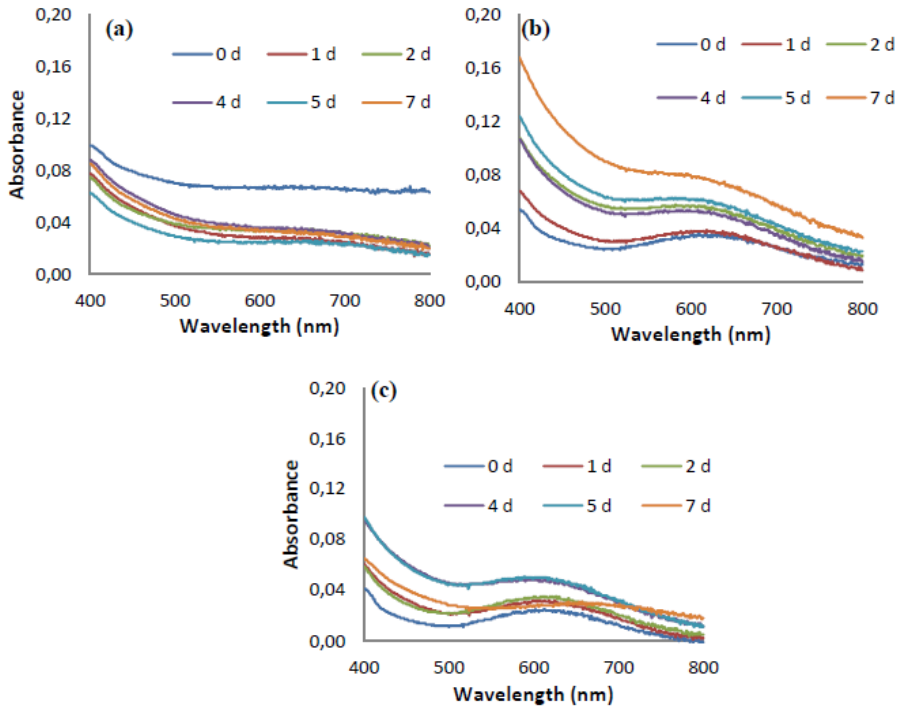

Figure 2. 10 Copper nanoparticles synthesis using $CuCl_2$ mediated by protein *S. hirsutum* in medium with 5 mM for 7 days of reaction. Figures correspond to $CuCl_2$ copper salt at different pH in the reaction solution at pH 5.0(a), pH 7.0(b) and pH 9.0(c).

Results that can see from Figure 2.11 (a, b) shows the TEM images and Figure 2.11(c) FTIR analysis. The TEM shows the effective formation of Cu-NPs synthesized using fungal extract of *S. hirsutum* a concentration of 5 mM at pH 9 after 7 days of incubation. The Cu-NPs show a spherical shape and monodispersity size. In addition, in Figure 2.11(a) and 2.11(b) TEM images show the nanoparticles embedded in the polymer. The synthesis of copper or copper oxide nanoparticles (Cu/CuO-NPs) can present different plasmon resonance peaks, being around 580 and 630 nm for Cu/CuO-NPs, respectively (Honary et al., 2012; Hasan et al., 2008). Besides,

the conversion of Cu-NPs into CuO-NPs is possible (Hasan et al., 2008). This conversion can be observed when shifts in the absorbance peak appear over time during the synthesis of Cu-NPs.

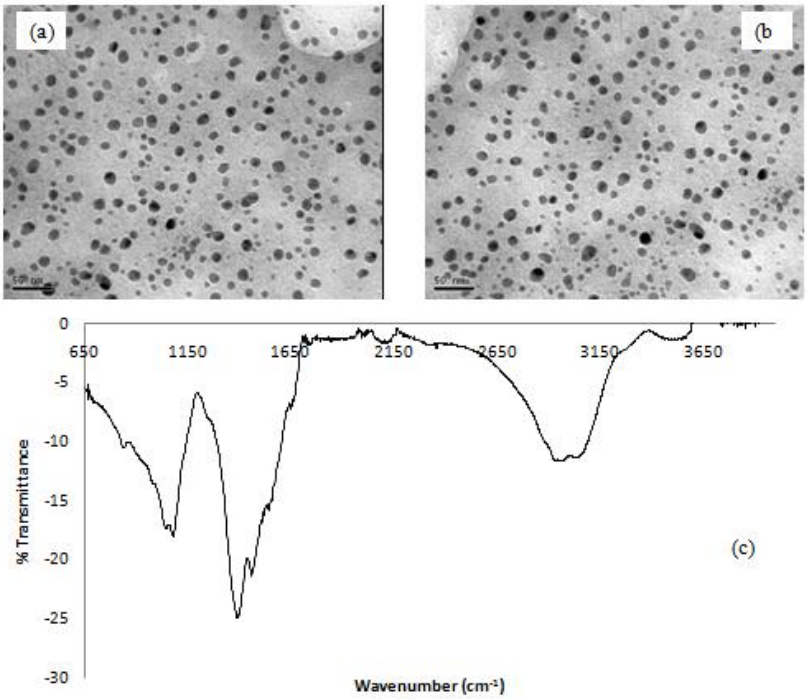

Figure 2. 11 Transmission electron microscopy (TEM) (a,b) and Fourier transform infrared spectroscopic (FTIR) (c) of copper nanoparticles produced by protein present in fungal extract of *S. hirsutum* at 7 days incubation (pH 9.0). Copper/copper oxide nanoparticles synthesis by *S. hirsutum* in medium with 5 mM $CuCl_2$ to alkaline conditions

Furthermore, the results of FTIR spectrum of the Cu/CuO-NPs are displayed in Figure 2.11(c), where bands at 835, 1076, 1387, 1457, 1539, 1646, 2091, 2114 and 3026 cm^{-1} were observed. In the FTIR spectra obtained with the synthesized nanoparticle bands found in the region of 3280 and 2924 cm^{-1}, these are reported as type movements of stretching vibrations in primary and secondary amides (Vigneshwaran et al., 2007, Chan et al., 2013), others report bands 1640 and 1540 cm^{-1} type movements corresponding to bending vibrations (Vigneshwaran et al., 2007; Basavaraja et al., 2008; Shaligram et al., 2009), another band of interest is 1243 and 1244 cm^{-1} which is designated for bending vibration movements in amides I and III (Hosseini et al., 2012). Another band is 1076 cm^{-1} corresponding to bending vibration movements in amides II, it was reported by Hosseini et al., (2012) in the synthesis of CuS nanoparticles; moreover, Chan et al. (2013) reported the same band synthesis of Ag-NPs used in the synthesis of white rot fungi. This evidence suggests that the release of extracellular protein by white rot fungi possibly performed the function of formation and stabilization of nanoparticles synthesized in aqueous medium (Vigneshwaran et al., 2007; Basavaraja et al., 2008; Shaligram et al., 2009).

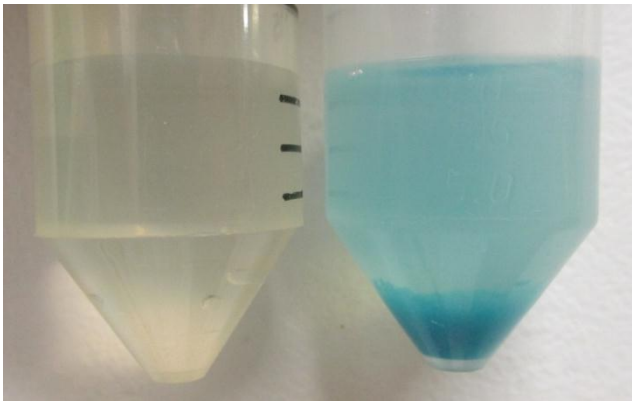

Figure 2. 12 Copper/copper oxides nanoparticles synthesized from fungal mycelium-free extract of *S. hirsutum* and formation of biopolymer in solution of reaction.

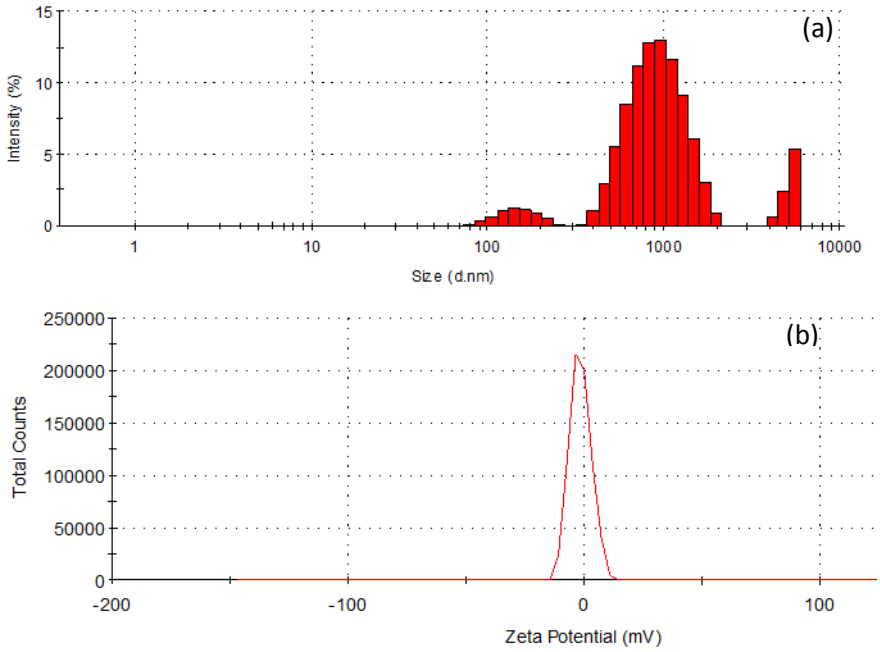

Figure 2. 13 (a) Dynamic Light Scattering (DLS) sizes distribution graph (Intensity) and (b) Zeta Potential for copper oxides nanoparticles synthesized from fungal extract-free mycelium of *S. hirsutum* using $CuCl_2$ in solution for alkaline conditions (pH 9.0).

The use of copper or copper derivatives in the biogenic synthesis of nanoparticles using fungal strains has only been reported using $CuSO_4$ copper salt (Hosseini et al., 2012, Honary et al., 2012) and not comparative studies have been performed using other copper salts such as $CuCl_2$ and $Cu(NO_3)_2$ with other fungal strains. Another aspect on which the results differ from the existing reports based on the use of fungal strains, is the change in coloration of yellow into brown in the reaction solution (Hosseini et al., 2012; Honary et al., 2012), but the experimental results showed a change in the coloration of yellow color to a light blue-green in solution resulting in formation of copper nanoparticles, results that can be seen in Figure 2.12. Moreover, it is reported that the particles of copper/copper oxide synthesized mainly present spherical forms (Guajardo et al., 2012, Gopalakrishsnan et al., 2012, Hosseini et al., 2012). The particles obtained during synthesis using copper salts showed a greater size which corresponds by definition to a nanoparticle. As shown in Figure 2.13(a) particles showed a distribution of its

larger size than 1000 nm by measuring applied by DLS and in relation to their zeta potential (Figure 2.13b) a value close to zero is observed.

In XRD analysis was carried out (Figure 2.14) and the sample produced by *S. hirsutum* showed the powder X-ray diffractometry pattern reported for copper or/and copper oxide, it can be seen that the sample prepared nanoparticles, shows the presence of two indices of monoclinic crystal phase, cupric oxide (CuO) and cubic cuprous oxide (Cu_2O). The positions of the peaks with values of 29.4°, 36.8°, 42.1°, 61.9° and 77.6° degrees of 2θ are indexed as (110), (111), (200), (220) and (222) planes have been reported for CuO (Abboud et al., 2014). In addition, peaks with values of 32.8°, 35.9°, 39.1°, 46.3°, 49.1°, 52.9°, 58.7°, 66.6°, 68.3°, 72.6° and 75.5° degrees of 2θ can be assigned to (-111) (002), (111), (-112), (-202), (020), (202), (-311), (113), (311) and (400) planes correspond to the values of Cu_2O monoclinic phase reported in the literature (Abboud et al., 2014; Volanti et al 2008). The percentage amount of copper incorporated into the Cu-NPs was characterized by XRF and it was obtained 5% of incorporation of metal into the nanoparticles, and approximately 94% is related to the organic component of the nanoparticles (CHON) and another group of elements less than 1%.

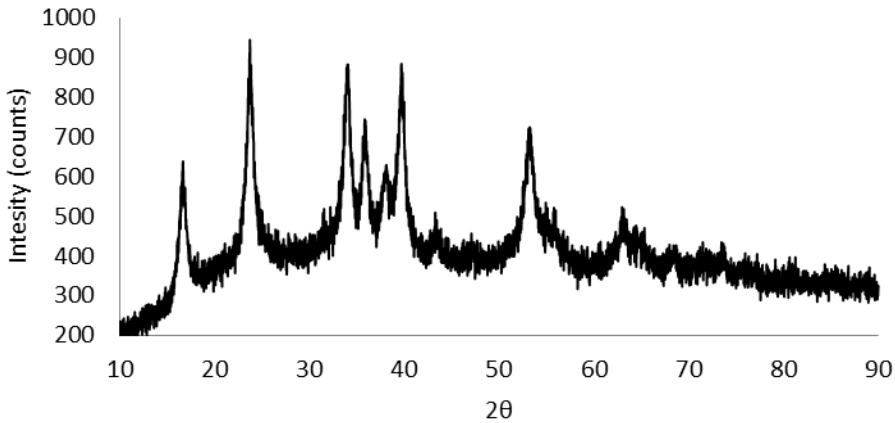

Figure 2. 14 XRD pattern of produced copper/copper oxide nanoparticles using fungal mycelium-free extract of *S. hirsutum.*

Currently, the synthesis of Cu/CuO-NPs is possible because several chemical and physical methods can be used (Ramyadevi et al., 2012; Chen et al., 2007). Moreover, their synthesis has been reported mainly using plant extracts such as soy (Guajardo et al., 2010), *Aloe barbadensis* Miller (Gunalan et al., 2012) and *Tridax procumbens* leaf extract (Gopalakrishsnan et al., 2012). In this context, a limited number of reports have been published, where different fungal strains have been evaluated for the synthesis of Cu-NPs. Fungi, as *Penicillium* strains and *F. oxysporum*, have been reported in the synthesis of CuO-NPs and Cu_2S-NPs (Honary et al., 2012; Hosseini et al., 2012). However, the use of white rot fungi in the synthesis of Cu-NPs has not been reported yet.

On the other hand, an effective synthesis of Cu-NPs under alkaline conditions using plant extracts has been reported (Guajardo et al., 2010). Similar results are indicated in this study using mycelium-free extract of white rot fungi for the synthesis of Cu-NPs. However, the opposite has been reported by Honary et al., (2012) and Hosseini et al., (2012), where synthesis of Cu-NPs occurred under acidic condition in the reaction solution (pH 5.0 to 5.5). The

synthesis of Cu/CuO-NPs can present different plasmon resonance peaks, being around 580 and 630 nm for Cu/CuO-NPs, respectively (Honary et al., 2012; Hasan et al., 2008). Besides, the conversion of Cu-NPs into CuO-NPs is possible (Hasan et al., 2008). This conversion can be observed when shifts in the absorbance peak appear over time during the synthesis of Cu-NPs. The use of copper or copper derivatives in the synthesis of nanoparticles using fungal strains has only been reported using $CuSO_4$ copper salt (Hosseini et al., 2012, Honary et al., 2012) and not comparative studies have been performed using other copper salts such as $CuCl_2$ and $Cu(NO_3)_2$ with other fungal strains. Another aspect on which the results differ from the existing reports based on the use of fungal strains, is the change in coloration of yellow into brown in the reaction solution (Hosseini et al., 2012; Honary et al., 2012), but the experimental results showed a change in the coloration of yellow color to a light blue-green in solution resulting in formation of Cu-NPs Moreover, it is reported that the particles of copper/copper oxide synthesized mainly present spherical forms (Guajardo et al., 2012, Gopalakrishsnan et al., 2012, Hosseini et al., 2012). Finally, it is important to note that the synthesis of Me-NPs using different fungal extracts is really clean and friendly environmental (Honary et al., 2012; Durán et al., 2005; Ahmad et al., 2003). In addition, metals, such as copper, have been shown to have a better antimicrobial activity with synthesized Cu-NPs than in nanoparticles synthesized in synthetic form (Lee et al., 2013).

2.3.4.- Characterization of the proteins present in the fungal mycelium-free extract by SDS-PAGE analysis

The results of SDS-PAGE analysis can be seen in Figure 2.15, four runs were observed, description from left to right, within the 15% polyacrylamide gel corresponding to the sample of silver nanoparticles (Ag-NP) lyophilized produced in the fungal extract of *S. hirsutum*, second-run the gel has the lyophilized fungal mycelium-free extract (extract), followed by copper/copper oxide nanoparticles (Cu-NP), and finally, the molecular weight marker (MW). The result showed the presence of two bands with molecular weights of 12.9 and 15.9 kDa in three runs of electrophoresis gel (Ag-NP / extract / Cu-NP) in study. In addition to the run, the gel corresponding to Ag-NP was observed additional three bands with molecular weights of 36.9, 47.4 and 61.0 kDa molecular weight, and some less intense bands were also observed in Cu-NP. Moreover, in the runs of Ag-NP and extract were observed the presence of bands with higher molecular weight, but the molecular weights were not determined due to the initial preparation of the gel. The election of molecular weights study initially was based on reports in the literature with a region of interest between 25 to 60 kDa.

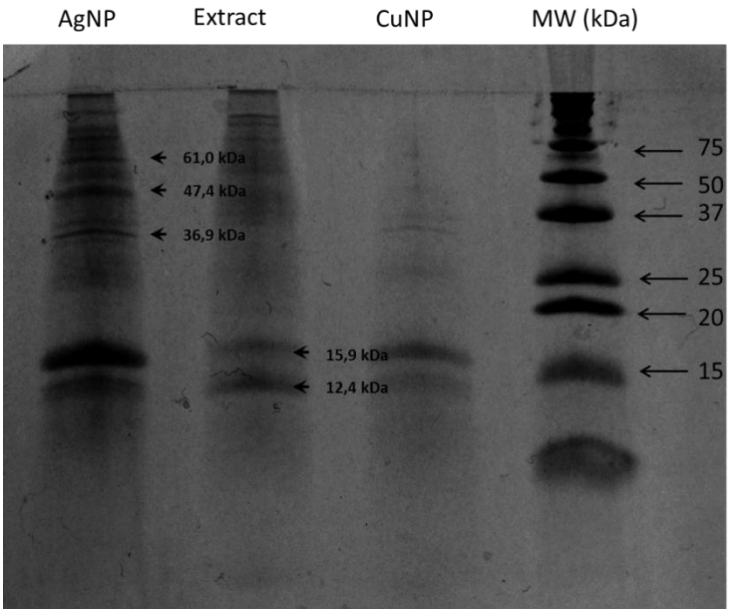

Figure 2. 15 SDS-PAGE analysis of AgNP (a), Mycelium-free Extract (b) and Cu/Cu_xO_x-NP. Protein was stained with Coomassie brilliant blue. Arrows indicate between 12 to 61 kDa proteins. Molecular weight marker (MW).

As can be seen in Figure 2.16 reported by Jain et al. (2011) suggested that a possible mechanism for synthesis of Ag nanoparticle by *Asperguillus flavus* could occur in two steps: the former step involves a 32 kDa protein, which may be the reductase enzyme secreted by the fungus and the latter step involves 35 kDa proteins, which are bound with nanoparticles and confer stability to nanoparticles.

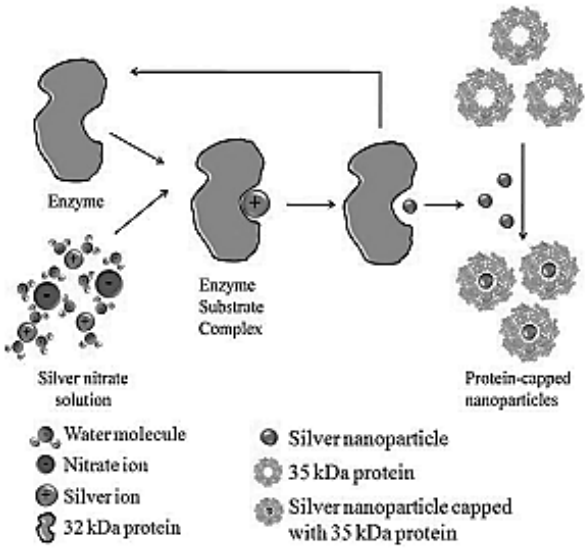

Figure 2. 16 Hypothetical mechanism showing the role of extracellular proteins in the synthesis of silver nanoparticles (Adapted of Nanoscale, Jain et al., 2011).

Similar results obtained by Bansal et al. (2004) demonstrated that the synthesis of zirconia nanoparticles by *F. oxysporium* showed two extracellular proteins with molecular weight of 24 and 28 kDa. Results are consistent with those reported by Mukherjee et al. (2002), who stated that at least four proteins of molecular masses between 66 and 10 kDa can be found in the crop extract produced by *F. oxysporium.*

A more recent study by Rodrigues et al. (2013) was used in the extracellular synthesis of Ag-NPs by *Aspergillus tubingensis* and *Bionectria ochroleuca*, this study reported that participating in the synthesis of proteins Ag-NPs are of a higher molecular weight in a range that varies between 75-328 kDa using *A. tubingensis*. For *B. ochroleuca* proteins were reported 25, 30, 44 and 49 kDa in the synthesis of Ag-NPs, but were informed bands of molecular weights in fungal extract in a range of 70-174 kDa. On the other hand, for the synthesis of Me-NPs, some researchers have mentioned that other organic molecule proteins are also involved in the synthesis of nanoparticles, thus, Balaji et al. (2009) postulated that proteins, polysaccharides and organic acid exudates are capable of producing crystals of different shapes, but with a growth directed to the production of spherical nanoparticles. In this context, Nithya and Ragunathan (2009) indicate that the protein released by the white rot fungus, could be involved in the stabilization of nanoparticles.

Currently, reports on the characterization and identification of enzymes and proteins involved in the biogenic synthesis using fungal extracts merely refer to the possible ranges of molecular weights. Furthermore, all reports only show that for each fungal species used there are varied ranges of possible proteins involved in the synthesis and stabilization of nanoparticle biogenic origin.

2.4.- Conclusions

Some general, promising conclusions may be derived for the results here obtained:

- In the selection process of fungal extract for the synthesis of different metal nanoparticles, the use of mycelium-free extract from *S. hirsutum* showed the best results in alkaline pH conditions compared with that observed for *A. discolor* and *T. versicolor* in the first selection. The use of fungal mycelium-free extract from native white rot fungi *S. hirsutum* was effective for the synthesis of silver, gold and copper/copper oxides nanoparticles formed from silver nitrate, chloroauric acid and copper chloride in aqueous solution, respectively.

- The presence of amine groups attached to the silver, gold, an copper/copper oxide nanoparticles was confirmed by FTIR, suggesting that the release of extracellular protein by white rot fungus of *S hirsutum* possibly performed the function of formation and stabilization of metal nanoparticles synthesized from mycelium-free extract. But, based on the results of gel electrophoresis of this study and those reported currently it is not possible to determine and/or identify the participant proteins contained in the mycelium-free extract involved in the synthesis and stabilization of biogenic nanoparticles.

- These positive results increase the consciousness towards green chemistry and to the development of environmentally friendly technologies. In this specific case the use of white rot fungi for the synthesis of nanoparticles is a technology with great potential for development new products. However, the use of a fungal extract for the synthesis of metal nanoparticles has the disadvantage of be a complex medium to determine a mechanism possible to explain the formation of the nanoparticles, since it is not possible to determine the molecules were as proteins, enzymes, sugars, organic acids and others who participated in the reduction and stabilization of the nanoparticles to be a complex mixture of different molecules previously mentioned.

CHAPTER III "SYNTHESIS AND CHARACTERIZATION OF METAL NANOPARTICLE (Cu, Ag and Au) PRODUCED BY LACCASE SEMI-PURIFIED AND LACCASE PURIFIED OBTAINED OF A WHITE ROT FUNGUS

Biogenic silver nanoparticles associated with silver chloride nanoparticles (Ag@AgCl) produced by laccase from *Trametes versicolor*. SpringerPlus 2014 3: 645

Abstract

White rot fungi isolated from template forests in southern Chile might have a high potential for synthesizing metal nanoparticles due to their high production of extracellular proteins and enzymes such as laccase and peroxidases. For the development of this new study used an oxido-reductase enzyme produced by a white rot fungus in the process of synthesis of the nanoparticles. The aim of this study was to evaluate the synthesis of metal nanoparticles (Cu, Ag and Au) by oxido-reductase enzyme of a mycelium-free extract of native white rot fungus and to propose a synthesis mechanism for their production. Laccase semi-purified and laccase purified (commercial) from *Trametes versicolor* were evaluated for synthesized metal (Ag, Au and Cu) nanoparticles. Laccase enzyme used for synthesis of metal nanoparticle was obtained from commercial purified laccase of *T. versicolor* $\geq$ 0.5 U/mg and them it was used a concentrated extract semi-purified laccase enzyme from *T. versicolor* with 2200 UL^{-1}. For synthesis of metal nanoparticle in aqueous solution of semi-purified and purified laccase enzyme in combination with the metal salt silver nitrate, gold tetrachloride and copper chloride under stirring 300 rpm and controlled temperature 50 °C were used. At the first step of the synthesis the metal nanoparticle formations were evaluated spectrophotometrically by UV-Vis (200-800 nm). The formation of different metal nanoparticles were characterized by hydrodynamic diameter by dynamic light scattering and zeta potential values of the produced silver, gold and copper nanoparticles were assessed and the reduction of metal ions was characterized by x-ray spectrophotometry (XRD). Furthermore, transmission electron microscope (TEM) model was used to observe the size and shape of the nanoparticles. The results showed that the laccase from white rot fungi (*T. versicolor*) had the potential to reduce metal ions of copper, silver and gold to form and stabilize metal nanoparticles of these metals. Through the XDR patterns were possible to identify the crystal structure of the different nanoparticles obtained for copper was possible to observe the formation of copper oxides nanoparticles. The presence of amine groups attached to the silver, gold and copper oxide nanoparticles was confirmed by FTIR, suggesting that the release of extracellular protein by white rot fungi possibly performed the function of formation and stabilization of nanoparticles synthesized in aqueous medium. Finally, the biogenic synthesis of metal nanoparticles mediated by laccase is an eco-friendly technology and also a simple process of reproduce, this oxido-reductase enzyme showed the potential to act as a reducing and stabilizing agent in the process of formation and synthesis of the nanoparticles when combined with metal salts in the aqueous medium.

3.1 Introduction

Currently it is possible to find numerous methods for preparation of metallic nanoparticles that have been reported in the literature for metals such as gold (Mukherjee et al., 2013), silver (Durán et al., 2014), iron oxides (Bharde et al., 2006), zinc oxide (Jain et al., 2013), titanium (Bansal et al., 2005) and copper (Lee et al., 2008), being studied and used in various nanotechnology applications related to food, cosmetics and medicine. According to Narayanan et al. (2010) there has been an increasing awareness towards green chemistry and biological processes that have led to develop nanoparticle synthesis without generation of toxic products. In general terms, the biogenic synthesis or synthesis of metallic nanoparticles does not have a clear mechanism of synthesis, but the literature has demonstrated that the mechanism used for the formation of metal nanoparticles is the action of a large number of enzymes secreted by fungi in special reductases (Ahmad et al., 2003; Durán et al., 2005; Durán et al., 2007; Durán et al., 2011; Jain et al., 2011).

The use of white rot fungi for the production of metallic nanoparticles is a recent branch of research that has had extensive development in the last decade (Vigneshwaran et al., 2006; Sanghi et al., 2011; Chen et al., 2013, 2014; Krishna et al., 2015). In recent years, has been reported the synthesis of different types of nanoparticles such as gold nanoparticles using extract of *Pleurotus sajor caju* (El-Batal et al., 2015), silver nanoparticle from *Schizophyllum radiatum* (Metuku et al., 2014); silver nanoparticles nanoparticles in extracellular synthesis using *Pycnoporus sanguineus* (Chan and Don, 2014), CdS nanoparticles (quantum dots) by *Phanerochaete chrysosporium* (Chen et al., 2014) and copper nanoparticles using free-mycelium extract of *S. hirsutum* (Cuevas et al., 2015).

In the context of the biotechnological potential of white rot fungi and its enzymatic system, Sanghi et al. (2011) reported synthesis of gold nanoparticles by laccase and ligninase enzymes secreted by the white rot fungus *P. chrysosporium* participates in the extra- and intra-cellular formation, but mechanism to explain the participation of laccase and ligninase in the formation of the nanoparticles is not mentioned. In general terms, the synthesis of metal nanoparticles is produced mainly by reaction of reduction/oxidation of the metal ions, being the responsible protein or enzymes of reduction of metal compounds that form nanoparticles. Similarly, an extract with presence of laccase from *Paraconiothyrium variabile* was used for the production of gold nanoparticles, but was to raise the temperature to 70 °C to obtain the formation of nanoparticles (Faramarzi and Forootanfar 2011).

In this context, white rot fungi isolated from temperate forests in southern Chile have potential for synthesizing metal nanoparticles due to their high production of extracellular protein and enzymes, such as laccase and peroxidases (Tortella et al., 2008; Rubilar et al., 2008; Acevedo et al., 2010), The aim of this study was to evaluate the synthesis of metal nanoparticles (Cu, Ag and Au) by oxido-reductase enzyme of a mycelium-free extract of native white rot fungus and to propose a synthesis mechanism for their production. The synthesis of silver, gold and copper nanoparticles were performed using semi-purified and purified of laccase enzyme from *Trametes versicolor*, a white rot fungus, as well as to characterize the nanoparticles by electronic microscopy, analysis of the distribution of size and shape by DLS measurements and micrographics TEM, stability of the nanoparticles by Zeta potential and, finally, by FTIR and XRD.

3.2 Material and methods

3.2.1 Chemicals and biological materials

$CuCl_2$, $AgNO_3$ and $AuCl_4^-$ were used for the synthesis of copper, silver and gold nanoparticles, respectively was used as substrate for spectrophotometric determination of laccase activity for enzyme semipurified. The commercial purified laccase of *T. versicolor* was obtained from SIGMA-ALDRICH with a concentration of ≥ 0.5 U/mg.

3.2.2 Microorganisms for synthesis of nanoparticles

Native fungi from Southern Chile used was *T. versicolor* were obtained from the culture collection of the Environmental Biotechnology Laboratory of Universidad de La Frontera.

3.2.3.1 Laccase production and semi-purification

The purification followed the previously published results of Cordi et al. (2007). The culture filtrate from the procedure described above in the presence of 0.1 mmol L^{-1} of copper sulfate (through 380 meshes) was frozen, thawed, filtrated through a Millipore 0.45 mm membrane and lyophilized. A solution containing 2.0 g of lyophilized crude extract, 30 mL of citrate-phosphate and buffer (75 mmol L^{-1}, pH 5.0) was precipitated with 90% ammonium sulfate. The precipitate was eluted in a Sephacryl S-200 (Sigma) column using the same buffer as the mobile phase. The fractions containing laccase activity were collected. Another precipitation and elution was performed to eliminate the dark pigments from the filtrate. The fractions with laccase activity were collected and lyophilized. The lyophilized sample was resuspended in 10 mmol L^{-1} (pH 5.0) citrate-phosphate buffer and applied to a column containing DEAE cellulose (Leonowicz and Grzywnowicz 1981). The laccase was eluted with 10 mmol L^{-1} citrate-phosphate buffer, and a NaCl gradient of zero to 1 mol L^{-1} was applied. The fractions obtained were lyophilized and stored in a freezer.

3.2.3.2 Enzyme activity assay

The reagent syringaldazine was used as a substrate for the spectrophotometric determination of the laccase activity. Briefly: a reaction mixture containing 0.6 mL of enzymatic solution, 0.3 mL of citrate-phosphate buffer 0.05 M (pH 5.0) and 0.1 mL of syringaldazine (1 mM) at a final volume of 1 mL was mixed for 5 min, and the absorption at 525 nm ($\varepsilon 525$= 65000 $M^{-1}cm^{-1}$) was measured. One laccase unit was defined as the enzyme quantity needed to oxidize 1 mmol of syringaldazine min^{-1} per liter of total enzymatic solution.

3.2.4 Synthesis of metal nanoparticles

3.2.4.1 Synthesis of copper, silver and gold nanoparticles by semi-purified laccase from *T. versicolor*

The semi-purified laccase from *T. versicolor* was used for synthesis of nanoparticles, which was obtained from the Biological Chemistry Laboratory of Unversidade Estadual de Campinas (Brasil). In preparation were taken 0.9 mL of concentrated semi-purified of laccase (2300 UL^{-1} determined using syringaldazine) in 9.1 mL of deionized water to obtain a final concentration of 200 UL^{-1} and pH was adjusted at 5.0 and 9.0. Then, 0.1 mL of a concentrated solution (100 mM) of metal salt ($CuCl_2$, $AgNO_3$ and $HAuCl_4$) was added separately to obtain a final

concentration of 1 mM in solution. The flasks were incubated for 24 h at 300 rpm and 50 °C in darkness. In each flask, aliquots at 0, 1, 6 and 24 h of reaction were removed periodically to evaluate the reduction of copper ions by measuring UV-Vis spectrophotometer (UV-1650 PC Shimadzu) at a range of 200-800 nm wavelengths.

3.2.4.2 Synthesis of silver, gold and copper nanoparticles by purified commercial laccase enzyme from *T. versicolor*

Laccase enzyme used for synthesis of silver, gold and copper nanoparticle was obtained of laccase purified commercial ≥ 0.5 U/mg from *T. versicolor*. For the preparation of the enzyme concentrate broth laccase used 1000 mg with activity ≥ 0.5 U/mg that were diluted in 1 mL in deionized and sterile water, obtained a standard of 500 U/mL. For synthesis of silver, gold and copper nanoparticle the aqueous solution of laccase purified commercial was prepared by adding 50 U/mL in deionized and sterile water in 5 mL final volume. Then, the aqueous solution (corresponding to 50 U/mL of laccase activity) was added to aqueous solution with 1 mM concentration of the metal salts ($CuCl_2$, $AgNO_3$ and $AuCl_4^-$), followed by incubation of reaction mixtures in dark at 50 °C.

3.2.5-. Characterization of metal nanoparticles (Ag, Au and Cu -Np)

3.2.5.1 UV-Visible Spectroscopy

Preliminary metal nanoparticles were detected by UV-Vis spectrophotometer (UV-1650 PC Shimadzu) and Spectronic Genesys GS at a range of 200-800 nm wavelengths.

3.2.5.2 Fourier Transform Infrared Spectroscopy (FTIR)

Characterization of metal nanoparticles was carried out by FTIR using CARY 630 FTIR Agilent Technologies at the 600-4000cm^{-1} range. The FTIR revealed the biomolecules responsible for the reduction of silver ions and stabilization of copper nanoparticles in the solution depicted.

3.2.5.3 X-Ray Diffraction (XRD) Studies

XRD spectra was recorded on a Shimadzu XRD 7000 instrument, and depicted number of Bragg reflections indexed on the basis of the face centered cubic (FCC) structure of metallic of metal nanoparticles.

3.2.5.4 Particle size Dynamic light scattering (DLS) analysis and Potential Zeta

The hydrodynamic diameter and zeta potential values of the produced metal nanoparticles were assessed with a Malvern Zetasizer Nanosystem ZS90 (Worcestershire, UK). The aqueous suspension of the synthesized silver nanoparticles was filtered through a 0.22 µm syringe driven filter unit and the size of the distributed silver nanoparticles were measured by using the principle of dynamic light scattering (DLS) technique made in a Malvern ZetasizerNano series compact scattering spectrometer.

3.2.5.5 Transmision Electron Microsocopy (TEM)

TEM images of the samples were obtained using a transmission electron microscope (model JEOL JEM 1200EX II), at a Filament; Tungsten Voltage, kV; 40-120kv. The elemental analysis was carried out in spectrum of energy dispersive X-ray technique.

3.3 Results and discussion

3.3.1 The biogenic synthesis of metal nanoparticles (Cu, Ag and Au) by semi-purified laccase from the white rot fungus *T. versicolor*

This section presents the results obtained in the synthesis of silver, gold and copper nanoparticles using the semi-purified laccase enzyme from the white rot fungus *T. versicolor*, the characterization of the obtained nanoparticles was performed.

3.3.1.1 The biogenic synthesis of silver nanoparticles by semi-purified laccase from white rot fungus

In the present study, semi-purified laccase from *T. versicolor* was applied for the synthesis of silver nanoparticles, and the produced nanoparticles were characterized. The obtained results showed that the absorption are present in the Figure 3.1, the spectra UV-Vis of silver solution in presence of laccase enzyme indicated formation of silver nanoparticles due to presence of the surface plasmon absorption of the silver nanoparticles between 420 to 450 nm (Figure 3.1a). In general, the UV-Vis spectrum is an important, simple and fast technique more used for the verification of the formation of metal nanoparticles by surface plasmon resonance in the processes of biogenic synthesis (Nithya and Ragunathan 2009; Chan and Don 2013; Metuku et al., 2013; El-Batal et al., 2015).

On the other hand, in the structure of the enzyme laccase is characterized by the presence of site is mononuclear (one copper atom) denominated as type 1 or T1 and gives the blue color to the enzyme in solution and is characterized by an absorption band at 600 nm. In the Figure 3.1b at first adsorption band performed at the laccase enzyme copper T1 600 nm before starting the synthesis of the nanoparticles, absorption of laccase (T1 site) at 600 nm, after the addition of silver ions, disappeared completely with the concomitant loss of laccase activity.

The wide plasmonic band (between 420 to 450 nm) of this interaction of silver ions and laccase is most likely an indication other nanometric species is present different to Ag^0, in Figure 3.1a can observe the absorption band produced by the nanoparticles formed. In this context, previously Gopinath et al. (2013) reported a plasmonic band at 440-460 nm for silver chloride nanoparticles.

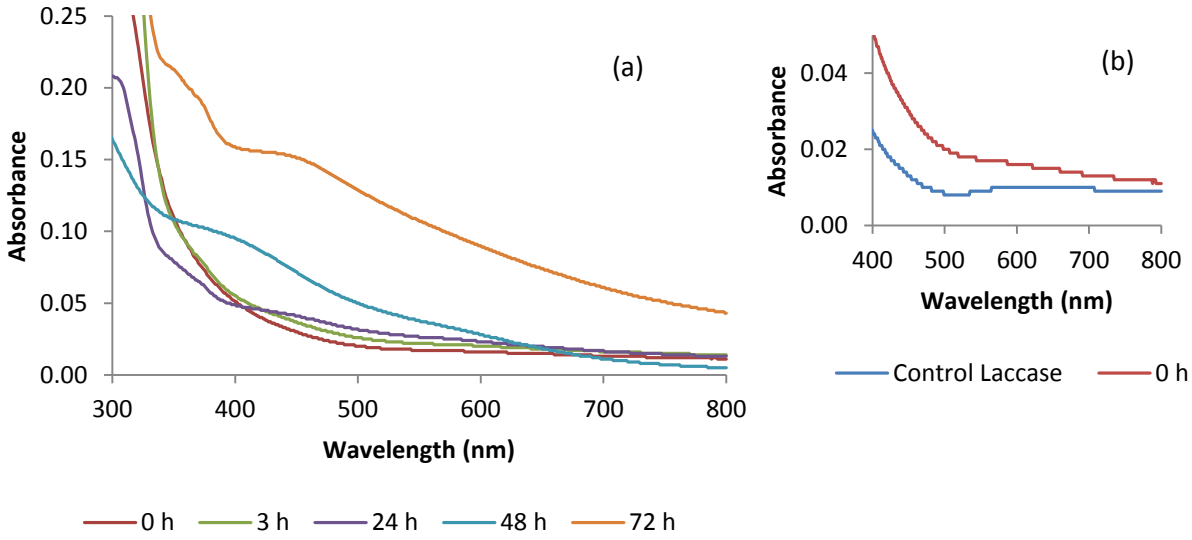

Figure 3. 1 (a) UV-Vis absorption spectra of silver nanoparticles using a 1 mM $AgNO_3$ solution in the presence of semi-purified laccase from *T. versicolor* (pH 9.0, 50 °C). (b) Absorption band characteristic of laccase enzyme copper T1 600 nm before starting the synthesis of the nanoparticles (before the addition of silver ions) and disappeared absorption band characteristic with loss of laccase activity (after the addition of silver ions).

In Figure 3.2 showed the results obtained in characterization by TEM, XRD, DLS and PZ of silver nanoparticles obtained in synthesis using semi-purified laccase. Figure 3.1(a) represents the effect of pH under acidic and alkaline conditions in the formation of silver nanoparticles; 50 °C was the temperature in which the silver nanoparticles were formed in the size range of 90 to 370 nm after 72 h incubation, the produced nanoparticles at showed particle size distributions around 90 nm at pH 9.0 best condition. Chan and Don (2013) reported the average size of silver nanoparticles produced from the culture supernatant of the white rot fungi *P. sanguineus* and *S. commune*, a particle average size of 50 and 65 nm diameters was observed respectively.

It was observed that there pH dependence of the size distribution, and at a lower pH, bigger sized nanoparticles were found (Gericke and Pinches, 2006) and increasing the temperature also yields smaller nanoparticles (Hosseiny et al., 2015). Also, in the Figure 3.2(b) shows the zeta potential of the silver nanoparticles formed at pH 9, which was -30.0 mV, showing a negative charge distribution of the silver nanoparticle surface. The results obtained using laccase in relation to the zeta potential were better in the same condition of pH 9.0 reported by Du et al. (2015) with a value of -13 mV, it is expected to higher value of greater stability of the particle in the solution.

Figure 3.2(c) shows an X-ray diffraction (XRD) pattern that is compatible with the cubic phase of Ag with diffractions points at 38°, 45°, 64.5°, 78° and 81.7° of 2θ, which can be indexed to the (111), (200), (220), (311) and (222) planes of the facet centered cubic (FCC) structure (JCPDS file: 65-871) that coexists with the cubic phase of AgCl at 27.9°, 32.3°, 46.3°, 55.0°, 57.6°, 67.6°, 74.6°,76.9°, and 85.7° and that corresponds to the (111), (200), (220), (311), (222), (400), (331), (420), and (422) planes (JCPDS file: 31-1238).

This XRD pattern clearly shows a pattern from the interaction of silver nanoparticles with silver ions (Ag complex) with chloride ions, the chloride ions likely came from the semi-purification

of laccase process. Represented nanocompex is normally as the Ag@AgCl product (Wang et al., 2008).

A transmission electron microscopy (TEM) image of silver nanoparticles is shown in Figure 1d. The micrographic image confirmed that the synthesized silver nanoparticles were spherical in shape, and the size of the particles was less than 100 nm, which correlates with DLS measurements.

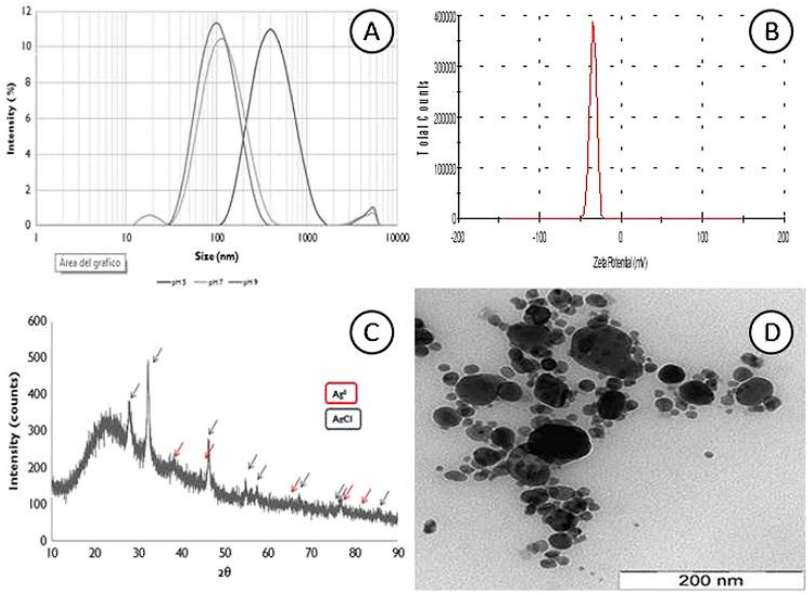

Figure 3. 2 Characterization of silver nanoparticles by (a) Dynamic Light Scattering, (b) Zeta potential, (c) XRD pattern and (d) Transmission electron micrograph (TEM) silver nanoparticles using semi-purified Laccase.

There are many possibilities for the reduction of silver, as previously described for other enzymes in the literature (Ahmad et al., 2003; Durán et al., 2005; Jain et al., 2011). Laccase from *T. versicolor* was used as the reductive agent for synthesis of silver nanoparticles. The production of silver nanoparticles by laccase is probably due to the presence of an ionic associated cysteine in its structure, as reducing group. The laccase from *T. versicolor* exhibits 1 cysteine associated with Cu1-Sγ (Cys-453) laccase and stabilized by a disulfide bridge to domain 1 (Cys-85–Cys-488), and a second disulfide bridge (Cys-117–Cys-205) connects domains 1 and 2 of laccase (Piontek et al., 2002).

In the case mechanism of laccase from *T. versicolor*, in the Figure 3.3 are presented two possible hypothetical mechanisms for synthesis using laccase: one involves cysteine associated to Cu type I (T1 site) (sulfhydryl group of cysteine) in the laccase structure reacting with the silver ion, reducing it to silver nanoparticles while the cysteine anion is oxidized to Cys-Cys in the laccase. The T1 site of laccase imparts a light blue color to the enzyme solutions and is characterized by a distinctly pronounced band of optic absorption at a wavelength of 600 nm (Morozova et al., 2007). This suggested mechanism is possible because, in this study, a rapid disappearance of the absorption band at approximately 600 nm in the *T. versicolor* laccase occurred after the addition of silver ions with complete inactivation of the enzyme (Figure 3.1).

The second possibility is the direct interaction of silver ions with the Cys-Cys moiety, generating silver nanoparticles, and the sulfhydryl moiety bound to silver nanoparticles as capped proteins (Cecil and McPhee 1957). This interaction of silver ions and the Cys-Cys moiety in the laccase domain most likely inactivates the enzyme, as observed in this study.

These hypothetical mechanisms no quinones or any other intermediates in this reaction of reduction by laccase were present, there were many possibilities as previously described for other enzymes in the literature. All data indicated cysteine as reductant.

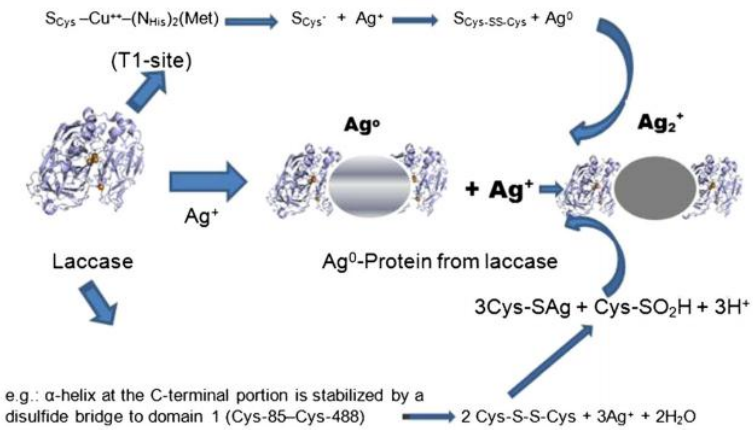

Figure 3. 3 Hypothetical mechanistic interactions between laccase from white rot fungus and silver ions producing silver nanoparticles.

Then, laccase from *T. versicolor*, a white rot fungi, showed reductive action for the synthesis of silver nanoparticles. Incubating the semi-purified laccase in the presence of silver ions reduced Ag^+ to Ag^0 and interaction with silver ions generated Ag@AgCl nanoparticles. The chloride ions most likely come from the semi-purification of laccase, as previously described.

3.1.2 Synthesis of copper nanoparticles used in the presence of semi-purified laccase from white rot fungus *T. versicolor*

In this section the results obtained for the synthesis of copper nanoparticles from use of laccase enzyme are presented. In Figure 3.4 the results of copper nanoparticle for color change (Figure 3.4a) and UV-Vis absorption spectra (Figure 3.4b) are presented. The solution containing the enzyme semi-purified laccase solution in combination with the initial copper chloride has a slightly bluish tinge the elapsed 24 h incubation with temperature that happens to have a dark yellow or light brown color indicating a positive reaction for the formation of copper nanoparticles in solution (Figure 3.4b), the synthesis of nanoparticles of copper oxides using biological extracts is characterized by obtaining a brown coloration in the solution (Honary et al., 2012).

The results observed in Figure 3.4b correspond to the UV-vis spectrum for copper nanoparticle synthesis using a semi-purified laccase. In the graph an increase can be seen in absorbance around 670 nm. The plasma band associated with zero-valent copper nanoparticles (Cu^0) present around 580 nm in the UV-Vis (Joshi et al., 1998), but the plasmonic bands when present on the 670 nm are associated to the formation of CuO-nanoparticles (Gunalan et al., 2012).

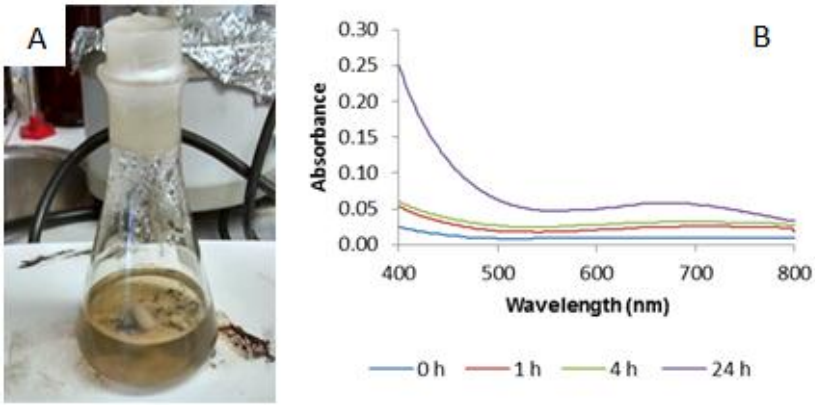

Figure 3. 4 (a) The visual identification for the formation of copper nanoparticles and (b) UV-Vis absorption spectra of nanoparticles using a 1 mM $CuCl_2$ solution in the presence of semi-purified laccase from *T. versicolor* (alkaline pH, 50 °C).

In Figure 3.5 the results obtained for the distribution of size and zeta potential of the particles resulting in the synthesis is presented. Figure 3.5a shows the size distribution determined by Dynamic light scattering (DLS) based on the intensity. In the results, a homogeneous sample shows a particle size that averages 94.3 nm in diameter with Poly Dispersity Index (PDI) with average values 0.23.

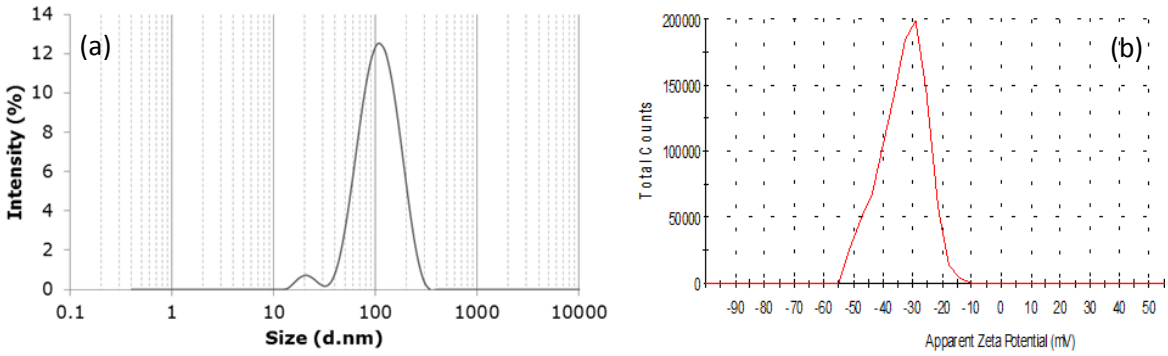

Figure 3. 5 (a) Dynamic Light Scattering (DLS) size distribution graph by Intensity and (b) Zeta potential (PZ) for copper nanoparticles using a 1 mM $CuCl_2$ solution in the presence of semi-purified laccase from *T. versicolor* (alkaline pH, 50 °C).

In Figure 3.5b presented the results for measurements of zeta potential of the nanoparticles showed an average value of -32.3 mV, the copper nanoparticle has a strong negative surface charge. Besides, the solution containing copper nanoparticles do not show the agglomerate formation or precipitate elapsed after two months of their initial training, which is related to a high stability of the nanoparticles obtained in the synthesis.

Figure 3.6 shows the results obtained for the diffraction pattern of X-rays, the following peaks with values of 27.3°, 31.7°, 45.4°, 56.4°, 66.1°, 75.2° and 83.9° degrees of 2θ can be seen. To confirm the crystalline properties of the nanoparticles, they were examined using XRD. Patterns of X-ray diffraction associated with the formation of copper nanoparticles are presented as

follows. The diffraction peaks are at 2θ of 43.5°, 50.6°, and 74.3° for elemental copper. However, the results of XRD pattern is not clear, as observed peaks associated with oxidized forms of copper. The peaks with values for 2θ of 29.4°, 36.8°, 42.1°, 61.9° and 77.6° were reported for CuO (Abboud et al., 2014) and peaks with values of 32.8 °, 35.9 °, 39.1 °, 46.3 °, 49.1 °, 52.9 °, 58.7 °, 66.6 °, 68.3 °, 72.6 ° and 75.5° degress of 2θ correspond to the values of Cu_2O (Volanti et al 2008; Abboud et al., 2014). Synthesis used semi-purified laccase as reducing and stabilizing agent that is a mix of nanoparticles of elemental copper and copper oxides.

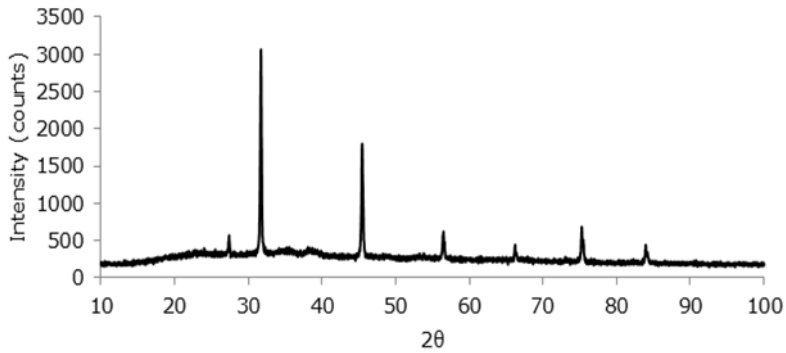

Figure 3. 6 The XRD pattern of produced copper nanoparticles using a 1 mM $CuCl_2$ solution in the presence of semi-purified laccase from *T. versicolor* (alkaline pH, 50 °C).

The results were quite consistent with those reported in biogenic processes: the obtained synthesis resulted in mixtures of nanoparticles of copper and copper oxides (Cuevas et al., 2015). Finally, we can indicate that it is possible to synthesize the metallic copper-based particles using the semi purified laccase enzyme as the reducing agent and the stabilizing agent in the formation reaction.

3.3.1.3 Synthesis of gold nanoparticles used in the presence of semi-purified laccase from the white rot fungus *T. versicolor*

The semi-purified laccase in exposure to aqueous solution of $AuCl_4^-$ ions 1 mM changed from light yellow to purple color after 24 h of reaction of fungal mycelium-free extract, indicating the formation of gold nanoparticles. Figure 3.7 are shown of results for UV-Vis absorption spectra (Figure 3.7a) and TEM micrograph of gold nanoparticles obtained using laccase semi-purified laccase enzyme (figure 3.7b). The UV-Vis spectra of semi-purified laccase enzyme from white rot fungus exhibited absorption band spectra around 580 nm (Figure 3.7a). These absorption bands confirm the synthesis of gold nanoparticles, because these color changes are typical of the surface plasmom resonance (SPR) of gold nanoparticles in solution (Mukherjee et al., 2001b; Gericke and Pinches, 2006a; Bhambure et al., 2009).

In this sense, the size range of gold nanoparticle synthesized by semi-purified laccase was 8 to 20 nm and nanoparticles formed presented a predominant spherical shape and a dispersal of its bounded size (Figure 3. 7b). The fungal extract produced from *Rhizopus oryzae* combined with chlorouric acid produces gold nanoparticles of 10 nm of mean diameter (Das et al., 2009).

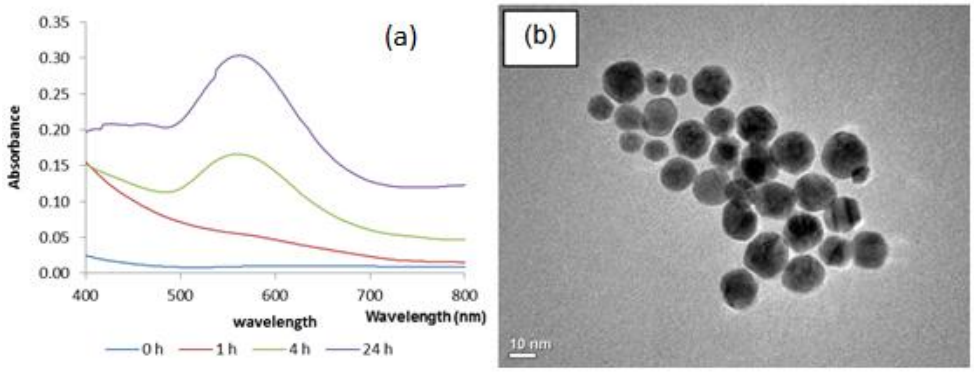

Figure 3. 7 (a) UV-Vis absorption spectra and (b) Transmission electron micrograph (TEM) of gold nanoparticles using $AuCl_4$- ions 1 mM with semi-purified laccase in solution from *T. versicolor.*

The XDR pattern spectrum of gold nanoparticles shows intense peaks in the spectrum of 2θ values ranging from 10 to 90. In Figure 3.8 the results obtained are presented (a) XRD patter and (b) Potential Zeta of gold nanoparticles. The results of the XRD scan spectroscopy showed the following values 21.11°, 27.40°, 31.74°, 38.20°, 45.54°, 56.48°, 64.50°, 66.72°, 75.30° and 84.22° degrees of 2θ (Figure 3.8a), the presence of intense peaks at 38°, 45°, 65°and 75° degrees of 2θ corresponding to gold nanocrystals, which correspond to the (111), (200), (220) and (311) (Ahmad et al., 2003; Shankar et al, 2004).

The lack of any peak resembling metal or metal oxide other than for pure gold in the diffraction data confirmed the purity of the synthesized gold nanoparticles. Identical XRD patterns with the strain *F. oxysporum* (Ahmad et al., 2003) were observed. In Figure 3.8(b) is observed value of zeta potential of the nanoparticles was -34.3 mV with a single peak signifying that the presence of repulsion among the synthesized nanoparticles was present. Similar result was reported by Gholami-Shabani et al. (2015) synthesis of gold nanoparticles with a zeta potential of -30 mV produced from a concentrated extract of sulfite reductase. Additionally, gold nanoparticles showed strong antifungal activity toward a wide range of human pathogenic fungi.

The production of metal nanoparticles by biogenic synthesis using a protein/enzyme acts on the reduction and stabilization of the particles; it is new technology for the development of new materials through new nanobiotechnological processes. Recent studies report the use of semi-purified laccase extracts for the biogenic synthesis of metal nanoparticles (El-Batal., 2015; Durán et al., 2014).

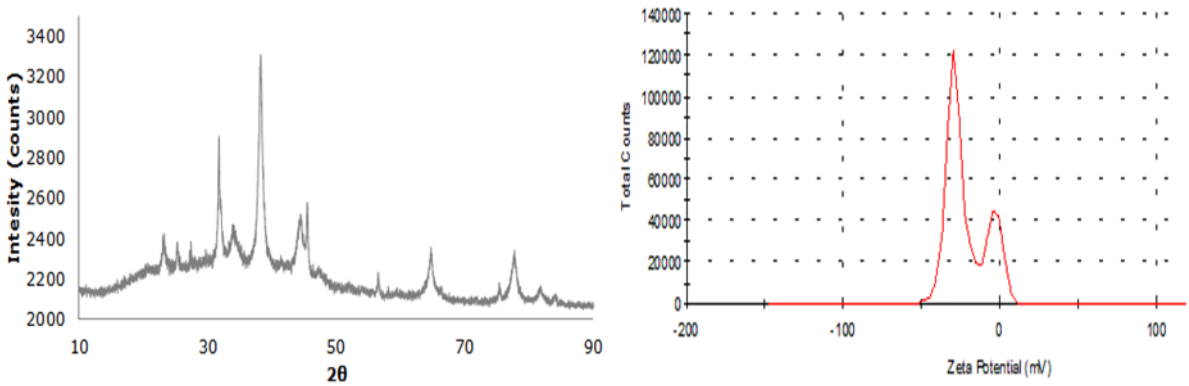

Figure 3. 8 (A) XRD patter and (B) Potential Zeta of gold nanoparticles using $AuCl_4^-$ ions 1 mM with semi-purified laccase in solution from *T. versicolor*.

In relation to the possible mechanism explaining the formation of metal nanoparticles exclusively in the presence of the laccase enzyme, the currently reported information indicates that the cysteine residues would be the reducing agent (Durán et al., 2014; Faramarzi et al., 2011), due to the lack of intermediary for the electron transport it is not possible by mechanism proposed by Durán et al. (2005) for the formation of the nanoparticle. Moreover, the mechanism could explain further the formation of the nanoparticle by the interaction of the metal ion with the disulfide bridges in the structure presenting the laccase enzyme, this interaction denature the enzyme losing its catalytic activity (Durán et al., 2014).

3.3.2 Synthesis of metal nanoparticles (Ag, Cu and Au) using purified commercial laccase from *T. versicolor*

The results when using commercial single purified laccase enzyme in the process of biogenic synthesis of gold nanoparticles was positive as shown in Figure 3.9 where one can appreciate the changes of coloration in solutions containing silver (3.9a), gold (3.9b) and copper (3.9c) nanoparticles, which were formed. This change in color is the preliminary sign of the formation of plasmon bands of metal nanoparticles. In Figure 3.9d resulting absorption spectrum is observed in the process of formation of copper nanoparticles, as had can be seen the band presented his highest absorbance between 650-700 nm. On the other hand, the formation of the plasmon band in the UV-Vis is observed around 560 nm for Au-NP and to 410 nm for Ag-NP (data not show). The Cu-NP, Au-NP and Ag-NP have an average zeta potential of -11.2, -15.7 and -20.4 mV, respectively, with a negative charge on their surface. Continuing with the characterization of nanoparticles, Figure 3.10 shows electron micrographs of the nanoparticles of copper, gold and silver obtained using purified laccase which is present in the synthesis process, as copper and silver nanoparticles showed a quasi-spherical with an average size smaller than 10 nm for copper and 90 nm for silver. In relation to gold nanoparticles more variables forms are presented as it can be seen in Figure 10a where forms triangular, hexagonal and other spherical particles obtained in the synthesis with an average size of 110 nm were observed.

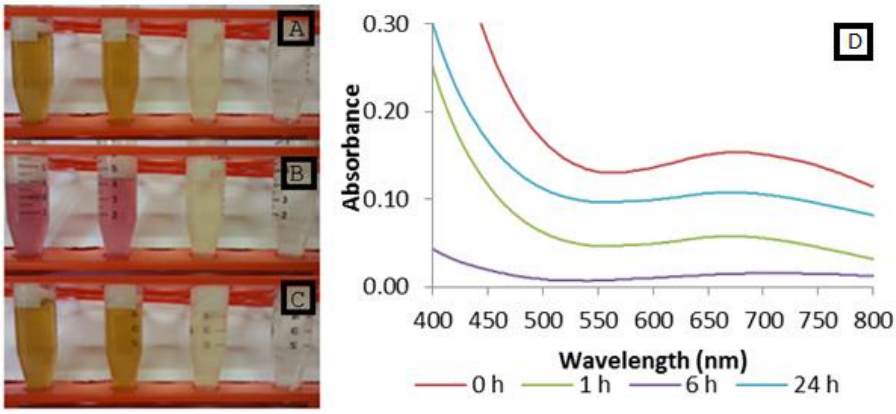

Figure 3. 9 the visual identification for the formations of (a) silver, (b) gold and (c) copper nanoparticles and (d) UV-Vis absorption spectrum of copper nanoparticles using purified commercial laccase from *T. versicolor* with 1 mM metal salt in solution.

On the other hand, diverse authors (Durán et al., 2005; Bhambure et al., 2009; Jain et al., 2011) have demonstrated that proteins could interact with metal salt for the metal nanoparticle formations and showing that the formation mechanism of metal nanoparticles is due to the action of a large number of enzymes secreted by the fungi, in a special by reductases (Ahmad et al., 2003; Durán et al., 2005, 2011, 2012; Jain et al., 2011). In this context the study the action of semi-purified and purified laccase is ratified as the reducing agent and stabilizer of the nanoparticles formed in the synthesis. Furthermore, for the formation of metal nanoparticles using laccase as a reducing agent it is necessary to deliver energy to the reaction system by increasing the temperature, as reported in the study Faramarzi et al. (2011).

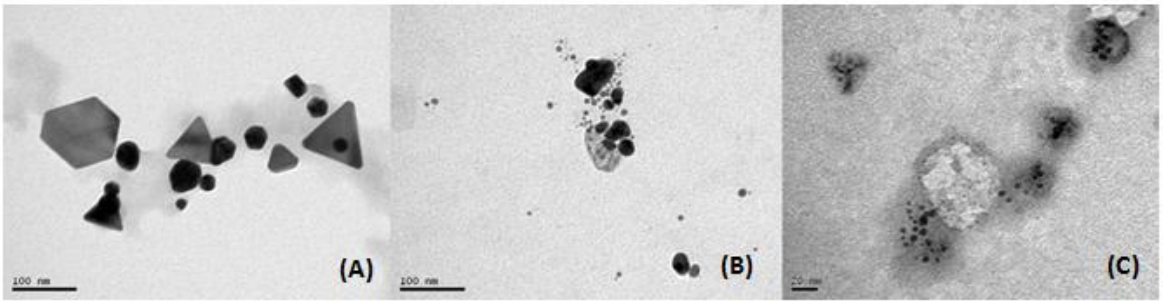

Figure 3. 10 Transmission electron micrographs (TEM) of (a) gold, (b) silver and (c) copper nanoparticles using purified laccase from *T. versicolor* for synthesis whit 1 mM metal salt in solution.

In Figure 3.11 is observed laccase tridimensional structure and representation of the active site multicopper, this is related to the possible mechanism explaining the formation of metal nanoparticles using laccase enzyme as reducing agent and stabilizing agent. The current information indicates that the cysteine residues would be the reducing agent present in the laccase structure; this is added to the laccase reducing potential due to the presence of the copper atoms at their active site (Durán et al., 2014, El-Batal et al., 2015).

The enzyme loses its catalytic activity during the process of synthesis of the nanoparticles, this is observed by the typical absorption band of this blue protein of approximately 600 nm

disappeared immediately after the addition of metal ions with the concomitant loss of laccase activity.

The ways for the formation of nanoparticle that could explain the formation of the nanoparticle by laccase enzyme: 1) It is by reducing the ion metal action of redox potential present in T1 copper having a cysteine residue in conformation and 2) it is possible to break the sulfur bridges sulfur stabilizing the molecule in domain 1 of the structure.

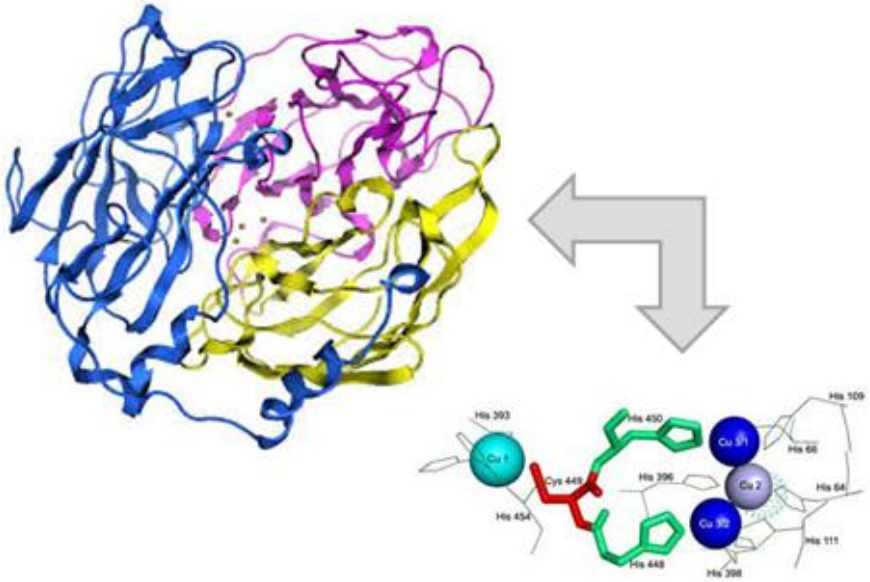

Figure 3. 11 Laccase tridimensional structure and representation of the active site multicopper.

In this same via relates to the use of purified enzymes from microorganisms reducers, it was reported the effective use of a reductase enzyme purified from microorganism and it used in process of reduction and stabilization in formation of biogenic nanoparticle is reported by Gholami-Shabani et al. (2015) synthesis of gold nanoparticles using sulfite reductase purified, gold nanoparticles which were spherical with an average size of 10 nm and a zeta potential of -30 mV. Another example of the use of not reductive enzyme with no catalytic function were reported by Mishra and Sardar (2012) in synthesis of Ag-NP in vitro by α-amylase as reducing and capping agent in synthesis process. The nanoparticles showed the absorption band at 422 nm and size of 22-44 nm diameters with triangular and hexagonal shape. The authors propose as formation mechanism interaction between thiol groups present in amylase enzyme and silver ions for synthesis of Ag-NP.

The results obtained in this work highlight by not depend on the enzymatic activity of the reducing agent for the synthesis of biogenic nanoparticles. This new concept of non-enzymatic catalytic biogenic silver nanoparticles expands the possibilities of the actual syntheses of the biogenic silver nanoparticles (Durán et al., 2014; El-Batal et al., 2015; Durán et al., 2015). This biogenic synthesis ability will have new economic and ecologically favorable perspectives in the field of nanoparticle synthesis from enzymes that have already been extensively studied and their biotechnological potential is known (Durán et al., 2015).

3.4.- Conclusions

Based on the results, the following conclusions are presented:

To our current knowledge, biological synthesis routes are not fully extended in the formation and preparation of metal nanoparticles yet, but based on the results obtained semi-purified laccase and commercial purified laccase have potential to form different metal nanoparticles (Cu, Ag and Au) using only laccase from white rot fungus, it can also be prepared easily and is friendly to the environment. Besides, the synthesis of metal nanoparticles using only semi-purified and purified commercial laccase were produced mainly by reaction of reduction/oxidation of the metal ions in solution beginning the process of nucleation for the formation of nanoparticle. Consequently, with the exclusive use of laccase in the process of synthesis it is possible to establish a hypothetical mechanism for the nanoparticle synthesis, based on the reduction potential of the laccase for metal ions and the presence of cysteine residues as necessary link points of the metal cores with protein structure that stabilize the formation of nanomaterial. In addition, through the XDR patterns it was possible to identify the crystal structure of the different nanoparticles obtained gold, silver and copper oxides were observed forming nanoparticles. In conclusion it is possible the effective synthesis of metal nanoparticles from the use semi-purified and purified laccase from the white rot fungus.

CHAPTER IV: BIOCIDAL PROPERTIES OF BIOGENIC METAL NANOPARTICLES (Cu, Ag, and Au) PRODUCED FROM PRECURSORS OF FUNGAL ORIGIN

Abstract

In the recent years, antibacterial activity against human and plant pathogens of metal nanoparticles have elicited high interest among researchers around the world, the metal nanoparticle antimicrobial properties have aroused great interest as an effective method against microorganisms that have developed resistance against most potent antibiotics. Therefore, this report aims to evaluate biocide activity of metal nanoparticles (Cu, Ag and Au) previously synthesized by fungal extract from white rot fungi. The minimum inhibitory concentration (MIC) and minimum bacterial concentration (MBC) of the metal nanoparticles (Ag, Au and Cu) for *E. coli* and *S. aureus* was determined. In addition, the antimicrobial activity by Scanning Electron Microscopy (SEM), Flow cytometer and Confocal Microscopy (CM) was evaluated in order for visualizing the cells damage by metal nanoparticles caused by reactive oxygen species (ROS). Results demonstrated that the biogenic copper/copper oxide nanoparticles synthesized using mycelium-free extract of *S. hirsutum* not exhibit antibacterial activity against *E. coli* and *S. aureus*, contrary effect showed the silver and gold nanoparticles show antimicrobial activity against bacterial strains of *E. coli* and *S. aureus*. Results of the MIC for silver nanoparticles against *E. coli* and *S. aureus* were 30 and 80 µg/mL; respectively. Scanning electron microscopy (SEM) and Confocal Microscopy (CM) revealed details silver nanoparticles adhering to bacteria membrane. In relation of antimicrobial activity using silver nanoparticles in combination with confocal microscopy and flow cytometer studies, fluorescence was observed and quantitate formation of reactive oxygen species was verified acting on the viability of the cell membrane. The results suggested that some Me-NPs (Ag and Au) may damage the structure of bacterial cell membrane which causes *E. coli* and *S. aureus* bacterial strains to die eventually, the biogenic metal nanoparticles have a potential use as an antibacterial. Finally, based on the results we can say that the biogenic nanoparticles of silver and gold synthesized from the fungal extract produced using a white rot fungus has biocide activity on a gram-negative bacterium *E. coli* such as more than about gram- positive bacteria such as *S. aureus*.

4.1 INTRODUCTION

In recent years, several investigations have been guided to study metal nanoparticles (Me-NP) with antimicrobial and antifungal activity against pathogenic, now also Me-NP are studied microorganisms resistant to multiple bactericides and fungicides (Li et al., 2014; He et al., 2011; Theivasanthi et al., 2011). In this context, we have studied the Me-NPs and promising results have been obtained based on their antimicrobial potential against various bacterial strains. An example is reported by Ahmad et al. (2013) reported the antimicrobial activity of gold and silver nanoparticles (Au- and Ag-NPs) produced from an cell free extract of *Candida albicans*, both nanoparticles were investigated against both *S. aureus* and *E. coli.* Moreover, Ramyadevi et al. (2012) demonstrated that Cu-NPs showed inhibitory effect in human gram negative pathogenic bacteria as *E. coli, Micrococus luteus, S. aureus, Klebsiella pneumonia and P. aeruginosa*. Another example of the antibacterial action of Copper nanoparticles (Cu-NPs) was reported by Yoon et al. (2007) was showed that *Bacillus subtilis* is more sensitive than *E. coli* to in this study the researchers showed that the Cu-NPs demonstrated higher antibacterial activity compared with Ag-NPs. In relation to antibacterial activity of Ag-NPs, it has been studied against diverse bacteria such as *Staphylococcus* sp (Ahmad et al., 2013), *Salmonella typhi* (Fayaz et al., 2010), *Bacillus* sp (Jaidev et al., 2010), *E. coli* (Ahmad et al., 2013; Ramyadevi et al., (2012), *Micrococcus luteus* (Fayaz et al., 2010), *P. aeruginosa* (Nithya et al., 2009). Another more recent example is reported by Husseiny et al. (2015) and bactericide potential of biogenic Me-NP synthesized from a fungal extract of *F. oxysporum* of Ag-NPs were used development antibacterial assays using *E. coli* and *S. aureus*. Use of nanoparticles and their possible applications in the area of health based on its antimicrobial potential has opened up opportunities for the design of multifunctional nanoparticles for medical and pharmaceutical applications (Simon de Dios and Diaz-Garcia, 2010). Their application of metal nanoparticles in medicine is based on the effectiveness of nanoparticles against many pathogens, including some resistant bacteria such as *Escherichia coli, Micrococus luteus, Klebsiella pneumonia* and *Streptococcus aureus*, the main focus of infections in hospitals (Theivasanthi et al., 2011; Ingle et al., 2008). In this context, Saravanan and Nanda (2010) and Ingle et al. (2008) tested bactericidal effect of Ag-NP against multiple drug resistant bacteria. Other example is the used Au-NPs chemical synthesis has been its bactericide effect against drug-resistant gram positive and gram-negative bacteria as reported by Li et al. (2014), the increase of microorganisms resistant to multiple antibiotics and antifungal many researchers have been guided to develop new and effective antimicrobial agents without resistance and cost-effective.
Another area of application of Me-NPs because of its antimicrobial properties is agriculture; Me-NPs have been used against plant fungal pathogens that cause severe crop damage (Kashyap et al., 2012; He et al., 2011). On the other hand, other an interesting study was reported by Durán et al. (2007) which tested antimicrobial activity in the Ag-NPs synthesized extracellular with *F. oxysporum* fungal strain against *S. aureus* bacterial strain, the nanoparticles were incorporated into a cotton cloth when it demonstrated its antimicrobial power. Besides, other medical applications of nanoparticles are dressings, nanogels and dental materials (Rai et al., 2009).

Fungi have gained much importance in the synthesis of different type of Me-NPs in the last decade (Ahmad et al., 2001; Bansal et al., 2005; Durán et al., 2005; Bharde et al., 2006; Sawle et al., 2008; Castro-Longoria et al., 2012), the extracellular secretion of enzymes that means an advantage in downstream processing and allows better handling of biomass in the process of synthesis (Gade et al .2008). At present there have been reported various enzymes secreted by

fungi that are capable of reducing metal ions through nonhazardous biological processes and allow controlled nanoparticle synthesis with the size and well defined shape (Jain et al., 2011; Rodriguez et al., 2013). An example is *Penicillium rugulosum*, was used to synthesize Au-NPs uniform sized, which is easier to handle as compared to other bacteria and yeast (Mishra et al., 2012). However scaling of biogenic synthesis processes nanoparticles requires the use of nonpathogenic human fungal strains, such as white rot fungi. Because of this it is necessary to conduct studies of synthesis and antimicrobial activity of the nanoparticles synthesized from fungal strains of the fungus type of white rot. Currently already it has been established that biologically synthesized nanoparticles metal have high antimicrobial activity (Rai et al., 2009; Rai et al., 2012; Husseiny et al., 2015) However, few studies have evaluated new strains of white rot fungi native and synthesis of metal nanoparticles with antimicrobial activity has been reported. This chapter aims to evaluate the biocide activity of nanoparticles of metal (Cu, Ag and Au), nanoparticles were previously synthesized from fungal extract produced by a white rot fungus.

4.2.- MATERIAL AND METHODS

Microorganisms for antimicrobial activity

Escherichia coli ATCC-25922 and *Staphylococcus aureus* ATCC-25923.

4.2.1.- Antimicrobial effect of metal nanoparticles (Ag, Au and Cu -NP) against bacteria pathogens by disc-diffusion method

Plates with Muller Hinton agar were inoculated with approximately 10^7 colony-forming units (CFU) of bacteria *E. coli* and *S. aureus*. The antimicrobial assays were done by disc-diffusion method with 100 µg/mL of metal nanoparticle. The plates were incubated in darkness at 32 ºC for 2 days and radial growth was registered. The zone around the nanoparticles was measured as zone of inhibition (ZOI) on the subsequent day using a millimeter scale. Antibiotic ampicillin was used for proposed comparative. The assays were performed in triplicate.

4.2.2.- Effect of metal nanoparticles (Ag and Cu) on the rate of bacterial growth in liquid medium

Different concentrations of metal nanoparticles (Ag and Cu) (100, 250 and 500 µg/mL) were added to a liquid culture and they were inoculated with approximately 10^5 colony forming units (CFU) of *E. coli* and *S. aureus*. Bacterial growth concentrations were determined by measuring optical density (OD) at 600 nm. Afterwards, an aliquot of liquid medium was seeded in Muller Hinton medium for observation of bacterial growth. The plates were incubated at 32 °C for 2 days. Assays were performed in triplicate.

4.2.3.- Determination of minimum inhibitory concentration (MIC) and minimum bactericidal concentration (MBC)

To examine the bactericidal effect of metal nanoparticles (Ag, Au and Cu -NP) on *E. coli* and *S. aureus*, approximately 10^5 CFU of bacterial strain were cultured on Muller Hinton agar plates supplemented with nanosized silver particles in concentrations of 10 to 100 µg/mL. Silver-free in Muller Hinton plates cultured under the same conditions were used as control. The plates were incubated for 24 h at 32 °C and the numbers of colonies were counted. The counts on the three plates corresponding to a particular sample were averaged. Growth rates and bacterial concentrations were determined by measuring optical density (OD) at 600 nm. The minimum inhibitory concentration (MIC) was defined as the lowest concentration of material that inhibits the growth of an organism. The minimum bactericidal concentration (MBC), i.e., the lowest concentration of nanoparticles that kills 99.9% of the bacteria was also determined from the batch culture studies.

4.2.4.- Transmision Electron Microsocopy (TEM)

TEM images of the samples were obtained using a transmission electron microscope (model JEOL JEM 1200EX II), at a Filament; Tungsten Voltage, kV; 40-120kv. The elemental analysis was carried out in spectrum of energy dispersive X-ray technique.

4.2.5.- Scanning Electron Microscopy (SEM) for metal nanoparticles

Micrograph was taken using a JEOL 6360LV instrument, 40kV. The samples were fixed with 2.5% glutaraldehyde overnight at room temperature followed by dehydration with gradient alcohol (10% to 95%) for 20 min and then in absolute alcohol for 2-5 min. The final specimen was prepared by coating the dehydrated sample with monolayer platinum for making the surface conducting

4.2.6.- Scanning Electron Microscopy - Microanalysis Elemental

The bacteria were washed for 1 times with deionized water for removing salts, the samples were glutaraldehyde fixed in buffered 4% 24hrs. SEM visualization under the following conditions Magnification 2000, 3500-6000X, BSE Detector 5 keV, WD ~ 5mm, 10 Pa. Microscope SU VP-SEM Hitachi-Japan 3500. EDX elemental microanalysis of samples was performed under the following conditions: 4000X magnification, BSE detector, 25KeV, WD ~ 10 mm and 10 Pa.

4.2.7.- Confocal microscopy

We performed a showing/show of bacterial and metal nanoparticles by the use of λ-scan that generated fluorescence emission at 405, 488 and 633 nm in a Fluoview FV1000 Confocal Laser Scanning Biological Microscope (Olympus, Japan). The FV10-ASW v.2.0c software program was used for obtaining emission intensities.

4.2.8.- Confocal microscopy. Cell viability staining

Cells were incubated for 15 minutes with 66 uM of PI (dead cells) and 10 µm of Syto9 (live cells) at room temperature in the dark. Samples were mounted and were visualized by Confocal Laser Microscope (CLSM), fluorescence emission was recorded Syto9 ʎ probe excitation/emission 488/530 nm and PI ʎ excitation/emission 546/590nm. Features of Image 1024 * 1024, 100X, 3x digital zoom. Olympus FV1000 CLSM-Japan. Image analysis was performed with FV10 Software v 0.2C.

4.2.9-. Confocal microscopy. Staining ROS production

Cells were incubated for 60 minutes with 25µM H2DCFDA (reactive species) at 37 °C. Positive Control sample is incubated in 1000um H_2O_2. Samples were mounted and were visualized by Confocal Laser Microscope (CLSM), fluorescence emission was recorded H2DCFDA ʎ excitation/emission 488/530 nm. Features of Image 1024 * 1024, 100X digital zoom 2.5x Olympus FV1000 CLSM-Japan. Image analysis was performed with FV10 Software v 0.2C

4.3.- Results and discussion

Metal nanoparticles antimicrobial activity

The use of fungal strains is a simple and easy method for obtaining Me-NPs in a friendly environment and generates no toxic agents in their synthesis. Currently, Me-NPs were showed inhibitory activity and biocide effect against bacteria and fungi (Durán et al., 2007; Fayaz et al., 2010). In this context, different Me-NPs synthesized from fungal mycelium-free extract of *S. hirsutum* have shown interesting results in their antimicrobial activity as shown in this investigation.

4.3.1.- Antimicrobial activity of copper nanoparticles

The effect of Cu-NP on *E. coli* and *S. aureus* bacterial strains with the disc diffusion assay 100 µg/mL was initially analyzed, in which it was not possible to observe any inhibition zone in culture plates as it can be seen in Figure 4.1. The same result was observed in other concentrations (50 µg/mL) tested with the Cu-NP synthesized from *S. hirsutum* fungal extract.

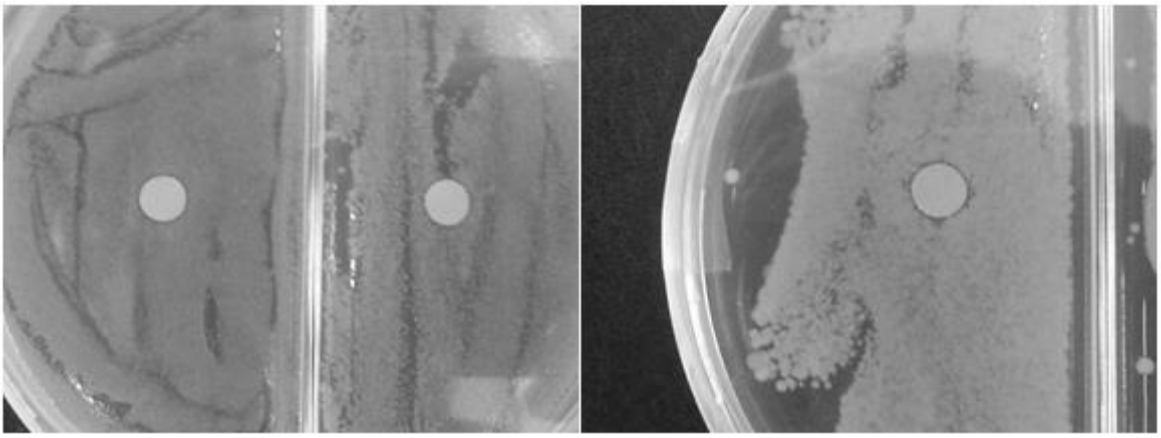

Figure 4.1 Disc diffusion assay for zone of inhibition of copper nanoparticles 100 µg/mL against *E. coli* after 48 h of incubation at 32 °C

The analysis tests was developed for evaluating the effects of concentration in solution of Cu-NPs (100, 250 and 500 µg/mL) on bacterial growth of *E. coli* and *S. aureus*. The results are presented in Figure 4.2, showing that there was no inhibitory effect by Cu-NPs on bacterial growth of *E. coli* and *S. aureus* in liquid medium. The study was conducted to compare the values of optical density between the initial and final state, which presented an increase in absorbance attributable to bacterial growth for the two bacterial strains under study. In the results obtained it can be observed that the optical density obtained absorbance is considerably higher for *E. coli* and *S. aureus* after 24 h incubation compared to initial optical density (time 0 h) for the concentrations 100, 250 and 500 µg/mL Cu-NPs in the culture solution, using these results may indicate that there was no inhibitory effect on growth in both strains of bacteria in concentrations of Cu-NPs used in the study.

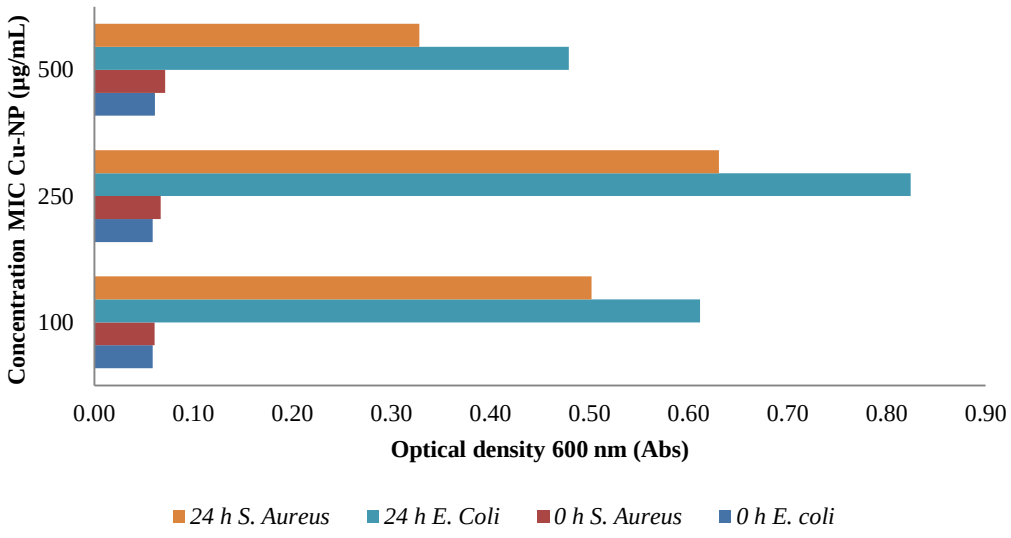

Figure 4.2 Effect of copper/copper oxides nanoparticles on bacterial strains *E. coli* and *S. aureus* growth rate.

However, opposite results have been reported in the literature, an example of the effective antibacterial action of Cu-NPs was reported by Yoon et al. (2007). In this study was reported an effectiveness of the antimicrobial activity of 90% at a concentration of about 40 µg/mL for *Bacillus subtilis* and *E. coli* bacterial strains. In the same study, it was demonstrated that Cu-NPs had a higher antibacterial activity compared with Ag-NPs (Yoon et al., 2007). Another example is reported by Ramyadevi et al. (2012), in their results show that the Cu-NPs of synthetic type at an approximate concentration of 500 mg/mL in their synthesis solution have biocide effect. To study inhibition zone disk were used 50 µL of solution Cu-NPs and study the effect against bacterial strains *E. coli*, *Micrococcus luteus*, *S. aureus*, *Klebsiella pneumoniae* and *P. aeruginosa*. It was reported that effective zones of inhibition with 5 bacterial strains were presented. Additionally it is concluded that the nanoparticles of copper has a greater antimicrobial effect of Ag-NPs (Ramyadevi et al., 2012). Lack of antimicrobial activity of Cu-NPs mixed synthesized from the extract of white rot fungus *S. hirsutum* can be attributed to these enveloping biopolymer nanoparticles, which are formed in the process of spontaneous synthesis studied, this biopolymer is withholding the particles which cannot effectively evaluate the potential use of antimicrobial nanoparticles. Hosseini et al. (2012) used fungal strain *F. oxysporum* in synthesis and used copper sulfide nanoparticles (CuS-NPs), in the same way they reported the formation of a peptide polymer encapsulating and limiting the growth of the nanoparticles.

4.3.2.- Antimicrobial activity of silver and gold nanoparticles

For the development of bacterial activity two bacterial strains *E. coli* and *S. aureus* were used. The results of the inhibition zone in disc diffusion assay for Ag-NP against two bacterial strains under study showed similar results as seen in Figure 4.3. The results showed that for *E. coli* and *S. aureus* it has diameter mean of 7.6 and 7.5 mm of inhibition zone, respectively. These results were subsequently compared with the broad-spectrum antibiotic ampicillin. Thus, the antibiotic were higher inhibition zone compared with the same Ag-NP concentration, where the diameter

of the zone of inhibition was greater than >10 mm. The results obtained in the test zone of inhibition was higher compared to that reported by Husseiny et al. (2015), in their results of antibacterial activity of biogenic Ag-NPs against *E. coli* and *S. aureus* were able to reach a maximum inhibition zone of only 2 mm and 1.6 mm, respectively. It was also observed an increased antimicrobial effect on *E. coli* bacteria corresponding to gram-negative type.

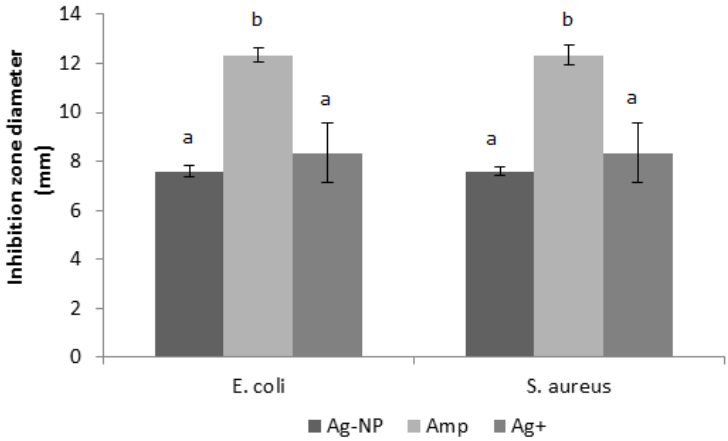

Figure 4. 3 Disc diffusion assay by inhibition zone of silver nanoparticles 100 µg/mL against *E. coli* and *S. aureus* after 48 h of incubation at 32 °C. Statistical analysis by multiple comparisons Tukey test ($\alpha < 0.05$).

In Addition Figure 4.3 are presented the results of Tukey's multiple comparison analysis with the results of the Ag-NPs, the statistical analysis showed similar results for both bacterial strains, no significant difference between the nanoparticle and the metal salt in the size of the zone of inhibition was observed, but when comparing the nanoparticles with the antibiotic if significant differences are observed in the results.

Test results for the MIC determination of Ag-NP are shown in Figure 4.4a based on the measurement of the optical density (OD) in the liquid culture medium. The results demonstrated that the MIC of Ag-NP for bacteria strain *E. coli* and *S. aureus* were 30 and 80 µg/mL respectively. The results for the determination of minimum bactericidal concentration (MBC) were performed by comparing the increase in optical density in the culture medium after 24 h incubation of both bacterial strains. The results of MBC were 40 µg/mL for *E. coli* and 90 µg/mL for *S. aureus*. Figure 4.4b the results obtained in studies of discrimination live/dead cell by flow cytometric of *E. coli* cells on being subjected to a concentration of 100 µg/mL Ag-NP with one hours of contact time are presented. It can be seen 60% of dead bacterial cells just 60 minutes after contact between the nanoparticle/bacteria cell. These results correlate with those obtained in studies plaque inhibition and determination of the minimum inhibitory concentrations and biocides, these studies demonstrate the good biocide activity of Me-NPs synthesized.

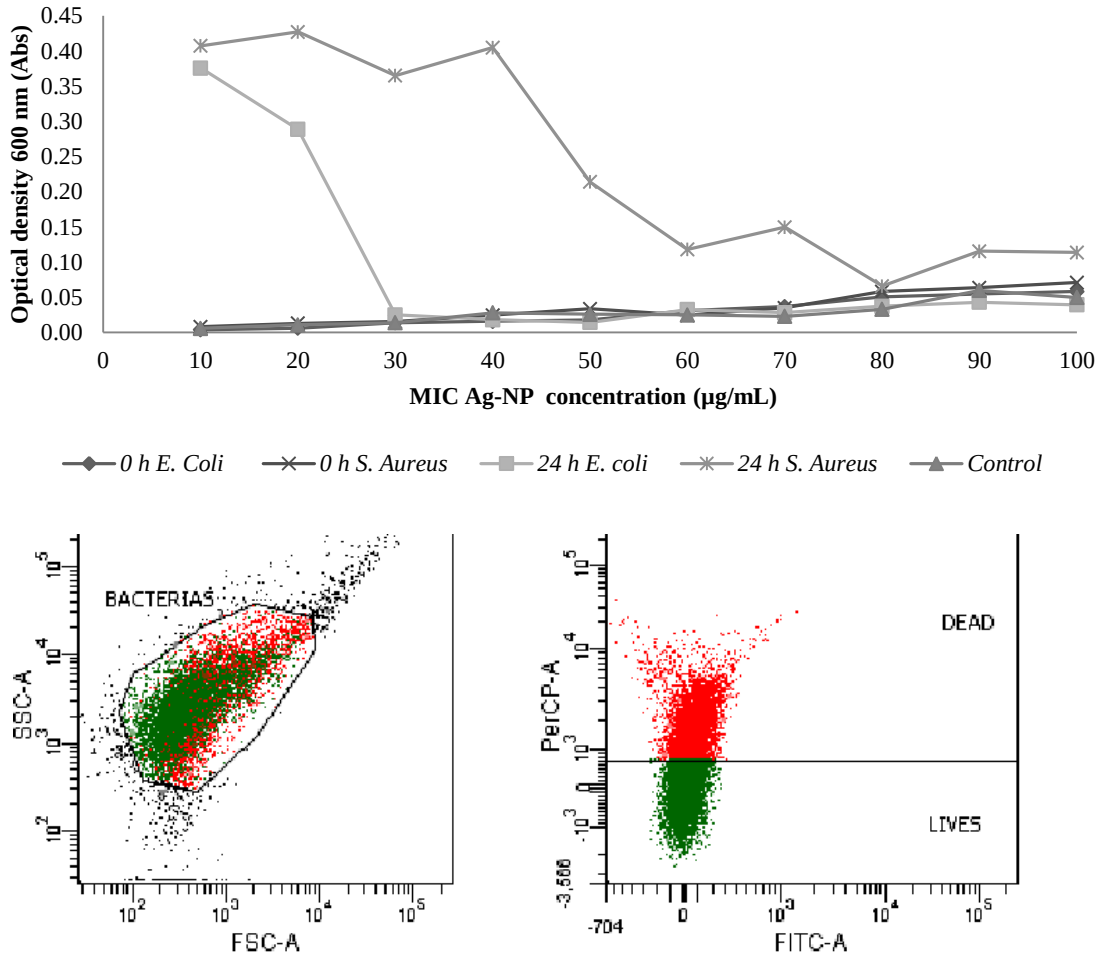

Figure 4. 4 (a) MIC assay for silver nanoparticles synthesized from fungal extract against *E. coli* and *S. aureus* bacterial strains by determination of increasing optical density (600 nm) in the culture medium after 24 h incubation. (b) Studies of discrimination live/dead cell by flow cytometric of *E. coli* cells on being subjected to a concentration of 100 µg/mL silver nanoparticles with one hours of contact time.

Figure 4.5 shows Confocal and SEM micrographs. The Figure 4.5a and 4.5b correspond to confocal microscopy. Initially, the Ag-NPs showed autofluorescence under laser excitation without the use of a chromophore, in the positive control. After the study, the auto-fluorescence Ag-NPs adhered to cell membrane of *E. coli*. The image 4.5a and 4.5d are the SEM microscopies of metal nanoparticles (Ag-NP) with bactericidal activity against *E. coli*. On one hand, the partial destruction of the cell membrane of *E. coli* can be seen in image 4.5c; it was also observed that most of the membrane was not destroyed and viable. The cell membrane is possible to be seen completely destroyed in 4.5d image. It is also possible to see the nanoparticles stuck to the membrane, white points corresponding to the nanoparticle that is observed.

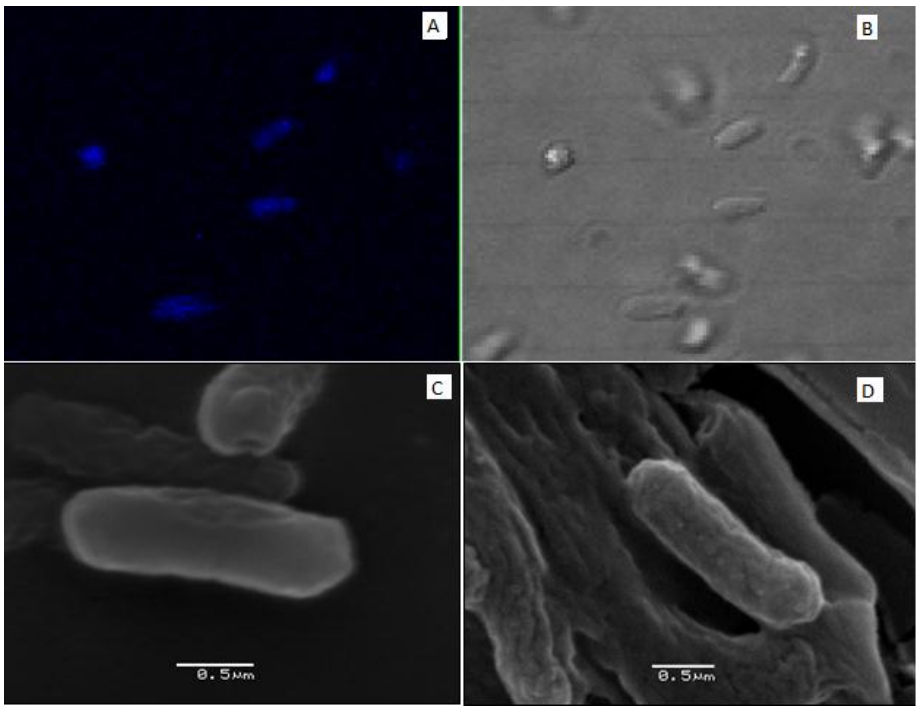

Figure 4. 5 the images (a) and (b) Confocal Microscopy. Autofluorescence detection of silver nanoparticles in combination microscopic analysis *E. coli* on antibacterial activity. Images (c) and (d) Microscopy SEM. Observation of the silver nanoparticles attached to the cell membrane of *E. coli* in microscopic analysis antibacterial activity

The results of the Au-NP showed similar results with silver nanoparticles where it was possible to observe inhibition around the paper discs but with minor areas inhibition, Au-NP had an area of inhibition of 6 mm diameter on average for both bacterial strains. Those observed for gold nanoparticles were 40 and 60 µg/mL using *E. coli* to the MIC and MBC, respectively. Moreover, using a strain *S. aureus* were the results of MIC 60 µg/mL and MBC exceeded the concentration of 100 µg/mL (data no show).

A similar result was by Ahmad et al. (2013) reported on the biological antimicrobial activity of Au-NP, the nanoparticles have a greater potential against *E. coli* and *S. aureus*. The MIC for Au-NP against *S. aureus* and *E. coli* were 512 and 128 µg/mL respectably. In addition it is reported that by Ahmad et al. (2013) that the mean diameters of the ZOI for Au-NPs against S. *aureus* were 11 mm, while as for *E. coli* showed 16 mm. One can point that *S. aureus* strain was less susceptible to Au-NPs and Ag-NPs than *E. coli* strain the antibacterial action (Kim et al., 2007; Ahmad et al., 2013; Husseiny et al., 2015). Li et al. (2014) reported the use Au-NP in confocal images; their results showed that the Au-NPs induced membrane damage in *E. coli and* methicillin-resistant *S. aureus.* Both bacteria strains were incubated with Au-NP 500 nM for 3 h, and them stained with Propidium Iodide (PI) was used to show the bacterial cells with damaged cell membrane. Finally, when is comparing the antibacterial potential of Me-NP produced from biogenic synthesis such as the use of fungal mycelium-free extracts, the results show that the Ag-NP have a greater antimicrobial potential against the two bacterial strains.

Figure 4.6 shows confocal micrographs for cell viability assay. Figure 4.6a corresponding of control negative *E. coli* without nanoparticles where no fluorescence is observed in the bacterial cell. In Figure 4.6b results are presented for the combination of bacterial cells with 30 µg/mL

Ag-NPs solution; in the image can see the presence of cell with green and yellow coloration in similar amounts corresponding to live and dead cell respectively. Addition, in Figure 4.6C results for the mixture are observed between *E. coli* cells and 100 µg/mL Ag-NPs; in this image was observe a predominance of yellow and red coloration in bacterial cells corresponding to high cell damage.

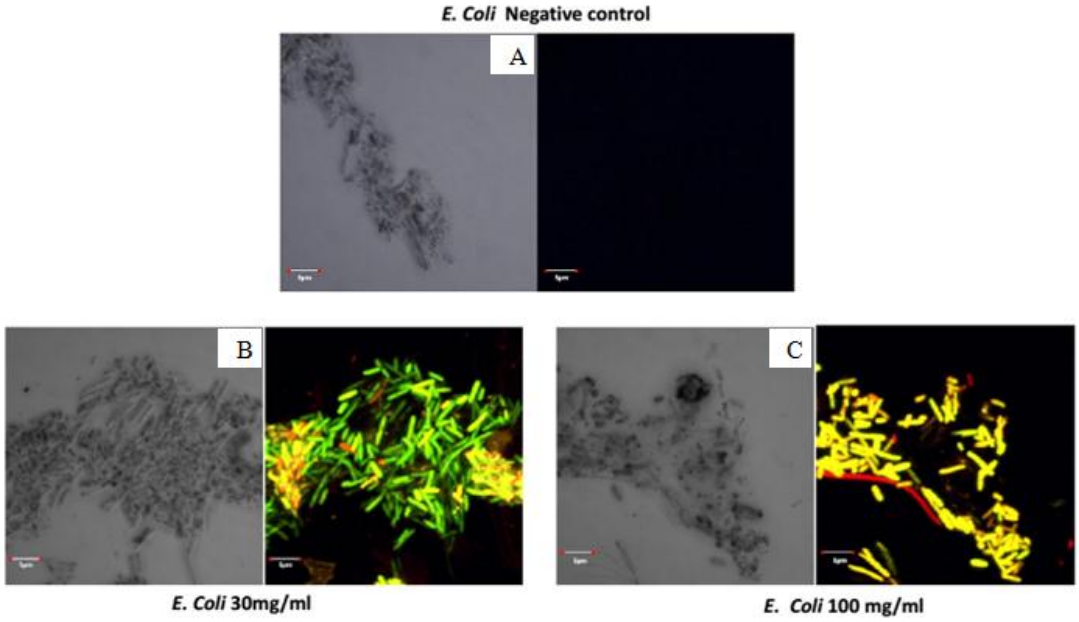

Figure 4. 6 Confocal microscopy images, cell viability studies of bacterial cell combined with silver nanoparticles. Images (a) Control *E. coli* without nanoparticles, (a) *E. coli* + 30 µg/mL Ag-NPs and (c) *E. coli* + 100 µg/mL Ag-NPs.

In Figure 4.7 in the results for scanning electron microscopy (SEM) and elemental microanalysis (EDX) are presented. On the image (4.7a) are presented the results of negative cell bacterial control, it is observed cell feasibility and EDX analysis not the presence of silver in the sample. By contrast in (4.7b) and (4.7c) is observed in bacterial cells one noticeable, and it is reflected in the decrease in the size of the damaged cell which correlates with the concentration of the nanoparticle, besides EDX analysis confirm it in the presence of silver as samples.

The observations made here should be supplemented with other techniques to determine the participation of the biocide Me-NPs. Besides, it is necessary to know the mechanism by which biocide of Ag-NP and the chemical species act on specific reaction that is activated. Antimicrobial activity of Me-NPs is a function of particle size, morphology shape and monodispersity (uniformly distributed) (Zhang et al., 2011). Small size, monodispersity and the high specific surface area of the nanoparticles enhance their antimicrobial ability as they interact directly with microbial membranes, generating cell death (Durán et al., 2010). The direct control of several reaction parameters, such as pH, substrate concentration, temperature and reaction time, has been studied to optimize the nanoparticle synthesis process (Gericke et al., 2006a; Nayak et al., 2011; Gericke et al., 2006b; Kathiresan et al., 2009).

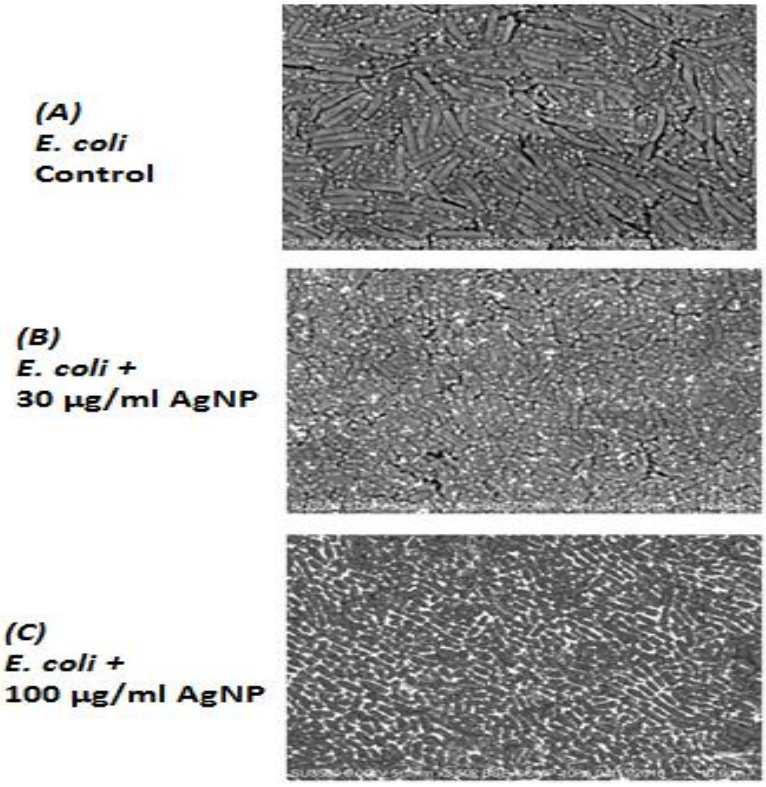

Figure 4. 7 Observation antibacterial activity on *E. coli* without and with silver nanoparticles in image of scanning microscopic analysis and Microanalysis Elemental. (a) Control *E. coli* without nanoparticles, (b) *E. coli* + 30 µg/mL Ag-NPs and (c) *E. coli* + 100 µg/mL Ag-NPs.

In Figure 4.8 they were observed the results obtained in studies of staining for the production of reactive oxygen species (ROS). Among the results the generation of ROS in the positive control (b) containing H_2O_2, images (c) and (d) corresponds to two concentrations in study 30 and 100 µg/mL, respectively, were observed. Staining of bacterial cells is observed, confirming qualitatively generation of ROS. Image (a) corresponds to the negative control, it fails to observe the generation of ROS detectable staining. Addition flow cytometer studies were performed to quantify the production of ROS species by combining and incubating bacterial and nanoparticles at two concentrations of 30 and 100 µg/mL cells. Additionally flow cytometer studies were performed to quantify the production of ROS species by combining and incubating bacterial cells and nanoparticles at concentrations of 30 and 100 µg/mL.

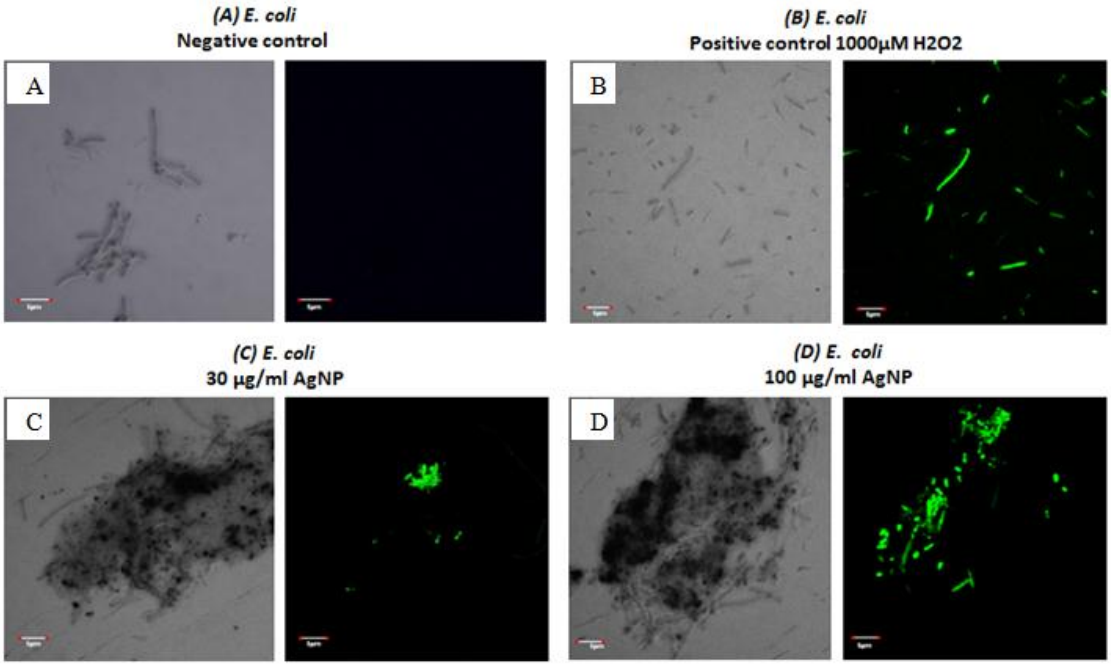

Figure 4. 8 Images confocal microscopy of generation of reactive oxygen species with silver nanoparticles on *E. coli*. (A) Negative control, (B) positive control 1000 µM H_2O_2, (C) *E. coli* + 30 µg/mL Ag-NPs and (D) *E. coli* + 100 µg/mL Ag-NPs.

Additionally flow cytometer studies were performed to quantify the production of ROS species by combining and incubating bacterial cells and nanoparticles at two concentrations of 30 and 100 µg/mL. In Figure 4.9 the results of the quantification of the generation of reactive oxygen species produced by the 100 µg/mL silver nanoparticles on *E. coli* is presented. Also it was used a negative control that originated the baseline and H_2O_2 which contained a positive control. The results showed an extra generation in average 15% of species ROS by bacterial when subjected to both nanoparticle concentration, compared to the baseline of the negative control cells. The positive control generated a production of 30% over the baseline.

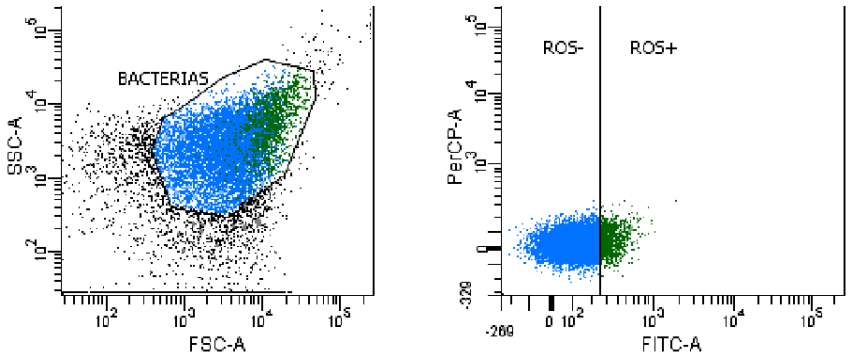

Figure 4. 9 Quantification by Flow cytometer of generation of reactive oxygen species produced by 100 µg/mL silver nanoparticles on *E. coli*

Metals can act as catalysts and generate ROS in the presence of dissolved oxygen, Marambio-Jones and Hoek (2010) in their review on nanomaterials and their implications on human health and environmental stand out especially for silver nanoparticles are two possible mechanisms of

action of antimicrobial activity from the ROS generated in the bacterial cell. The generation of ROS could act on different parts of the bacterial cell; (1) interact with proteins and membrane phospholipids affecting proper operation and integrity and (2) the ROS species generated inside the cell directly cause damage bacterial DNA. Kim et al. (2007) to confirm the production of free radicals in bacterial cells caused by the action of silver nanoparticles was performed a study by electron spin spectroscopy (ESR), values found in the ESR spectrum generation relate free radicals with Ag nanoparticles.

The antibacterial efficacy of Me-NPs is investigated for its high specific area and antibacterial effect at low concentrations against bacteria and fungi (Durán et al., 2007, Fayaz et al., 2010; Musarrat et al., 2010). Different authors have reported on bactericidal action and the possible mechanism of action of Ag-NP, Lok et al. (2006) determined that a short exposure of Ag-NP to *E. coli* resulted in an increase of permeability of cell membrane and a massive loss of intracellular potassium generating the loss of cell viability. In the same way, Sondi et al. (2004) reported that *E. coli* treated with Ag-NP showed the formation of “pits” in its cell wall with accumulation of nanoparticles on cell membrane, leading to increased permeability and cell death.

The bacterial cell showed aggregates composed of Ag-NPs and cell death, suggesting that Ag^+ binds to functional groups, resulting in protein denaturation. Rai et al. (2009) described that antimicrobial action mechanism of Ag-NPs is related to the amount and rate of ionized silver release. This is highly reactive and binds to tissue proteins and causing structural changes in bacterial cell wall and nuclear membrane, which leads to warping and cell death. In Figure 4.10 summary of all possible behaviors multi-action of Ag-NP against bacteria, shown can be seen as a possibility of damage to cell death in the cell membrane or the formation of reactive oxygen species (ROS) between other possibilities (Rai et al., 2012, Kan and Rai, 2013). Ruparelia et al. (2008) determined that a similar action mechanism is attributed to Cu-NPs, but in general the mechanism of action of other nanoparticles as copper and gold nanoparticles, different Ag-NP, is still not well understood, especially effect and mechanism of action of nanoparticle combinations on bacterial cells (Kon and Rai, 2013). Silver and copper ions are released by nanoparticles and these may attach to negatively charged bacterial cell wall generating their rupture, thereby leading to protein denaturation and cell death (Lin et al., 1998). This antibacterial activity is related to total surface area of nanoparticles providing a better interaction with microbes (Baker et al., 2008; Musarrat et al., 2010; Kon and Rai, 2013). In addition, antimicrobial potency of nanoparticles is directly proportional to concentration of nanoparticles in solution (Ruparelia et al., 2008; Husseiny et al., 2015).

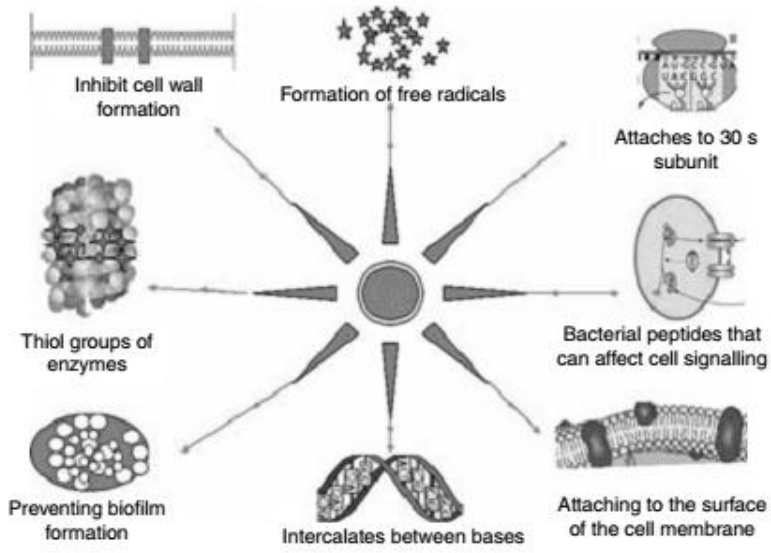

Figure 4. 10 Schematic representations of silver nanoparticles showing multiple bactericidal actions (figure taken from Rai et al., 2012)

This antibacterial activity is related to total surface area of nanoparticles providing a better interaction with microbes (Baker et al., 2008; Musarrat et al., 2010). Besides, antimicrobial potency of nanoparticles is directly proportional to concentration of nanoparticles in solution. Sondi et al. (2004) studied antimicrobial effect of different concentrations of Ag-NP (10, 50 and 100 µg/mL) on 10^7 UFC of *E. coli*. The results demonstrated that at higher nanoparticles concentration the growth delay of bacteria increased. However, these concentrations are considerably lower, if the antimicrobial effect of Me-NP and metal salts is compared according to this, nanomolar concentrations are used in the case of nanoparticles and micromolar ranges are used in the case of metal salts (Durán et al., 2010). In summery bactericidal potential of nanoparticles is influenced by size, shape, concentration and dose, bactericidal potential can be increased by manipulating the size at nano-scale and leading to increased surface area/volume ratio (Rai et al., 2012). Finally, antibacterial activities of NPs depend on two main factors: (i) physicochemical properties of NPs as type metal using in process of synthesis and (ii) type of bacteria as gram negative and gram positive (Hajipour et al., 2012) .

4.4.- Conclusions

To our knowledge, routes biocide activity or inhibitory activities of different Me-NPs do not extend completely yet. Currently the most studied and reported in biogenic Ag-NP remains, find information about other possible mechanisms of Me-NP is very limited.

- Based on the results we can say that the biogenic nanoparticles synthesized from the fungal extract produced using a white rot fungus has greater biocide activity on a gram-negative bacterium *E. coli* such as more than about positive bacteria such as gram- *S. aureus*.

- In conclusion with relation of antimicrobial activity, the inhibition zone formed in the screening test indicated that Ag-NPs and Au-NPs have antibacterial activity against bacteria *E. coli* and *S. aureus*. The bactericidal effect of metal nanoparticles has been attributed to their small size and high surface to volume ratio, which allows them to interact closely with microbial membranes. The results suggested that some Me-NPs (Ag and Au) may damage the structure of bacterial cell membrane which causes *E. coli* and *S. aureus* bacterial strains to die eventually.

- Additionally it is possible to conclude that developed based on studies and obtained results in the Confocal microscopy and Flow Cytometry for generation of reactive oxygen species acting on the feasibility of cell membrane are consistent with the information in the scientific literature on the antimicrobial activity having the Me-NP biogenic, this results showed that one of the routes for the biocide activity of metal nanoparticles is related to the generation of reactive oxygen species and possible effect on cell membrane proposed by other researchers.

CHAPTER 5: GENERAL DISCUSSION AND CONCLUSION, FUTURE PERSPECTIVES

5.1.- General discussion

Nanobiotechnology is a new field of investigation emerging of nanotechnology and broad technological application, in nanobiotechnology is involved with different research fields of expertise, such as physics, chemistry, biology, medicine, engineering and material science (El-batal et al., 2015; Husseiny et al., 2015). In this direction, 'green nanomaterials' are now a major objective of research in nanobiotechnology as biogenic metal nanoparticles synthesized from biological extracts (Husseiny et al., 2015; Gholami-Shabani et al., 2015). Synthesis of nanomaterials by microorganisms offers a reliable and alternative approach to traditional chemical and physical methods (El-Batal et al., 2015; Husseiny et al., 2015). Saravanan and Nanda, (2010) defined microorganisms as potential biofactories; this concept is used to mention the ability of unicellular or multicellular microorganisms for biogenic synthesis of metal nanoparticles or oxide metal nanoparticles. Fungi are organisms, which produce nanoparticles in form intra and extracellular way due to the high secretion of proteins and enzymes that are involved in the reduction of metal ions and limiting nanoparticles (Narayanan et al., 2010).

In this context, the Chilean native white rot fungi *Stereum hirsutum, Anthracophyllum discolor* and *Trametes versicolor* were evaluated for its potential for synthesis of silver nanoparticle. In this assays, the effect of an acid and alkaline condition (5.0 and 9.0) was evaluated in the silver nanoparticle formation by the mycelium free extract of the white rot fungi using UV-vis spectrum. The results of this assays showed that the fungal extracts produced from *S. hirsutum* and *A. discolor* demonstrated to have the greater potentials for the synthesis of silver nanoparticles. The synthesis process occurs under conditions of alkaline pH (pH 9.0); this is corroborated with the formation of the plasma band associated with the silver nanoparticles around 400 nm, but the highest band intensity was observed in the use the mycelium-free extract of *S. hirsutum*. The synthesis reaction does not proceed when the pH is adjusted to an acidic condition in mycelium-free extract.

Additionally, the mycelium-free extract of *S. hirsutum* showed a surface plasmon absorption band higher only under alkaline condition, which occurred at 420 nm, being the peak higher when the incubation time increases. During the process of the synthesis of biogenic synthesis of silver nanoparticles have an average size of 100 nm and quasi-spherical shape. In the synthesis was effective in the formation of silver nanoparticles zero valent (Ag^0), which was ratified by the formation of the plasmon band around 420 nm (Krishna et al., 2015; Metuku et al., 2014; Chan and Don, 2013) and the peak at 38.24°, 44.40°, 64.74° and 77.44° degrees of 2θ that correspond to a structure of silver nanoparticles in study of X-ray diffraction (Mukherjee et al., 2008; Feng et al., 2010). The similar results have been reported using white rot fungi in the synthesis of silver nanoparticles as *Trametes sp, Schizophyllum radiatium, Pycnoporus sanguineus* and *Schizophyllum commune* (Chan et al., 2012; Chan and Don, 2013; Metuku et al., 2014; Krishna et al., 2015). An initial pH condition in the reaction solution affects the shape and size of synthesized nanoparticles, currently possible to find several reports on pH effect on the formation of nanoparticles (Navazi et al., 2010).

On the other hand, the size and morphology of the nanoparticles in formation are affected by the temperature in the synthesis reaction (Fayaz et al., 2009; Kathiresan et al., 2009). Among the main results obtained in relation to the effect of temperature on synthesis of metal nanoparticles in fungal extract of *S. hirsutum* reaction proceeded synthesis at room temperature (25 °C) without the need to deliver energy to the system, the resulting nanoparticles had lower sizes at 100 nm in the three metals in studied. The formation of nanoparticles using extract of fungal

strains is simple and that the synthesis of nanomaterials do not need special conditions of temperature and this training is feasible at ambient temperatures (Rajamukar et al., 2012).

Moreover, this fungal mycelium-free extract produced using *S. hirsutum* was used for the synthesis of nanoparticles of gold and copper. Gold nanoparticles synthesized using the fungal extract showed the formation of plasmon band characteristic for gold around 560 nm in the UV-Vis spectrum (Mukherjee et al., 200; Sanghi et al., 2011). In synthesis process using the fungal extract from white rot fungus was effective in acid conditions has on the solution to pH 5.0, this condition acidity of the solution is consistent with that reported in other biogenic synthesis using fungal extract (Sanghi et al., 2011; Mishra et al., 2012; El-Batal et al., 2015). The XDR pattern spectrum of gold nanoparticles shows intense peaks in 21.11°, 27.40°, 31.74°, 38.20°, 45.54°, 56.48°, 64.50°, 66.72°, 75.30° and 84.22° degrees of 2θ, the presence of intense peaks at 38°, 45°, 65° and 75° degrees of 2θ corresponding to gold nanocrystals, which correspond to the (111), (200), (220) and (311) corresponding to the planes of a crystal structure of gold (Ahmad et al., 2003; Shankar et al, 2004).

Finally, in the biogenic synthesis of copper nanoparticles by the mycelium-free extract of *S. hirsutum* using a concentration 5 mM of different copper salts $CuCl_2$, $Cu(NO_3)_2$ or $CuSO_4$. Particularly, with mycelium-free extract of *S. hirsutum* combined with $CuCl_2$ in under neutral or basic conditions was effective synthesis of these nanomaterials, the nanoparticles obtained were monodisperse, spherical, and between 4 and 5 nm in size. In an opposite direction they were reported the results obtained in the synthesis of nanoparticles using fungal extracts three different *Penicillium sp*, where it is indicated that the pH of the solution can strongly influence the average size of the copper nanoparticles, the size of nanoparticles copper was lower in the acid pH (5.0) to be compared with average sized obtained from neutral and alkaline pH conditions.

On the other hand, the maximum absorbance peak was observed to 620 nm when $CuCl_2$ was used as the substrate, this peak is indicating the synthesis of copper oxide nanoparticles with a small particle size (Lisiecki and Pileni, 1995; Banerjee and Chakravorty, 2000). Also, it was observed that the surface of the copper nanoparticles was surrounded by a biopolymer by microscopy TEM; similar situation was reported by Hosseini et al. (2012) where it is produced nanoparticles copper combined with sulfur (CuS-NPs). Among its findings highlight that the nanoparticles have a size of 5 nm but were entangled in spherical shells which were peptide about 20 nm in diameter.

In this context, to the characterization of biogenic nanoparticles obtained, the FTIR spectra of the nanoparticles biogenic synthesized using mycelium-free extract from *S. hirsutum* revealed bands in the regions of 3280 and 2924 cm^{-1}, which are reported as type movements of stretching vibrations in primary and secondary amines (Vigneshwaran et al., 2007; Chan and Mashitah, 2013). Other researchers reported bands at 1640 and 1540 cm^{-1}, which are associated with type movements corresponding to bending vibrations (Vigneshwaran et al., 2007; Basavaraja et al., 2008; Shaligram et al., 2009). The bands near 1029 cm^{-1} are reported to be C–N stretching vibrations of aromatic and aliphatic amines (Shaligram et al., 2009), and another band of interest found in this study was observed at 1243 and 1244 cm^{-1}, which is designated for bending vibration movements in amides I and amides III (Hosseini et a., 2012). A band at 1076 cm^{-1}, which corresponds to bending vibration movements in amides II, was reported by Hosseini et al. (2012) for the synthesis of CuS nanoparticles; moreover, Chan and Mashitah (2013) reported the same band in the synthesis of silver nanoparticles synthesized by white rot

fungi. The overall observations confirm the presence of protein in the samples of metal nanoparticles (Ag, Au and Cu -NPs) using mycelium-free extract produced from *S. hirsutum*.

This evidence suggests that the release of extracellular protein by white rot fungi may have resulted in the formation and stabilization of biogenic metal nanoparticles synthesized in aqueous medium (Vigneshwaran et al., 2007; Basavaraja et al., 2008; Shaligram et al., 2009). The FTIR studies allowed concluding that the fungal extract with presence of proteins containing an amino acid with S-H bond participates in the reducing process of metal ions, and probably cysteine is the amino acid involved in metal ion reduction to form metal nanoparticles (Mukherjee et al., 2008; Sanghi and Verma, 2009).

In the context of the synthesis process and mechanism of synthesis using fungal mycelium-free extract, due to the presence of different types of biomolecules in the mycelium-free extract produced from *S. hirsutum*, determine which were the forerunners of the reduction of metal salts which began the process of nucleation and formation of metal nanoparticles is very difficult to determine. The fungal mycelium-free extract produced from fresh biomass of *S. hirsutum* biomolecules contained as sugars, aminoacids and proteins that have been reported as possible reducing agents in the synthesis of these nanomaterials. However, in the literature demonstrates that the formation mechanism of metal nanoparticles is due to the action of a large number of enzymes secreted by the fungi, in special reductase enzymes (Durán, et al., 2005; Jain et al., 2011; Sanghi et al., 2011; Durán et al., 2014). The analysis results of SDS-PAGE protein profile present in the mycelium-fre extract produced from *S. hirsutum*, the presence of bands 12.9, 15.9, 36.9, 47.4 and 61.0 kDa were observed molecular weight. These molecular weights are related to the enzyme laccase produced by white rot fungi.

In this context, results are consistent with reported by Mukherjee et al. (2002), which indicated that at least four proteins of molecular mass between 66 kDa and 10 kDa can be found in the culture extract produced by *F. oxysporum.* Based on current information, a possible mechanism for synthesis of Ag nanoparticles in two stages: the first stage involves kDa 32 protein, which may be the reductase enzyme secreted by the fungus and the second step is 35 kDa, which are associated with nanoparticles and give stability to the nanoparticles (Jain et al., 2011). In this context, Nithya and Ragunathan (2009) indicate that the protein released by the white rot fungus, could be involved in the stabilization of nanoparticles.

However, the biological systems are the exact biological reduction mechanism of Ag^+ to Ag^0 or other metal are not fully understood, but generally partition of reductase enzyme in the synthesis is by reduction non-enzymatic catabolic (Durán et al., 2014; Gholami-Shabani et al., 2015). On relation to the possible mechanism explaining the formation of metal nanoparticles exclusively in the presence of the laccase enzyme, the currently reported information indicates that cysteine residues would be the reducing agent (Faramarzi et al., 2011; Durán et al., 2014). The laccase from *T. versicolor* exhibits one cysteine associated with Cu1-Sγ (Cys-453) laccase and is stabilized by a disulfide bridge to domain 1 (Cys-85–Cys-488), and a second disulfide bridge (Cys-117–Cys-205) connects domains 1 and 2 of laccase (Piontek et al., 2002). Based on this background Durán et al. (2014) proposes two possible ways for the formation of nanoparticle that could explain the formation of the nanoparticle by the interaction of the metal ion with the disulfide bridges in the structure presenting the laccase enzyme: 1) It is by reducing the ion metal action of the redox potential present in T1 copper having a cysteine residue in conformation and 2) it is possible to break the sulfur bridges sulfur stabilizing the molecule in domain 1 of the structure.

In general, metabolic complexity of fungal strains complicates the analysis and identification of active species in the reduction, nucleation, growth and stabilization of metal nanoparticles. The clarification of the biochemical pathways involved in the biogenic synthesis of the nanoparticles is necessary to develop and rational approach to this technology and its biotechnological application. The use of biogenic nanoparticles opens new and different fields of study in medicine, agriculture, bioremediation among others.

A property of great importance in metal nanoparticles is its antimicrobial activity; several studies stand out as the new generation of antimicrobial metal nanoparticles (Rai et al., 2009). In this context, the antimicrobial potential of nanoparticles previously synthesized and characterized was studied.

The inhibitory effect of copper nanoparticles on *E. coli* and *S. aureus* bacterial strains with the disc diffusion assay 100 µg/mL and analysis tests the effects on bacterial growth by increasing the optical density in the liquid medium with increasing concentration in solution (100, 250 and 500 µg/mL) of *E. coli* and *S. aureus* were analyzed. The results obtained showed that there copper nanoparticles were not inhibitory effect on bacterial growth of *E. coli* and *S. aureus* in liquid medium and the same result was observed in the diffusion assay plate. These results may indicate that there was not inhibitory effect or bactericide on growth in both strains of bacteria in concentrations of copper nanoparticles used in the study. However, opposite results have been reported in the literature, an example of the effective antibacterial action of Cu-NPs was reported by Yoon et al. (2007), this study was reported an effectiveness of the antimicrobial activity of 90% at a concentration of about 40 µg/mL for *Bacillus subtilis* and *E. coli* bacterial strains.

Other studies obtained positive results for the antimicrobial activity of copper nanoparticles at higher concentration; a case is reported by Ramyadevi et al. (2012), in their results show that the Cu-NPs of synthetic type at an approximate concentration of 500 mg/mL in their synthesis solution have biocide effect. Another possible cause of the lack antimicrobial activity of copper nanoparticles synthesized from the extract of white rot fungus *S. hirsutum* can be attributed to these enveloping biopolymer nanoparticles, which are formed in the process of spontaneous synthesis studied, this biopolymer is withholding the particles which cannot effectively evaluate the potential use of antimicrobial nanoparticles. Hosseini et al. (2012) used fungal strain *F. oxysporum* in synthesis and used copper sulfide nanoparticles (CuS-NPs), in the same way they reported the formation of a peptide polymer encapsulating and limiting the growth of the nanoparticles.

On the other hand, the development of bacterial activity of silver and gold nanoparticles were used bacterial strains *E. coli* and *S. aureus*, bacterial strains of Gram-negative and Gram-positive type respectively. The results demonstrated that the MIC of silver nanoparticle for bacteria strain *E. coli* and *S. aureus* were 30 and 80 µg/mL, respectively. Complementarily, gold nanoparticles were in solution 40 and 60 µg/mL for *E. coli* and *S. aureus*, respectively. Currently, silver nanoparticles of size 10 – 100 nm have strong bactericidal potential against both Gram-positive and Gram-negative bacteria (Rai et al., 2009). Antibacterial activity of nanoparticles also depends on the target species of microorganism as Gram-negative or Gram-positive type. Some of reports showed higher antibacterial action of silver nanoparticles against Gram-negative than against Gram-positive (Kon and Rai, 2013; Kora et al., 2015).

The results of the development this work investigate may indicate that the biogenic silver nanoparticles synthesized from extract of *S. hirsutum* have better antimicrobial activity that

biogenic gold nanoparticles synthesized from the same fungal extract against two bacterial strains. Toxic effect of metal nanoparticles is related to addition to time, dose, and temperature, including particle size, shape, surface coatings, and cell type (Wei et al., 2015). More simplified manner it is possible to note that antibacterial activities of NPs depend on two main factors: (i) physicochemical properties of NPs as type metal using in process of synthesis and (ii) type of bacteria as gram negative and gram positive (Hajipour et al., 2012).

In this direction, the results obtained in studies of staining for the production of reactive oxygen species (ROS), confirming qualitatively generation of ROS by means of the Confocal Microscope images obtained by subjecting both bacterial strains contact with the nanoparticles. Addition flow cytometer studies were performed to quantify the production of ROS species by combining and incubating bacterial and nanoparticles, the results showed an extra generation in average 15% of species ROS by bacterial when subjected interaction with nanoparticles. Complementarily, it was possible to observe the damage caused on the viability of the bacterial membrane through the images obtained in the TEM and SEM microscopies. These results show an association between ROS generation and cell membrane damage in the antibacterial action of silver nanoparticles (Kora et al., 2015). The silver nanoparticles can induce ROS production, the possible chemical reaction involves: $2Ag + H_2O_2 + 2H^+ \rightarrow 2Ag^+ + 2H_2O$ (AshaRani et al., 2009).

In relation to mechanism of antimicrobial activity of silver nanoparticles are not fully characterized, but in this direction hypothetical mechanism hypothesis of the silver nanoparticles as antimicrobial activity and discussed the three most common mechanisms: (a) silver nanoparticle direct damage to cell membranes, (b) the silver nanoparticle and silver ion generation of ROS, (c) the uptake of free silver ions followed by disruption of ATP production and DNA replication (Marambio-Jones and Hoek; 2010). Nevertheless, antimicrobial mechanism of action of other metal nanoparticles as copper and gold nanoparticles, is still not well understood, especially effect and mechanism of action of nanoparticle combinations on bacterial cells (Kon and Rai, 2013).

At the present there are many opportunities to grow nanotechnology using biological systems for the synthesis of metal nanoparticles with antimicrobial activity, but for scaling to industrial level and the commercialization of nanoparticles produced from biological precursors it is necessary to use non-pathogenic biological system that produces the metallic nanoparticles as the white rot fungus.

5.2.- General conclusions

- As a first conclusion it can say that use of fungal mycelium-free extracts produced from white rot fungi for the production of different metal nanoparticles proved to be effective in the process of synthesizing the three types of study nanoparticles (Ag, Au and Cu), this results show a high potential for research and development in the area of nanobiotechnology from the use of white rot fungi. However the use of fungal mycelium-free extract in the synthesis of the nanoparticles has some drawbacks, since the use of a matrix that combines different organic molecules such as proteins, enzymes, sugars, animo-acids, organic acids, including all reported as potential participants in the mechanism of formation of nanoparticles. Due to the high complexity of the fungal mycelium-free extract the possibility of establishing a mechanism for the formation of nanoparticles synthesized difficult.
- Another limitation occurs in use of fungal mycelium-free extract in addition to ignoring the molecules or biological particles involved in the reduction and stabilization of the metal nanoparticles lies in the complexity of controlling the size and shape of the nanoparticles decrease poly-dispersity of particles obtained in the synthesis and replication.
- As second conclusion of this work we can say that the use of an oxidoreductase enzyme produced for white rot fungus, with the power of different participants reduce metals in the formation of biogenic nanoparticles is a viable and highly productive alternative. The laccase enzyme shown to be effective in the process of formation of the nanoparticle silver, gold and copper, acting in a dual role of reducing agent and later as the stabilizing agent of the nanoparticles formed. From the results obtained in the synthesis process using Laccase; it is possible to propose a mecanism possible of nanoparticle formation based on reducing properties of this enzyme and its protein structure.
- It can be concluded on the anti-microbial activity of nanoparticles of silver and gold, they are have the potential to inhibit bacteria growth and/or kill the bacterial cell of Gram positive and Gram negative type such as *S. aureus* and *E. coli*, respectively. Through the results we can say that one of the ways of action of the metal nanoparticle is the destruction of the cell membrane, through the generation of reactive oxygen species (ROS) that have the potential to destabilize integrity membrane cell, the result observed in the electronic microscopies. However although effective synthesis nanometrics copper structures (average size 5 nm) was obtained by being produced using the laccase enzyme, these did not show greater antimicrobial activity in the ranges studied.

5.3.- Nanotechnology perspectives

Today, nanotechnology is a very fast growing area, with the generation of large number of patents and products already on the market and should be expected that the number of products and therefore their economic and social impact is much greater in the coming years. Nanotechnology, working on a scale equal to or less than 10^{-9} meter, allowing the development of new materials and applications that are used in many industrial sectors, some of the sectors with the highest growth prospects and that are becoming a reality and applications in this field have the potential to transform biotechnology through its emerging area of nanobiotechnology, in addition to other areas such as medicine, agriculture, manufacturing, materials science, among others.

Nanotechnology gives small steps based on the discovery of new properties of certain nanoparticles or manufacture of new materials with really promising properties such as nanotubes, nanowires, graphene, nanoparticles of different synthesis as chemical, physical or biogenic processes for synthesis and they can be synthesized using different metals or metal oxides as precursors in the synthesis. The use of nanoparticles in commercial products and materials follows an increasing rate and there is almost no industry that can do without them. The nanoparticles are added to cosmetics, textiles, pharmaceuticals, paints, food, fertilizers, electronics among others, these provide improvements to the product or material such as providing antibacterial properties, ability to repel water, improve drug absorption and drug delivery, extend the life food of new type packing, fertilizer controlled, new dental resins, release enter other applications.

Additionally, the biogenic metal nanoparticles acquire increasing interest, not only from the academic or research point of view but also toward diverse industrial and medical applications, also the biogenic nanoparticles are environmentally friendly process based on non-toxic reagents become an urgent need. Biogenic metal nanoparticles can be implemented in every possible application which already uses chemically produced metal nanoparticles, for example, as catalysts and biosensors, in antimicrobial surfaces, biomedical applications, etc. At the moment, a lot of studies have been performed to analyze the general antimicrobial activity of biogenic silver and gold. Therefore, it is making a great effort to methods of synthesis of biogenic nanoparticles. Most of these methods are based on the direct application of extracts produced from the fungal biomass. However, the identification of the chemical components that are actually responsible for nanoparticle formation and stabilization is still at early stages and therefore much research is needed in this direction.

The antimicrobial activity of metal nanoparticles in combination with their anti-inflammatory and wound healing features, makes them interesting for biomedical applications such as bandages for the treatment of burns. Therefore, the ability to fully understand the mechanism of antimicrobial action of nanoparticles. The main advances are associated with the formation of reactive oxygen species, but it is still unknown which ROS are activated with greater force by the nanoparticles and where they would be affecting the cells of the microorganisms

Moreover, certain microorganism (fungi) and plants have medical properties which could give an added value to the nanoparticles. Nevertheless, the biocompatibility and toxicity must be tested carefully for every type of biogenic metal nanoparticles. The number of biotechnological applications and antimicrobial silver primarily or other biogenic metals nanometric cannot be limited to biomedical treatments can also expand to technologies applied to new materials for

food packaging, textiles, filters, water purification or formulation of agricultural chemicals with controlled release. As for biomedical applications, pathogenic fungi should not be the first choice for the production of biogenic metal nanoparticles. The production technology of biogenic metal nanoparticle technology must focus on the use of non-pathogenic microorganisms like white rot fungi or edible mushrooms with favorable properties for human health.

Biogenic silver nanoparticles is due to its green synthesis using fungal mycelium-free extract are stable nanoparticles an interesting alternative for chemically produced nanoparticles. However, the large scale production of biogenic silver has not been explored so far. To be able to compete with chemically produced nanosilver on the market, biogenic silver needs to have the same price or be cheaper. But the biggest and main challenge for the technological applications of biogenic nanoparticles is finding the balance between industrial upgrading process synthesis, price, and applicability.

REFERENCES

REFERENCES

- Abboud, Y., Saffaj, T., Chagraoui, A., El Bouari, A., Brouzi, B., Tanane, O., Ihssane, B. (2014) "Biosynthesis, characterization and antimicrobial activity of copper oxide nanoparticles (CONPs) produced using brown alga extract (Bifurcaria bifurcata),"Applied Nanoscience 4: 571–576.
- Acevedo, F., Pizzul, L., Castillo, Md. P., González, M. E., Cea, M., Gianfreda, L., Diez, M. C. (2010) Degradation of polycyclic aromatic hydrocarbons by free and nanoclay-immobilized manganese peroxidase from *Anthracophyllum discolor*. Chemosphere 80: 271-278.
- Ahmad, A., Mukherjee, P., Mandal, D., Senapati, S., Khan, M. I., Kumar, R., Sastry, M. (2002) Enzyme mediated extracellular synthesis of CdS nanoparticles by the fungus, *Fusarium oxysporum*. Journal of the American Chemical Society 124: 12108–12109.
- Ahmad, A., Mukherjee, P., Senapati, S., Mandal, D., Khan, M. I., Kumar, R., Sastry, M. (2003) Extracellular biosynthesis of silver nanoparticles using the fungus *Fusarium oxysporum*. Colloids and Surfaces B: Biointerfaces 28: 313-318.
- Azim, A., Zare, D., Farhangi, A., Mehrabi, M. R. Norouzian, D., Tangestaninejad, S., Moghadam, M., Bararpour. S. (2009) Synthesis and Characterization of gold nanoparticles by Tryptophane. American Journal of Applied Sciences. 6: 691-695.
- Baker, C., Pradhan, A. Pakstis, L., Pochan, D. J., Shah, S. I. (2005) Synthesis and antibacterial properties of silver nanoparticles. Journal of Nanoscience and Nanotechnology. 5: 244-249.
- Bansal, V., Rautaray, D., Ahmad, A., Sastry, M. (2004) Biosynthesis of zirconia nanparticles using the fungus *Fusarium oxysporum*. Journal of Materials Chemistry 14: 3303-3305.
- Bansal, V., Rautaray, D., Bharde, A., Ahire, K., Sanyal, A., Ahmad, A., Sastry, M. (2005) Fungus-mediated biosynthesis of silica and titania particles. Journal of Materials Chemistry 15: 2583-2589
- Bansal, V., Poddar, P., Ahmad, A., Sastry, M. (2006) Room-temperature biosynthesis of ferroelectric barium titanate nanoparticles. Journal of the American Chemical Society 128: 11958-11963.
- Balaji, D. S., Basavaraja, S., Deshpande, R., Bedre Mahesh, D., Prabhakara, B. K., Venkataramanb, A. (2009) Extracellular biosynthesis of functionalized silver nanoparticles by strains of *Cladosporium cladosporioides* fungus. Colloids and Surfaces B: Biointerfaces 68: 88–92.
- Basavaraja, S., Balaji, S. D., Lagashetty, A., Rajasab, A. H., Venkataraman, A. (2008) Extracellular biosynthesis of silver nanoparticles using the fungus *Fusarium semitectum*. Materials Research Bulletin 43: 1164–1170.
- Baker, C., Pradhan, A., Pakstis, L., Pochan, D. J. and Shah, S. I. (2005) Synthesis and antibacterial properties of silver nanoparticles. Journal of Nanoscience and Nanotechnology 2: 244 – 249.
- Banerjee, S. and Chakravorty, D. (2000) Optical absorption by nanoparticles of Cu2O, Europhysics Letters 52: 468–473.
- Bhainsa, K. C. and D'Souza, S. F. (2006). Extracellular biosynthesis of silver nanoparticles using the fungus *Aspergillus fumigates*. Colloids and Surfaces B: Biointerfaces 47: 160–164
- Bharde, A., Rautaray, D., Bansal, V., Ahmad, A., Sarkar, I., Yusuf, S. M., Sanyal, M., Sastry, M. (2006) Extracellular biosynthesis of magnetite using fungi. Small 2: 135-141.
- Bhambure, R., Bule, M., Shaligram, N., Kamat, M., Singhal, R. (2009) Extracellular biosynthesis of gold nano-particles using *Aspergillus niger* – its characterization and stability. Chemical Engineering and Technology 32:1036-1041 .

- Behnood, M., Nasernejad, B., Nikazar, M. (2013) Biodegradation of crude oil from saline waste water using white rot fungus *Phanerochaete chrysosporiu.* Journal of Industrial and Engineering Chemistry 20; 1879–1885
- Castro-Longoria, E., Vilchis-Nestor, A. R., Avalos-Borja, M. (2011) Biosynthesis of silver, gold and bimetallic nanoparticles using the filamentous fungus *Neurospora crassa*. Colloids and Surfaces B: Biointerfaces 83: 42–48.
- Cecil, R. and McPhee, J. R. (1957) Further studies on the reaction of disulphides with silver nitrate. Biochemical Journal 66:538–543
- Chan, Y. S. and Don, M. M. (2013) Biosynthesis and structural characterization of Ag nanoparticles from white rot fungi. Materials Science and Engineering 33:282 – 288
- Chan, Y. S., Don, M. M. (2012a). Characterization of Ag nanoparticles produced by white rot fungi and it's in vitro antimicrobial activities. The international Arabic Journal of Antimicrobial Agents. 2: 3.
- Chan, Y. S., Don, M. M. (2012b). Biosynthesis and structural characterization of Ag nanoparticles from white rot fungi. Materials Science and Engineering 33: 282–288.
- Chen, Q., Shen, Y., Gao, H. (2007) Formation of nanoparticles in water-in-oil microemulsions controlled by the yield of hydrated electron: The controlled reduction of $Cu2^{+}$. Journal of Colloid and Interface Science 308: 491–499.
- Chen, G., Yi, B., Zeng, G., Niu, Q., Yan, M., Chen, A., Du, J., Huang, J., Zhang, Q. (2014) Facile green extracellular biosynthesis of CdS quantum dots by white rot fungus *Phanerochaete chrysosporium.* Colloids and Surfaces B: Biointerfaces 117:199–205.
- Cordi, L., Minussi, R. C., Freire, R. S., Durán, N. (2007). Fungal laccase: copper induction, semi-purification, immobilization, phenolic effluent treatment and electrochemical measurement. African Journal of Biotechnology 6:1255–1259.
- Cuevas, R., Durán, N., Diez, M. C., Tortella, G. R., Rubilar, O. (2015). Extracellular biosynthesis of copper and copper oxide nanoparticles by *Stereum hirsutum*, a native white rot fungus from Chilean forests. Journal of Nanomaterials, Article ID 789089, 7 pages
- El-Batal, A., ElKenawy, N., Yassin, A., Magdy A. Amin, M (2015) Laccase production by *Pleurotus ostreatus* and its application in synthesis of gold nanoparticles. Biotechnology Reports 5: 31–39.
- El-Rafie, M. H., Mohamed, A. A., Shaheen, Th. I., Hebeish, A. (2010) Antimicrobial effect of silver nanoparticles produced by fungal process on cotton fabrics. Carbohydrate Polymers 80: 779–782.
- Das, S. K., Das, A., Guha, A. K. (2009) Gold Nanoparticles: Microbial synthesis and application in water hygiene management. *Langmuir* 25: 8192–8199.
- Dhas, N. A., Raj, C. P., Gedanken, A. (1998). Synthesis, characterization, and properties of metallic copper nanoparticles. Chemistry of Materials 10:1446-1452.
- Du, L., Xu, Q., Huang, M., Xian, L., Feng, J. (2015) Synthesis of small silver nanoparticles under light radiation by fungus *Penicillium oxalicum* and its application for the catalytic reduction of methylene blue. Materials Chemistry and Physics. dx.doi.org/10.1016/j.matchemphys.2015.04.003
- Durán, M. Silveira, C., Durán, N. (2015) Catalytic role of traditional enzymes for biosynthesis of biogenic metallic nanoparticles: a mini-review. IET Nanobiotechnology 9: 314–323
- Durán, N., Cuevas, R., Cordi, L., Rubilar, O. Diez, M. C. (2014). Biogenic silver nanoparticles associated with silver chloride nanoparticles (Ag@AgCl) produced by laccase from *Trametes versicolor*. SpringerPlus 2014 3: 645.
- Durán, N., Marcato, P.D. (2012) Biotechnological Routes to Metallic Nanoparticles Production: Mechanistic Aspects, Antimicrobial Activity, Toxicity and Industrial Applications. Nano-Antimicrobials: 337-374.
- Durán, N., Marcato, P.D., Durán, M., Yadav, A., Gade, A., Rai, M. (2011) Mechanistic aspects in the biogenic synthesis of extracellular metal nanoparticles by peptides, bacteria, fungi, and plants. Applied Microbiology and Biotechnology 90: 1609–1624.

- Durán, N., Marcato, P., De Conti, R., Alves, O., Costa, F., Brocchi, M. (2010) Potential use of silver nanoparticles on pathogenic bacteria, their toxicity and possible mechanisms of action. Journal of the Brazilian Chemical Society 21: 949-959.
- Durán, N., Marcato P. D., De Souza, G., Alves, O., Esposito, E., (2007) Antibacterial effect of silver nanoparticles produced by fungal process on textile fabrics and their effluent treatment. Journal Biomedical Nanotechnology 3: 203–208.
- Durán, N., Marcato, P.D., Alves, O., De Souza, G., Esposito, E. (2005) Mechanistic aspects of biosynthesis of silver nanoparticles by several *Fusarium oxysporum* strains. Journal Nanobiotechnology. 3: 8.
- Fayaz, A. M., Balaji, K., Girilal, M., Yadav, R., Kalaichelvan, P. T., Venketesan, R. (2010). Biogenic synthesis of silver nanoparticles and their synergistic effect with antibiotics: a study against gram-positive and gram-negative bacteria. Nanomedicine: Nanotechnology, Biology and Medicine. 6: 103-109.
- Fayaz A. M., Balaji K., Kalaichelvan P. T., Venketesan R. (2009). Fungal based synthesis of silver nanoparticles – An effect of temperature on the size of particles. Colloids and Surface B: Biointerfaces. 74: 123-126.
- Faramarzia, M.A., Forootanfar, H. (2011). Biosynthesis and characterization of gold nanoparticles produced by laccase from *Paraconiothyrium variabile*. Colloids and Surfaces B: Biointerfaces 87: 23 – 27.
- Feng, H. L., Gao, X. Y., Zhang, Z. Y., Ma, J. M. (2010) Study on the Crystalline Structure and the Thermal Stability of Silver-oxide Films Deposited by Using Direct-current Reactive Magnetron Sputtering Methods. Journal of the Korean Physical Society 56: 1176-1179.
- Ferrando-Climent, L., Cruz-Morató, C., Ernest Marco-Urrea, E., Vicent, T., Sarràb. M., Rodriguez-Mozaz, S., Barceló, D. (2015) Non-conventional biological treatment based on *Trametes versicolor* for the elimination of recalcitrant anticancer drugs in hospital wastewater. Chemosphere 136 (2015) 9–19.
- Gade, A., Bonde, P. P., Ingle, A. P., Marcato, P., Durán, N., Rai, M. K. (2008) Exploitation of *Aspergillus niger* for synthesis of silver nanoparticles. Journal of Biobased Materials and Bioenergy 2:1–5.
- Gaikwad, S. C., Birla, S. S., Ingle, A. P., Gade, A. K., Marcato, P. D., Rai, M., Durán, N. (2013). Screening of different *Fusarium* species to select potential species for the synthesis of silver nanoparticles. Journal of the Brazilian Chemical Society 24:1974–1982.
- Ghaseminezhad, S. M., Hamedi, S., Shojaosadati, S. A. (2012) Green synthesis of silver nanoparticles by a novel method: Comparative study of their properties. Carbohydrate Polymers 89: 467-472.
- Gericke, M., Pinches, A. (2006a) Microbial production of gold nanoparticles. Gold Bull 39: 22-28.
- Gericke, M., Pinches, A. (2006b) Biological synthesis of metal nanoparticles. Hydrometallurgy 83: 132–140
- Gholami-Shabani, M., Shams-Ghahfarokhi, M., Gholami-Shabanid, Z., Akbarzadeh, A., Riazi, G., Ajdari, S., Amani, A., Razzaghi-Abyaneh, M (2015) Enzymatic synthesis of gold nanoparticles using sulfite reductase purified from *Escherichia coli*: A green eco-friendly approach. Process Biochemistry 50: 1076–1085.
- Gopinath, V., Priyadarshini, S., Priyadharsshini, N. M., Pandian, K., Velusamy, P. (2013) Biogenic synthesis of antibacterial silver chloride nanoparticles using leaf extracts of *Cissus quadrangularis* Linn. Materials Letters 91:224 – 227.
- Gopalakrishsnan, K., Ramesh, C., Ragunathan, V., Thamailselvan, M. (2012) Antibacterial activity of Cu_2O nanoparticles on *E. coli* synthesized from *Tridaxprocumbens* leaf extract and surface coating with polyaniline. Digest Journal of Nanomaterials and Biostructures 7: 833 – 839.
- Govender, Y., Riddin, T., Gericke, M., Whiteley, C. G. (2009) Bioreduction of platinum salts into nanoparticles: a mechanistic perspective. Biotechnology Letters 31: 95–100

- Guajardo-Pacheco, Ma. J., Morales-Sáncheza, J.E., González-Hernández, J., Ruizb, F. (2012) Synthesis of copper nanoparticles using soybeans as a chelant agent. Materials Letters. 64: 1361–1364 .
- Gunalan, S., Sivaraj, R., Venckatesh, R. (2012) *Aloe barbadensis Miller* mediated green synthesis of mono-disperse copper oxide nanoparticles: Optical properties. Spectrochimic Acta Part A: Molecular and Biomolecular Spectroscopy 97: 1140–1144.
- Hasan, S. S., Singh, S., Parikh, R., Dharne, M., Patole, M., Prasad, B. L. V., Shouche, Y.S. (2008) Bacterial Synthesis of Copper/Copper Oxide Nanoparticles. Journal of Nanoscience and Nanotechnology 8: 3191–3196.
- Hajipour, M. J., Fromm, K. M., Ashkarran, A. A., Jimenez de Aberasturi, D., de Larramendi, I. R., Rojo, T., Serpooshan, V., Parak, W. J., Mahmoudi, M. (2012) Antibacterial properties of nanoparticles. Trends in Biotechnology 30:499-511.
- He, L., Liu, Y., Mustapha, A., Lin, M. (2011). Antifungal activity of zinc oxide nanoparticles against *Botrytis cinerea* and *Penicillium expansum.* Microbiological Research. 166: 207-215.
- Honary, S., Barabadi, H., Gharaie-fathabad, E., Naghibi F. (2012) Green synthesis of copper oxide nanoparticles using *Penicillium aurantiogriseum*, *Penicillium citrinum* and *Penicillium waksmani*. Digest Journal of Nanomaterials and Biostructures 7: 999 – 1005.
- Hosseini, M. R., Schaffie, M., Pazouki, M., Darezereshki, E., Ranjbar, M. (2012) Biologically synthesized copper sulfide nanoparticles: Production and characterization. Materials Science in Semiconductor Processing 15: 222-225.
- Husseiny, S., Salah, T., Anter, H. (2015) Biosynthesis of size controlled silver nanoparticles by *Fusarium oxysporum*, their antibacterial and antitumor activities. Journal of basic and applied sciences 4: 225–231 .
- Ingle, A., Rai, M., Gade, A., Bawaskar, M. (2009). *Fusarium solani:* a novel biological agent for the extracellular synthesis of silver nanoparticles. Journal of Nanoparticle Research 11: 2079–2085.
- Ingle, A., Gade, A., Pierrat, S., Sönnichse, C., Rai, M. (2008) Mycosynthesis of silver nanoparticles using the fungus *Fusarium acuminatum* and its activity against some human pathogenic bacteria. Current Nanoscience 4: 141-144.
- Jaidev, L. R., Narasimha, G. (2010). Fungal mediated biosynthesis of silver nanoparticles, characterization and antimicrobial activity. Colloids and Surfaces B: Biointerfaces 81: 430–433.
- Jain, N., Bhargava, A., Majumdar, S., Tarafdar, J. C., Panwar, J. (2013) A biomimetic approach towards synthesis of zinc oxide nanoparticles. Applied Microbiology and Biotechnology 97:859-69
- Jain, N., Bhargava, A., Majumdar, S., Tarafdar, J. C., Panwar, J. (2011) Extracellular biosynthesis and characterization of silver nanoparticles using *Aspergillus flavus* NJP08: A mechanism perspective. Nanoscale 3: 635-641.
- Joshi, S. S., Patil, S. F., Iyer, V., Mahumuni, S. (1998) Radiation induced synthesis and characterization of copper nanoparticles. Nanostructured Materials 10: 1135-1144.
- Kalimuthu, K., Babu R. S., Venkataraman, D., Bilal, M., Gurunathan, S. (2008). Biosynthesis of silver nanocrystals by *Bacillus licheniformis*. Colloids and Surfaces B: Biointerfaces. 65: 150-153.
- Kathiresan, K., Manivannan, S., Nabeel, M. A., Dhivya, B. (2009) Studies on silver nanoparticles synthesized by a marine fungus, *Penicillium fellutanum* isolated from coastal mangrove sediment. Colloids Surf. B 71: 133–137.
- Kashyap, P. L., Kumar, S., Srivastava, A. K., Sharma, A. K. (2012) Myconanotechnology in agriculture: a perspective. World Journal of Microbiology and Biotechnology 29; 191–207
- Kersten, P. J., Kalyanaraman, B., Hammel, K. E., Reinhammar, B., Kirk, T. K. (1990) Comparison of lignin peroxidase, horseradish peroxidase and laccase in the oxidation of methoxybenzenes. Biochemical Journal 268: 475-480.

- Kim S., Kim K., Lamsal K., Kim Y., Kim S., Jung M., Sim S., Kim H., Chang S., Kim J., Lee Y. (2009) An in vitro study of the antifungal effect of silver nanoparticles on oak wilt pathogens *Raffaelea sp.* Journal Microbiology and Biotechnology. 19: 760-764.
- Kitching, M., Ramani, M., Marsili, E. (2015) Fungal biosynthesis of gold nanoparticles: mechanism and scale up. Microbial Biotechnology 8: 904–917.
- Kora, A. J., Sashidhar, R. B. (2014) Biogenic silver nanoparticles synthesized with *rham nogalacturonan* gum: Antibacterial activity, cytotoxicity and its mode of action. Arabian Journal of Chemistry. doi.org/10.1016/j.arabjc.2014.10.036.
- Kon, K. and Rai, M. (2013) Metallic nanoparticles: mechanism of antibacterial action and influencing factors. Journal of Comparative Clinical Pathology Research 1:160 - 174.
- Krishna, G., Prasad, M. R., Krishna, P. S., Bindu, N. S. H., Samatha, B., Charya, M. A. (2015a) Fungus-mediated synthesis of silver nanoparticles and their activity against Gram positive and Gram negative bacteria in combination with antibiotics. Walailak Journal of Science and Technology, 12(7).
- Krishna, G., Kumar, S. S., Pranitha, V., Alha, M., Charaya, S. (2015b) Biogenic synthesis of silver nanoparticles and their synergistic effect with antibiotics: a study against *Salmonella* sp. International Journal of Pharmacy and Pharmaceutical Sciences. ISSN- 0975-1491 7(10).
- Kumar, S. A., Peter, Y., Nadeau, J. L. (2008) Facile biosynthesis, separation and conjugation of gold nanoparticles to doxorubicin. Nanotechnology 19: 495101 .
- Lee, H., Song, J. Y., Kim, B. S. (2013) Biological synthesis of copper nanoparticles using *Magnolia kobus* leaf extract and their antibacterial activity. Journal of Chemical Technology and Biotechnology 88: 1971–1977.
- Lee, Y., Choi, J., Lee, K. J., Stott, N. E., Kim, D. (2008). Large-scale synthesis of copper nanoparticles by chemically controlled reduction for applications of inkjet-printed electronics. Nanotechnology 19: 41pp.
- Li, X., Robinson, S., Gupta, A., Saha, K., Jiang, Z., Moyano, D., Sahar, A., Riley, M., Rotello, V. (2014) Functional Gold Nanoparticles as potent antimicrobial agents against multi-drug-resistant bacteria. ACSNANO 8: 10682–10686.
- Lin, Y. E., Vidic, R. D., Stout, J. E., Mccartney C. A., Yu, V. L. (1998) Inactivation of *Mycobacterium avium* by copper and silver ions. Water Research 32: 1997– 2000.
- Lisiecki, I. and Pileni, M. P. (1995) Copper metallic particles synthesized 'in situ' in reverse micelles: influence of various parameters on the size of the particles. Journal of Physical Chemistry 99: 5077–5082.
- Liu, W. (2006) Nanoparticles and their biological and environmental applications. Journal of Bioscience and Bioengineering. 1: 1–7.
- Lok, C.N., Ho, C. M., Chen, R., He, Q. Y., Yu, W. Y., Sun, H., Tam, P.K., Chiu. J. F.,Che, C. M. (2006) Proteomic analysis of the mode of antibacterial action of silver nanoparticles. Journal of Proteomic Research 5: 916–924.
- Mandal, D., Bolander, M.E., Mukhopadhyay, D., Sarkar, G., Mukherjee, P. (2006) The use of microorganisms for the formation of metal nanoparticles and their application. Applied Microbiology and Biotechnology 69: 485–492.
- Mashitua, M. D. and Chan, Y. S. (2011) *Schizophyllum commune* As Nano-Factory for biosynthesis of silver nanoparticles (U. Sains Malaysia, Pulau Pinang). ICCE-19 July 24-30, Shangai, China. www.icce-nano.org.
- Marambio-Jones, C. and Hoek, E. M. V. (2010) A review of the antibacterial effects of silver nanomaterials and potential implications for human health and the environment. Journal of Nanoparticle Research 12: 1531–1551
- Metuku, R. P., Pabba, S., Burra, S., Hima, B. N., Gudikandula, K., Charya, M. A. S. (2014) Biosynthesis of silver nanoparticles from *Schizophyllum radiatum* HE 863742.1: Their characterization and antimicrobial activity. 3 Biotech 4:227–234.
- Mirzadeh, S., Darezereshki, E., Bakhtiari, F., Fazaelipoora, M. H., Hosseini, M. R. (2013) Characterization of zinc sulfide (ZnS) nanoparticles Biosynthesized by *Fusarium oxysporum*. Materials Science in Semiconductor Processing 16: 374–378

- Mishra, A. and Sardar, M. (2012) Alpha-amylase mediated synthesis of silver nanoparticles' Science of Advanced Materials 4: 143–146, 2012.
- Mishra, A., Tripathy, S. K., Yuna, S. (2012) Fungus mediated synthesis of gold nanoparticles and their conjugation with genomic DNA isolated from *Escherichia coli* and *Staphylococcus aureus*. Process Biochemistry 47: 701–711.
- Moaveni, P., Karimi, K., Valojerdi, M. Z. (2011) The nanoparticles in plants: review paper. Journal of Nanostructure in Chemistry 2:59–78.
- Mohanpuria, P., Rana, N.K., Yadav, S.K. (2008) Biosynthesis of nanoparticles: technological concepts and future applications. Journal of Nanoparticle Research 10: 507–517.
- Morozova, O. V., Shumakovich, G. P., Gorbacheva, M. A., Shleev, S. V., Yaropolov, A. I. (2007) "Blue" laccases. Biochemistry Moscow 72:1136–1150.
- Mukherjee, P., Ahmad, A., Mandal, D., Senapati, S., Sainkar, S. R., Khan, M. I., Ramani, R., Parischa, R., Ajayakumar, P. V., Alam, M., Sastry, M., Kumar, R. (2001a) Bioreduction of $AuCl_4^-$ Ions by the Fungus, *Verticillium* sp. and Surface Trapping of the Gold Nanoparticles Formed. Angewandte Chemie International Edition 40: 3585-3588
- Mukherjee, P., Ahmad, A., Mandal, D., Senapati, Sudhakar R. S., Mohammad I. S., Parishcha, R., Ajaykumar, P. V., Alam, M., Kumar, R., Sastry, M. (2001b) Fungus-Mediated Synthesis of Silver Nanoparticles and Their Immobilization in the Mycelial Matrix: A Novel Biological Approach to Nanoparticle Synthesis. Nano Letters 10: 515-519.
- Mukherjee, P., Senapati, S., Mandal, D., Ahmad, A., Khan, M. I., Kumar, R., Sastry, M. (2002) Extracellular Synthesis of Gold Nanoparticles by the Fungus *Fusarium oxysporum*. Chembiochem 3: 461-463.
- Mukherjee, P., Roy, M., Mandal, B. P., Dey, G. K., Mukherjee, P. K. Ghatak, J., Tyagi A. K., Kale, S. P. (2008) Green synthesis of highly stabilized nanocrystalline silver particles by a non-pathogenic and agriculturally important fungus *T. asperellum*. Nanotechnology 19: 7.
- Musarrat, J., Dwivedi, S., Singh, B. R. Al-Khedhairy, A. A., Azam, A., Naqvi, A. (2010) Production of antimicrobial silver nanoparticles in water extracts of the fungus *Amylomyces rouxii* strain KSU-09. Bioresource Technology 101: 8772–8776.
- Narayanan, K. B., Sakthivel, N. (2010) Biological synthesis of metal nanoparticles by microbes. Advances in Colloid and Interface Science 156: 1–13.
- Navazi, Z. N., Pazouki, M., Halek, F. S. (2010) Investigation of culture conditions for biosynthesis of silver nanoparticles using *Aspergillus fumigates*. Iranian Journal of Biotechnology 8: 56-61.
- Nayak, R. R., Pradhan, N., Beher,a D., Pradhan ,K. M., Mishra, S., Sukla, L. B. Mishra, B. K. (2011). Green synthesis of silver nanoparticles by *Penicillium purpurogenum* NPMF: the process and optimization. Journal of Nanoparticles Research. 13: 3129-3137.
- Nithya, R., Ragunathan, R. (2009) Synthesis of silver nanoparticle using *Pleurotus sajor caju* and its antimicrobial study. Digest Journal of Nanomaterials and Biostructures 4: 623-629.
- Oh, S., Lee, S., Choi S., Lee I., Lee, Y., Chun, J., Park, H. (2006). Synthesis of Ag and Ag-SiO_2 by y-irradiation and their antibacterial and antifungal efficiency against Salmonella enteric serovar *Thyphimurium* and *Botrytis cinerea*. Colloids and Surface A: Physicochemical Engineering Aspects. 275: 228-233.
- Palma, C., Carvajal, A., Vásquez, C., Contreras, E. (2011) Wastewater treatment for removal of recalcitrant compounds: A hybrid process for decolorization and biodegradation of dyes. Chinese Journal of Chemical Engineering, 19: 621-625.
- Piontek, C. K., Antorini, M., Choinowski, G. J. (2002) Crystal structure of a laccase from the fungus *Trametes versicolor* at 1.90-Å resolution containing a full complement of coppers. The Journal of Biological Chemistry 277:37663–37669.
- Prasad, K., Jha, A., Prasad, K., Kulkarni, A.R. (2010) Can microbes mediate nano-transformation?. Indian Journal Physical. 84: 1355-1360.

- Prasad, Metuku, R., Pabba, S., Burra, S., Hima Bindu, N., Gudikandula, K., Singara Charya, M.A. (2014) Biosynthesis of silver nanoparticles from *Schizophyllum radiatum* HE 863742.1: their characterization and antimicrobial activity. 3 Biotechn 4:227–234.
- Rai, M., Ingle, P., Gade, A (2012) Silver nanoparticles: the powerful nanoweapon against multidrug-resistant bacteria. Journal of Applied Microbiology ISSN 1364-5072.
- Rai, M., Yadav, A., Gade, A. (2009) Silver nanoparticles as a new generation of antimicrobials. Biotechnology Advances 27: 76–83.
- Rajakumar, G., Abdul Rahuman, A., Mohana Roopan, S., Gopiesh Khanna, V., Elango, G., Kamaraj, C., Abduz Zahir, A., Velayutham, K. (2012) Fungus-mediated biosynthesis and characterization of TiO_2 nanoparticles and their activity against pathogenic bacteria. Spectrochimica Acta Part A 91: 23– 29.
- Ramyadevi, J., Jeyasubramanian, K., Marikani, A., Rajakumar, G., Rahuman, A. A. (2012) Synthesis and antimicrobial activity of copper nanoparticles. Materials Letters. 71: 114–116.
- Rodrigues, A., Ping, L., Marcato, P., Alves, O., Silva, M., Ruiz, R., Melo, I., Tasic, L., De Souza, A. O. (2013) Biogenic antimicrobial silver nanoparticles produced by fungi. Applied Microbiology and Biotechnology 97:775–782.
- Rubilar, O., Tortella, G. R., Cuevas, R., Cea, M., Rodríguez-Couto, S., Diez. M. C. 2012. Adsorptive removal of pentachlorophenol (PCP) by *Anthracophyllum discolor* in a fixed-bed column reactor. Water, Air and Soil Pollution 2235:2463-2472.
- Rubilar, O., Feijoo, G., Diez, M. C., Lu-Chau, T. A., Moreira, M. T., Lema, J. M. (2007) Biodegradation of pentachlorophenol in soil slurry cultures by *Bjerkandera adusta* and *Anthracophyllum discolor*. Ind Engin Chem Res 46:744-6751.
- Rubilar, O., Diez M. C., Gianfreda, L. (2008) Transformation of chlorinated phenolic compounds by white rot fungi. Critical Reviews in Environmental Science and Technology 38: 227-268.
- Rubilar, O., Tortella, G.R., Cuevas, R., Cea, M., Rodríguez-Couto, S., Diez, M. C. (2012) Adsorptive removal of pentachlorophenol (PCP) by *Anthracophyllum discolor* in a fixed-bed column reactor. Water Air Soil Poll 223: 2463-2472.
- Rubilar O., Tortella G., Cea M., Acevedo F., Bustamante M., Gianfreda L., Diez M.C. 2011. Bioremediation of a Chilean Andisol contaminated with pentacholophenol (PCP) by solid substrate cultures of white rot fungi. Biodegradation 22: 31-41.
- Ruparelia, J. P., Chatterjee, A. K., Duttagupta, S. P., Mukherji, S. (2008) Strain specificity in antimicrobial activity of silver and copper nanoparticles. Acta Biomaterialia 4: 707–716.
- Saravanan, M. and Nanda, A. (2010) Extracellular synthesis of silver bionanoparticles from *Aspergillus clavatus* and its antimicrobial activity against MRSA and MRSE. Colloids and surfaces B: Biointerfaces 77: 214-218.
- Sanghi R. and Verma P. (2010). pH dependant fungal proteins in the green synthesis of gold nanoparticles. Advanced Materials Letters. 1: 193-199.
- Sanghi, R. and Verma, P. (2009a) Biomimetic synthesis and characterization of protein capped silver nanoparticles. Bioresource Technology 100: 501-504.
- Sanghi, R. and Verma, P. (2009b) A facile green extracellular biosynthesis of CdS nanoparticles by immobilized fungus. Chemical Engineering Journal 155: 886–891.
- Sanghi, R., Verma, P., Puri, S. (2011) Enzymatic formation of gold nanoparticles using *Phanerochaete chrysosporium.* Advances in Chemical Engineering and Science 1: 154-162.
- Shamaila, S., Zafar, N., Riaz, S., Sharif, R., Nazir, J., Naseem, S. (2016) Gold Nanoparticles: An Efficient Antimicrobial Agent against Enteric Bacterial Human Pathogen. Nanomaterials 6(4): 71.
- Sastry, M., Ahmad, A., Khan, I., Kumar, R. (2003). Biosynthesis of metal nanoparticles using fungi and actinomycete. Current Science 85:162-170.
- Sawle B,D., Salimath, B., Deshpande, R., Dhondojirao Bedre, M., Krishnamurthy Prabhakar, B., Venkataraman, A. (2008) Biosynthesis and stabilization of Au and Au–

Ag alloy nanoparticles by fungus, *Fusarium semitectum.* Science and Technology of Advanced Materials. 9: 035012.

- Senapati, S., Ahmad, A., Khan, M. I., Sastry, M., Kumar, R. (2005) Extracellular biosynthesis of bimetallic Au-Ag alloy nanoparticles. Small 1: 517-520.
- Shankar, S., Rai, A., Ahmad, A., Sastry, M. (2004) Rapid synthesis of Au, Ag, and bimetallic Au core–Ag shell nanoparticles using Neem (*Azadirachta indica*) leaf broth. Journal of Colloid and Interface Science 275: 496–502.
- Shaligram, N.S., Bule, M., Bhambure, R., Singhal, R. S., Singh, S. K., Szakacs, G., Pandey, A. (2009) Biosynthesis of silver nanoparticles using aqueous extract from the compactin producing fungal strain. Process Biochemistry 44: 939–943.
- Sharma, D., Kanchi, S., Bisetty, K. (2015) Biogenic synthesis of nanoparticles: A review. Arabian Journal of Chemistry. http://dx.doi.org/10.1016/j.arabjc.2015.11.002.
- Simón de Dios, A., Díaz-García M. E. (2010) Multifunctional nanoparticles: Analytical prospects. Analytica Chimica Acta 666: 1–22.
- Sondi, I., Salopek-Sondi, B. (2004) Silver nanoparticles as antimicrobial agent: a case study on *E. coli* as a model for Gram-negative bacteria. Journal of Colloid and Interface Science 275: 177–182.
- Soni, N., Prakash, S. (2012) Efficacy of fungus mediated silver and gold nanoparticles against *Aedes aegypti* larvae. Parasitology Research. 110: 175-184 .
- Thakkar, K. N., Snehit, M. S., Mhatre, S., Rasesh M. S., Parikh, M. S. (2010) Biological synthesis of metallic nanoparticles. Nanomedicine: Nanotechnology, Biology, and Medicine 6: 257–262.
- Tortella G., Diez M. C., Durán N. 2005. Fungal diversity and use in decomposition of environmental pollutants. Critical Reviews in Microbiology 31: 197-212.
- Tortella, G. R., Rubilar, O., Gianfreda, L., Valenzuela, E., Diez, M. C. (2008) Enzymatic characterization of Chilean native wood-rotting fungi for potential use in the bioremediation of polluted environments with chlorophenols. World Journal of Microbiology and Biotechnology 12: 2805-2818.
- Theivasanthi, T., Alagar, M. (2011). Studies of copper nanoparticles effect on microorganisms. Annals of Biological Research. 4:368-373.
- Vahabi, K., Mansoori, G. A., Karimi, S. (2011) Biosynthesis of silver nanoparticles by fungus *Trichoderma Reesei* (A Route for Large-Scale Production of AgNPs). Insciences Journal. 1: 65-79.
- Vigneshwaran, N., Ashtaputre, N. M., Varadarajan, P. V., Nachane, R. P., Paralikar K. M., Balasubramanya, R. H. (2007) Biological synthesis of silver nanoparticles using the fungus *Aspergillus flavus*. Materials Letters 61: 1413–1418.
- Vigneshwaran, N., Kathe, A., Varadarajan, P.V., Nachane, R., Balasubramanya, R. H. (2006) Biomimetics of silver nanoparticles by white rot fungus, *Phaenerochaete chrysosporium*. Colloids and Surfaces B: Biointerfaces 53: 55–59.
- Volanti, D. P., Keyson, D., Cavalcante, L. S., Simões, A. Z., Joya, M. R., Longo, E., Varela, J. A., Pizani, P. S., Souza, A. G. (2008) Synthesis and characterization of CuO flower-nanostructure processing by a domestic hydrothermal microwave. Journal of Alloys and Compounds.459:537–542.
- Yoon, K., Byeon, J.H., Park, J., Hwang, J. (2007) Susceptibility constants of *Escherichia coli* and *Bacillus subtilis* to silver and copper nanoparticles. Science of the Total Environment 373: 572–575.
- Wei, L., Lu. J., Xu, H., Patel, A., Chen, Z., Chen, G. (2015) Silver nanoparticles: synthesis, properties, and therapeutic applications. Drug Discovery Today 20: 595–601.
- Zhang, X., Yan, S., Tyagi, R. D., Surampalli, R. Y. (2011) Synthesis of nanoparticles by microorganisms and their application in enhancing microbiological reaction rates. Chemosphere 82: 489–494.